

UNIVERSIDADE DE SÃO PAULO
ESCOLA POLITÉCNICA

GUILHERME DE FARIA GIACHERO

**A METHOD OF ECONOMIC ANALYSIS AND COST
ASSESSMENT FOR THE INSTALLATION OF MARINE
STREAM TURBINES**

São Paulo, SP, Brazil

2022

GUILHERME DE FARIA GIACHERO

**A METHOD OF ECONOMIC ANALYSIS AND COST
ASSESSMENT FOR THE INSTALLATION OF MARINE
STREAM TURBINES**

Submitted to the department of Naval
Architecture and Ocean Engineering,
Polytechnic School of the University of Sao
Paulo in fulfillment of the requirements for
the degree of Master in Engineering.

Advisor:

Prof. Dr. Gustavo Roque da Silva Assi

São Paulo, SP, Brazil

2022

Autorizo a reprodução e divulgação total ou parcial deste trabalho, por qualquer meio convencional ou eletrônico, para fins de estudo e pesquisa, desde que citada a fonte.

Este exemplar foi revisado e corrigido em relação à versão original, sob responsabilidade única do autor e com a anuência de seu orientador.

São Paulo, 25 de maio de 2022

Assinatura do autor: Guilherme Giachero

Assinatura do orientador: [Assinatura]

Catálogo-na-publicação

Giachero, Guilherme
A METHOD OF ECONOMIC ANALYSIS AND COST ASSESSMENT
FOR THE INSTALLATION OF MARINE STREAM TURBINES / G. Giachero --
versão corr. -- São Paulo, 2022.
106 p.

Dissertação (Mestrado) - Escola Politécnica da Universidade de São Paulo. Departamento de Engenharia Naval e Oceânica.

1.Energia de correntes de maré 2.Energia oceânica 3.Disco atuador
4.Avaliação de custos 5.Modelagem econômica I.Universidade de São Paulo.
Escola Politécnica. Departamento de Engenharia Naval e Oceânica II.t.

ACKNOWLEDGMENTS

I would first like to thank my thesis advisor Prof. Dr. Gustavo Assi who was always open whenever I ran into trouble or had questions about my research and writing. He consistently allowed this paper to be my own work but steered me in the right direction whenever he thought I needed it.

I would also like to express my very profound gratitude to my parents Teresa and Osvaldo for providing me with unfailing support and continuous encouragement throughout my years of study and through the process of researching and writing this thesis. This accomplishment would not have been possible without them.

Finally, I must thank the experts who were involved in the validation survey for this project, especially my colleagues at Monte Bravo. Without their passionate participation and input, this work would not have been successfully conducted.

Guilherme de Faria Giachero

CONTENTS

| | |
|---|----|
| ACKNOWLEDGMENTS | 1 |
| CONTENTS | 2 |
| LIST OF SYMBOLS..... | 5 |
| ABSTRACT | 6 |
| 1 INTRODUCTION | 8 |
| 1.1 Subject and background..... | 8 |
| 2 OBJECTIVES..... | 16 |
| 2.1 Problem description | 16 |
| 2.2 Study goals..... | 17 |
| 3 REVIEW OF PHYSICAL MODELING OF STREAM TURBINES..... | 18 |
| 3.1 Tidal power | 18 |
| 3.2 Tidal Turbines and design performance | 21 |
| 3.3 Existing commercial turbines | 23 |
| 3.4 Calculation of turbine power through actuator disc models..... | 25 |
| 3.4.1 Analytical modelling based on Betz’s actuator disc model..... | 25 |
| 3.4.2 Actuator disc model based on a finite flow and constant pressure..... | 28 |
| 3.5 Physical modelling of turbines in a blocked channel | 30 |
| 4 REVIEW OF ECONOMIC METRICS FOR EVALUATING ARRAY DESIGNS ... | 34 |
| 4.1 Power | 34 |
| 4.2 Break-even calculations..... | 35 |
| 4.2 Net Present Value | 37 |
| 4.3 Net Present Value and Internal Interest Rate..... | 38 |
| 4.4 Levelized cost of energy | 39 |
| 4.5 Pay-back period | 40 |
| 4.6 CAPEX, OPEX and DECEX..... | 40 |
| 4.7 Alternative metrics to be considered | 43 |

| | | |
|--------|---|----|
| 4.7.1 | Environmental Costs | 43 |
| 4.7.2 | Location Based Costs | 44 |
| 4.7.3 | Volume Savings..... | 45 |
| 4.7.4 | Scale Savings..... | 46 |
| 4.7.5 | Energy generation..... | 47 |
| 4.7.6 | Revenue inputs | 48 |
| 4.7.7 | Relationship between cost and size of array..... | 49 |
| 4.7.8 | Discount rate..... | 50 |
| 4.7.9 | Lifetime of array | 52 |
| 4.7.10 | Cost model inputs | 53 |
| 4.7.11 | Downtime and degradation..... | 54 |
| 4.7.12 | Final considerations regarding the economic metrics | 55 |
| 5 | METHODOLOGY | 57 |
| 5.1 | Concept and market research costs | 59 |
| 5.2 | Purchase Costs | 60 |
| 5.3 | Installation Costs..... | 60 |
| 5.4 | Operation and Maintenance Costs | 62 |
| 5.5 | Costs not considered in this methodology | 63 |
| 5.6 | Proposed methodology | 64 |
| 6 | BUSINESS CASE DEFINITION | 67 |
| 6.1 | Characterization of the São Sebastião Channel | 67 |
| 6.2 | Characterization of the renewable energy farm | 72 |
| 6.3 | Characterization of costs for São Sebastião channel | 73 |
| 6.3.1 | Installation Procedures | 74 |
| 6.3.2 | Maintenance procedures | 75 |
| 6.4 | Cost overview | 76 |
| 6.5 | Characterization of the turbine farm problem..... | 80 |

| | | |
|-------|---|-----|
| 6.5.1 | Definition of premises | 81 |
| 7 | BUSINESS CASE RESULTS..... | 84 |
| 7.1 | Results of C_p by altering the arrangement of the turbine array | 84 |
| 7.2 | Comparison of generated power employing two physical models | 85 |
| 7.3 | Power, IRR, and cashflow for $N=105$ | 87 |
| 7.4 | Power, IRR, and cashflow varying the number of turbines..... | 90 |
| 7.5 | Results by increasing flow speed..... | 93 |
| 7.6 | Calculation of IRR depending on the number of turbines, using $v=2,0\text{m/s}$ | 94 |
| 7.7 | General result varying speed and suggestion of location | 95 |
| 8 | CONCLUSIONS | 98 |
| 8.1 | Suggestions for future work..... | 100 |
| | REFERENCES..... | 101 |

LIST OF SYMBOLS

| Variable | Meaning |
|------------|---|
| u | Flow velocity |
| ρ | Fluid density |
| g | Gravity |
| p | Pressure |
| h | Height |
| α_2 | Turbine speed coefficient |
| α_4 | Turbine belt speed coefficient |
| β_4 | Speed coefficient of the deviation region |
| A | Area |
| R | Area ratio |
| b | Flow width, bounded by the channel walls |
| B | Blocking ratio of the turbine or actuator disk |
| T | Thrust force applied to the turbine |
| X | Thrust reaction force |
| P | Power extracted from the turbine |
| P_m | Power extracted from the mixture |
| C_P | Dimensional power coefficient |
| C_{P^*} | Dimensionalized normalized power coefficient |
| C_{PW} | Dimensionalized normalized power dissipation coefficient |
| C_T | Dimensional buoyancy coefficient normalized by kinetic pressure |
| C_{TL} | Dimensional thrust coefficient normalized by turbine pressure |
| F_r | Froude Number $F_r = u/\sqrt{gh}$ |

ABSTRACT

Efficient energy generation is a pressing challenge inherent to human activity and development. From the installation of industries on the riverside to the expansion of nuclear technology, humanity must be prepared for the increasing demand of the next 20 years, with intense electrification and reduction of fossil fuels. By then, it is expected that the demand for electricity doubles. Climate change due to the emission of greenhouse gases put tight constraints on our use and generation of electricity. In this scenario, accounting for environmental problems and market issues, a change in the conventional energy matrix is inevitable, creating space for the use of other sources, especially renewables. This master's thesis addresses research on conversion of marine current energy to supply electricity proposing a methodology for economic feasibility analysis. In the first part of this work, a literature review is presented, delineating current endeavors regarding stream energy harnessing. In the second part, a methodology is presented to assess the cost and power generation capability of a generic tidal farm. In the third part, a business case using real-world conditions is presented, to test the proposed methodology and to offer results regarding the feasibility of a specific endeavor. Lastly, an analysis of the results is presented, as well as the suggestion for future work in this current field.

Keywords: Tidal Stream Energy, Ocean Energy, São Sebastião Channel, Renewable Energy, Cost Assessment, Economic Modelling, Actuator Disc.

RESUMO

A geração eficiente de energia é um importante desafio inerente à atividade e ao desenvolvimento humano. Da instalação de indústrias ribeirinhas à expansão da tecnologia nuclear, a humanidade deve estar preparada para a demanda crescente dos próximos 20 anos, com intensa eletrificação e redução de combustíveis fósseis. Até lá, espera-se que a demanda por eletricidade dobre. As alterações climáticas devido à emissão de gases de efeito estufa colocam fortes restrições à utilização e geração de eletricidade. Nesse cenário, levando em conta os problemas ambientais e de mercado, é inevitável uma mudança na matriz energética convencional, abrindo espaço para a utilização de outras fontes, principalmente renováveis. Esta dissertação de mestrado aborda a pesquisa sobre conversão de energia de corrente marítima para fornecimento de energia elétrica propondo uma metodologia para análise de viabilidade econômica. Na primeira parte deste trabalho, é apresentada uma revisão de literatura, delineando os esforços atuais em relação ao aproveitamento de energia de correnteza. Na segunda parte, é apresentada uma metodologia para avaliar o custo e a capacidade de geração de energia de uma fazenda de marés genérica. Na terceira parte, é apresentado um business case utilizando condições físicas reais para testar a metodologia proposta e oferecer resultados sobre viabilidade de um empreendimento específico. Por fim, é apresentada uma análise dos resultados, bem como a sugestão de trabalhos futuros nesta área.

Palavras-chave: Energia das Correntes das Marés, Energia Oceânica, Canal de São Sebastião, Energias Renováveis, Avaliação de Custos, Modelagem Econômica, Disco Atuador.

1 INTRODUCTION

1.1 Subject and background

The energy sector worldwide is undergoing a substantial transformation driven by concerns about climate change, involving topics such as sustainability, energy security, and changing demand patterns. The importance of affordable, reliable, and sustainable energy as a key aspect of development and prosperity has been listed as one of the 17 Sustainable Development Goals adopted by the United Nations (UN) (Vogel et al. 2019). There is an expanding international concern regarding the necessity of reduction of climate impact within the energy sector, as outlined in numerous climate events, such as UN Climate Change Conference (COP26), held in Glasgow in 2021.

For this reason, it is necessary to explore the renewable potential of different locations worldwide in an attempt to mitigate the emission of greenhouse gases, largely caused by the exploration of fossil fuels to generate electricity. South America, for instance, has a very long coastline, dominated by Brazil on the East and Chile on the West, presenting an interesting scenario for the development of renewable energy generation from the ocean. To extract energy from the bulk motion of water in tidal and marine currents, stream turbines arranged in large offshore farms are required to explore this hydrokinetic potential. Marine currents generated by tidal efforts are the most reliable source of hydrokinetic energy.

Currents that present economic potential can be found in several spots worldwide, such as in the fjords in Southern Chile, particularly where narrow bathymetries and estuaries result in substantial tidal amplification (Cáceres et al. 2003; Aiken 2008). Typically, peak flow speeds over 2 m/s are required for economically viable energy extraction (Vogel et al. 2019).

Peak flow speeds of up to 4 m/s and turbulence intensities of 10–20% have been observed in the Chacao Channel, located in the northernmost part of Chilean Patagonia (Guerra et al. 2017), and around 4,5 m/s in the Magellan Strait (Hassan 2009). It is believed that there is little prospect for tidal stream energy in northern and central Chile. There may also be regions with favorable bathymetry including headlands in the mid Rio de la Plata Estuary in Uruguay where tidal stream energy may be feasible to exploit (Alonso et al. 2017).

Focusing on Brazil, the studies conducted by Retec in 2016 also have demonstrated Brazil's huge potential for hydroelectricity, largely owed to its many rivers and geographical features, as shown in figure 1. In fact, hydropower accounted for 68,1% of the country's energy

sources in 2016. Hydropower is predominantly harnessed through hydroelectric power plants, such as the Itaipú power plant, located on the Paraná River (on the Brazil-Paraguay border), with an installed capacity of 14.000 MW (Retec, 2016). Despite generating large amounts of power, hydroelectric power plants are extremely costly to build and have a negative impact on the environment, as detailed in 1.2.2, which includes a review of the available literature and a discussion on the advantages and disadvantages of the various types of equipment used to transform water power into electricity. Given the negative aspects associated with current energy sources, efforts to use alternative sources are being stepped up, mostly as a result of their reduced environmental impact, which is considered one of their main benefits.

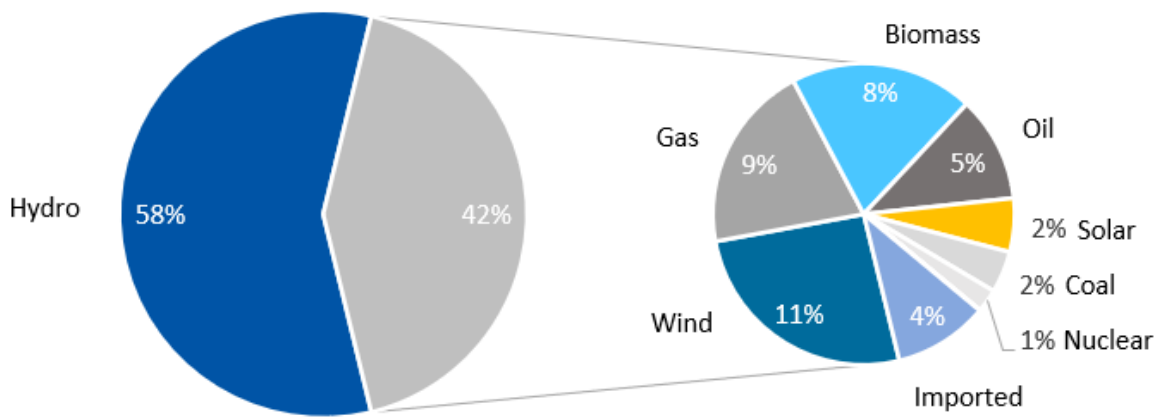


Figure 1 – Energy sources in Brazil. Adapted from ABSOLAR (2022)

It is important to mention that marine stream energy is not contemplated within the hydraulic share of the above illustrated pie graph. The tidal barrages function as an intermediate solution that uses tides to accumulate water volume inside the reservoirs and conventional turbines are responsible to harness the hydroelectric energy.

One of the key differences between stream turbines in the open seas and the more established tidal barrage technology is that a barrage stores water in a reservoir using tidal elevation, whether an ocean stream farm explores the kinetic energy in an open ocean current. One of the challenging aspects of tidal stream energy is that there is a complex and multi-scale interaction between the available tidal resource, flow past and through turbine farms, and the hydrodynamics of the turbines themselves (Vogel et al. 2019).

The increasing worldwide demand for renewable energy sources, together with the ability to generate electricity from wave and tidal power, has driven the development of hydropower technologies in recent decades, as shown in the studies conducted by Denny (2009). Extensive research has led to significant advances in countries with large marine-energy potential such as the United Kingdom, as evidenced by several initiatives, namely the Marine Energy Challenge (Carbon Trust, 2007) and the Global Atlas for Renewable Energy (DTI, 2007).

Regarding ocean energy exploration in Brazil, wave and tidal power technologies are still in their infancy. As an example, several research articles have been published on the Pecém wave power station, in Ceará, a proof-of-concept facility designed to generate 50 kilowatts (kW), which cannot be compared to the amount of power generated by river hydroelectric power plants (Shadman, 2017). Private company Tractebel has invested R\$ 15 million in this facility; however, the existing equipment is currently out of operation, as technological improvements and maintenance are required. Tidal variation in Brazil is significant mainly in the North and Northeast regions of the country, in areas such as the estuary of the River Bacanga, in São Luís (MA), which has tides of up to 7 meters, and on the island of Macapá (AP), with tides of up to 11 meters (Vogel et al., 2019). But little is known about the tidal streams associated with such large tide amplitudes.

Assessment of the tidal energy resource in South America has been limited to a small number of potential sites to date as shown in Figure 2, and further work is required to better understand the potential resource that is available. The highest tidal current flow speeds in Chile are found towards the South and are dominated by the M2 tidal constituent by an order of magnitude (Guerra et al. 2017). The high flow speeds of the Chacao Channel, for example, have attracted a number of studies, with the energy density in the channel comparing favorably to other energetic sites around the world. Guerra et al. (2017) performed field measurements and developed a numerical model of the Chacao Channel and showed that the average kinetic power density is greater than 5 kW/m^2 more than 20% of the time, presenting an interesting scenario for tidal stream exploration. The Chacao Channel is relatively isolated, and Villalón et al. (2019) showed that any tidal stream plant would be limited to 45.6 MW unless the transmission system could be upgraded. However, strong lateral shear in tidal flow speeds has been observed in the channel, which may affect planning of tidal stream energy developments (Cáceres et al. 2003). The Chacao Channel is also an important marine ecological area, including a feeding ground and nursery for blue whales (Hucke-Gaete et al. 2004).



Figure 2 - Regions where potential for tidal stream energy development has been identified in South America. Reproduced from Vogel et al. (2019)

Tidal stream energy potential has been also evaluated at a few locations in Brazil. González-Gorbeña et al. (2015) identified that in São Marcos Bay (Maranhão) has a region with annual power density in the range from 9.2 to 11.2 MWh/m². Marta-Almeida et al. (2017) investigated the energy available in the estuary of Baía de Todos os Santos, located in Brazil's Northeast the second largest bay in Brazil and near Salvador, the third-largest city in Brazil. A numerical assessment estimated that the power density in this region reaches a daily average around 400 W/m², peaking at around 2.5 kW/m² for the surface layer when allowing for a minimum operating flow speed of 1 m/s.

South America also benefits from large estuaries such as the Amazon and Rio de la Plata (van Els and Junior, 2015) and significant ocean currents near its coastlines, including the Brazilian and Malvinas currents (Kirinus et al. 2018). Hydrokinetic turbines may still present a feasible technology for harnessing this energy. The Rio Grande do Sul littoral off the South-eastern coast of Brazil was found to have peak current speeds of over 1.5 m/s, with flow speeds further enhanced in some coastal areas through headlands or straits between islands (Kirinus et

al. 2018). South America faces challenges in achieving efficient power extraction using tidal stream turbines, as there are relatively few sites that meet the requirements of peak tidal current speeds between 2 and 2.5 m/s at moderate depths of 20 to 50 m in regions where the seabed is favorable to offshore foundations (González-Gorbeña et al. 2015). However, as tidal stream technologies develop, there may be the potential for further sites to become feasible for development.

Regions in which tidal stream energy may be most economical to harness are those in which the tidal energy flux in the oceans is concentrated by the bathymetry of the continental shelf and geographical features such as islands, headlands, and straits or channels. Analytical models of the tidal stream energy available at such sites have been studied by a number of researchers (Garrett and Cummins 2005; Draper et al. 2010; Vennell 2010), as idealized representations of real channels such as the Pentland Firth, UK, or Cook Strait, NZ, in order to establish upper limits to the power available at those sites. Tidal flows may be driven by a head difference or phase difference across a region or a combination of both. Given the large scale (tens of kilometers) of regional-scale models, the turbines are represented as momentum sinks, which means care is required when relating turbine thrust to the hydrodynamic power available. Site-specific investigations of tidal energy extraction necessitate a numerical modelling approach (Vogel et al. 2019). The large horizontal extent, relative to the vertical dimension, of the regional models required for site investigations means that depth-averaged shallow water modelling is usually the most appropriate modelling technique. Shallow water flow models are well-established and have been applied in many different applications, including coastal flows, flood modelling, and pollutant dispersal (Cummins et al. 2010; Roos and Schuttelaars 2011). Application to tidal stream energy problems is a more recent phenomenon and has required addition of energy extraction terms in the governing shallow water equations (Vogel et al. 2017).

Regarding the numerical modelling, one of the key differences between wind and tidal flows is the close proximity of boundaries to tidal turbines, including the seabed, surface, and potentially neighboring turbines. Approximating the tidal turbine as an actuator disk, Garrett and Cummins (2007) demonstrated that operating turbines in a confined flow increase the maximum power coefficient C_p , turbine power normalized on the undisturbed kinetic flux through the rotor swept area, above the well-established Betz limit $C_p = 16/27$ for wind turbines. (Vogel et. al 2016)

The increase in maximum power coefficient for the idealized turbine in confined flows is due to the acceleration of flow in the bypass region around the turbine leading to a reduction in the downstream static pressure and the consequent increased pressure drop across the turbine plane. The turbine can thus achieve a higher thrust and therefore power for a given flow rate through the turbine. Maximizing turbine power in a blocked environment requires that the turbine operates at a higher thrust than for an unblocked turbine, increasing energy output potential. (Vogel et. al 2016)

For this reason, it is important to measure the ideal number of turbines to be installed in channel in order to have maximum energy output without impeding the tidal flow within a confined channel.

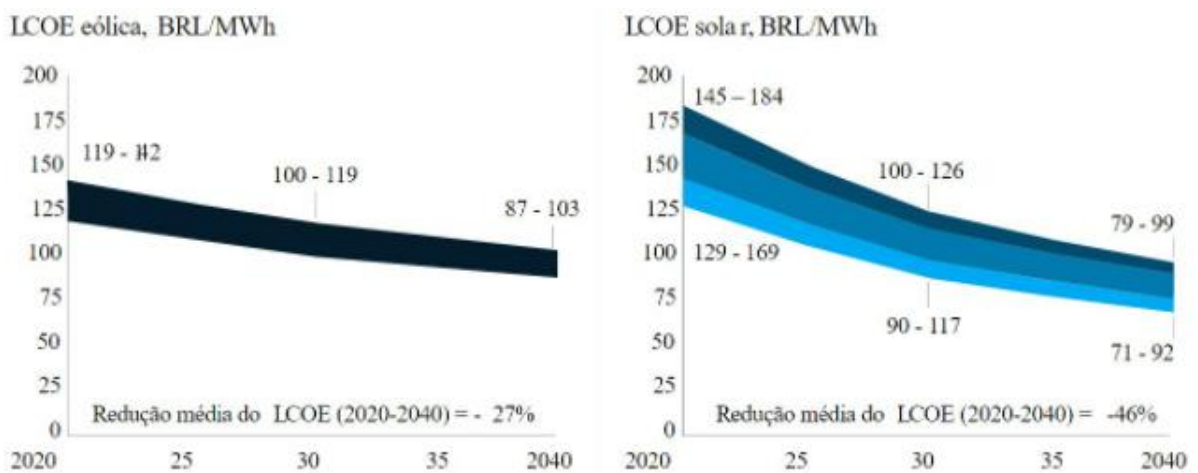
The impact of the tidal farm on the tidal resource is also a topic of concern. As it is a function of both the total resistance presented by the turbine farm and the underlying dynamics of the tidal site, the power that can be extracted from a site is thus a balance between increasing numbers of turbines and the resulting reduction in energy flux (Garrett and Cummins 2005). Large straits with high levels of background friction are relatively insensitive to the resistance presented by the turbine farm, and therefore changes in tidal flows are relatively small (Garrett and Cummins 2005). Tidal stream turbines extract energy from an open channel flow without using a barrage to establish a drop in static pressure across the turbines.

Tidal energy also faces challenges such as current energy generation cost. Despite the recent successful deployments of tidal devices in the UK, further reductions in the levelized cost of energy (LCOE) are required for commercial success. Revenue support for renewable energy technologies in the UK is offered through the contract for difference (CfD) programme. Draft strike prices of USD 230/MWh in 2023/2024 and USD 227/MWh in 2024/2025 were quoted in 2017 (Vogel et al 2019); although without specific allocation of funding to tidal stream energy, it is unlikely to be competitive in an auction in competition with offshore wind, which is forecast for strike prices of USD 60/MWh and USD 57/MWh in 2023/2024 and 2024/2025, respectively. (Melo and Jeffrey 2018)

Significant cost reductions are expected to be achieved through further technical innovations, financing cost reductions as the technologies mature, and economies of scale, with LCOE estimated to reduce to USD 93/MWh once 1GW has been deployed (Smart and Noonan 2018). According to McKinsey Brazil's study in 2021, the LCOE of wind energy is currently in the range of USD 25 to 30 per MWh, with an expected reduction of 27% by 2040; solar

energy, on the other hand, has a current cost in the range of USD 35 to 40 per MWh in the Southeast region and 38 to 42 in the Northeast region, but it presents a 46% drop trend in the average LCOE until 2040. No results have been presented for tidal energy, but it shows that wind energy can reach an LCOE of 20-24 USD/MWh in 2030 and 17-21 USD/MWh in 2040; on the other hand, solar energy can reach an LCOE of 17-21 USD/MWh in 2030 and 13-17 USD/MWh in 2040, thus being able to surpass wind energy in the five-year period 2025 - 2030 in this attribute.

This information is important to measure the necessary LCOE for tidal farms to be achieved in order to study economic feasibility. As already mentioned, Brazil offers very interesting areas of tidal energy exploration but the technology itself must have a competing cost value in order to attract private investments that will be naturally attracted to solar and wind endeavors within the mentioned time range.



Fonte: linha de serviço de hidrogênio da McKinsey



Figure 3 - Large scale solar and wind LCOE forecast in Brazil. Reproduced from McKinsey v8 p12 (2021)

Tidal stream energy presents a significant and worthwhile opportunity as a predictable and renewable source of energy in countries with significant tidal resources. Different locations in Europe as well as South America in particular benefit from established offshore energy sectors, primarily focused on oil and gas, driving the development of industrial and academic

knowledge for developing new offshore technologies. In order to drive renewable energy transition, costs must be reduced before tidal stream energy will be competitive with alternative technologies such as wind and solar photovoltaics.

Besides, as the present work discusses, stream velocity is also a main factor to be considered when studying the implementation of a tidal energy farm, as it is the most important parameter to achieve interesting economic projections. The fluid dynamic similarities between wind and tidal stream energy have allowed significant transfer of knowledge from the former industry to the later, although there are important differences between the two applications, in particular the effects of blockage. Whilst the harsh marine environment, including the effects of waves, shear profile, and high levels of ambient turbulence, presents challenges in the design and operation of tidal turbines, blockage also presents an opportunity to substantially boost tidal turbine performance relative to that for wind turbines. Indeed, recent experiments on turbines designed for operating in a blocked environment have shown that a substantial uplift in performance of approximately 20% can be achieved (McNaughton et al. 2019). Of course, advanced materials, coatings, and control strategies will be required to fully benefit from tidal stream technology at a commercial scale.

A significant challenge in the development of renewable energy technologies is that they typically involve large upfront investments, with payback occurring over extended periods. Investor confidence in the sector will therefore benefit from the long-term demonstration of performance and maintainability of tidal turbines, as is currently being demonstrated by a number of global tidal energy companies at testing centers and the first commercial arrays. This will also demonstrate to policymakers the potential of tidal stream energy to contribute to national electricity supplies and develop the case for supporting nascent technologies. The existing offshore energy infrastructure in countries such as Brazil and the UK provides opportunities for integrating tidal energy into the existing energy network.

2 OBJECTIVES

Taking into consideration the presented context, this research project has its grounds in the Brazilian marine power potential, focusing on the necessity to provide an economic model assessment for future endeavours, taking into account available marine stream resources and the country's geographical features. In the first part of this work, a literature review is presented, delineating current endeavours regarding tidal energy harnessing. In the second part, a methodology is presented to assess the cost and power generation capability of a generic tidal farm. In the third part, a business case using real world conditions is presented, to test the proposed methodology and to offer results regarding the feasibility of this specific endeavour. Lastly, an analysis of the results is presented, as well as the suggestion of future work in this current field.

2.1 Problem description

After analyzing the current existing tidal energy scenario more specifically in South America and the existing hydropower systems, this work provides a step-by-step methodology to analyze the economic feasibility of a generic ocean stream farm, involving the calculation of costs of implementation and revenue of an energy venture. Different outputs of this study will be analyzed, such as for how many years the undertaking must exist until it becomes economically feasible.

The following stages are involved:

1. Study of various physical models, starting with Betz analysis and incrementing details into the proposed model to understand the effect of local and global water flux blockage into the power output.
2. Building of the cost assessment methodology, taking into account different aspects of the construction of a tidal farm, including maintenance, installation, project management costs and others, which will be mentioned in the literature review.
3. Development of a business case analysis, to evaluate the proposed model. The business case calculation will receive real inputs from a location in South America and will determine the different conditions into which the project would become feasible.

2.2 Study goals

The primary goal of this work is to create and present a scalable methodology to assess the economic feasibility of tidal energy farms, given certain parameters such as flow velocity, blockage effect and size of the channel. No alterations to the existing theoretical physical models are proposed in this study. The calculation parameters will be provided using literature information from previous works regarding the topology of São Sebastião channel, located between the city of São Sebastião and Ilha Bela, state of São Paulo, Brazil.

The main question to be answered is whether the installation of a tidal farm construction in this region would be economically viable, and if so, in which conditions. A second analysis will present a scenario overview by changing certain parameters, such as the number of turbines installed and flow velocity, to predict the conditions in which the undertaking would become feasible. With this study, a second location can be suggested for the implementation of the tidal farm.

Note that it is not our intention to develop a hydrodynamic, geological or electrical technical study on the installation of the farm. Given that the installation of a turbine farm would be feasible in this channel, our focus is on its economic viability.

3 REVIEW OF PHYSICAL MODELING OF STREAM TURBINES

In the first part of this section an overview of existing tidal power initiatives is presented. Subsequently, an investigation into different parameters of different types of turbine will be conducted. An analysis of these parameters and an appropriate definition of their values are necessary to ensure optimal performance, therefore an entire section will be dedicated to optimal parameter setting. The second part of this section presents an overview of the economic parameters of the project, which will be used to construct a model for the energy produced by the farm presented in following sections.

3.1 Tidal power

Tidal power or tidal energy is the form of hydropower that converts energy obtained from tides into electricity. Two forms of energy may be used for this purpose, namely kinetic energy from water currents or potential energy resulting from the height difference between high and low tides. The available technologies employing these forms of energy generations are summarized below, including a brief description of the equipment currently used and a comparative analysis of efficiency.

Tides are the alternating rise and fall of sea levels caused by the combined effects of the gravitational forces exerted by the celestial bodies closer to the Earth (the Moon and the Sun), and the Earth's rotation. Tide tables provide information on predicted times and amplitude at any location. Predictions are based on multiple factors, namely the alignment of the Sun and the Moon, tidal patterns in the deep ocean, the amphidromic systems (movement of the tides deflected by Coriolis and blocked by land masses, these rotary systems are formed in oceans basins, bays and seas that are counter-clockwise in the Northern Hemisphere and clockwise in the Southern Hemisphere) of oceans and the shape of the coastline and the near shore. Nevertheless, tide tables are mere predictions; the actual time and height of tide variation is also influenced by wind and atmospheric pressure. Tidal timescales range from hours to years, depending on the factors that determine the lunitidal interval. Tide gauges located at fixed stations, which measure water level over time, are used to obtain accurate records. Gauges ignore variations caused by waves with time periods shorter than minutes. Data are subsequently compared with a reference level usually known as the mean sea level.

Although tides are usually the main source of short-term sea-level fluctuations, sea levels are also subject to forces such as wind and barometric pressure changes, resulting in tidal surges, especially in shallow seas and near coasts. The speed of tidal flows depends on coastal morphology. For instance, the Venturi effect enhances tidal flow speed in estuaries and bays, facilitating energy extraction. Therefore, it makes sense to install tidal power stations at locations when topographical characteristics allow for increased energy conversion, focusing on ways to use the movement of rising and falling sea levels to generate horizontal streams to drive the rotors.

A turbine is a device that converts energy from a fluid flow, which is extracted by a rotor assembly, into useful work or energy. Turbines subsequently generate electricity for human consumption through a suitable means, such as electromagnetic induction. Several types of turbines are commonly used, namely steam, wind, gas and water turbines. These devices were already found in ancient Greece, where the first windmills extracted wind energy through a series of shafts and wheels in order to power machinery. Windmills and waterwheels are early examples of turbines used for milling grain and other purposes (Rouse, 2008).

Water flow energy was one of the first renewable energy sources to be harnessed, firstly by means of watermills. This type of energy can also be harvested through modern devices known as tidal stream generators (TSGs), which extract kinetic energy from moving water to propel turbines. TSGs may be installed near bridges, such as to make the most of existing infrastructures, or in peninsulas or inlets, where topographical features allow for greater flow speeds, leading to better yields. Axial, radial, cross-flow and inward-flow turbines are usually installed near the bottom of water columns (GE Power Conversion, 2017).

In 2008, an experimental turbine was installed in the East River, near New York (USA). In 2013 a 35kW turbine was installed in the Mississippi River (USA), to mention only two examples (Figure 4).

However, geographical limitations represent a major drawback, as location is key to ensuring economic feasibility, which prevents large-scale implementation. In an attempt to find a suitable solution, Delta Stream Energy has developed a device based on this technology, equipped with 3 blades (Figure 5), which can generate up to 400kW per turbine (Deltastreamenergy.ca, 2018).



Figure 4 – Illustration of an axial turbine installed in the Mississippi river. Reproduced from RETEC (2016)

Delta Stream Energy has developed a gravity-based system that reduces installation and maintenance costs, as well as an automated hydraulic mechanism that aligns turbines with water flow in order to maximize efficiency. However, this system does not allow for power to be extracted from reverse flows, due to design limitations.



Figure 5 - Generators attached by triangular base to generate up to 1.2MW. Reproduced from Deltastreamenergy.ca (2018)

Another promising, although untried, technology dynamic tidal power (DTP) might also be used to convert kinetic energy from tidal currents into electricity. DTP would involve the

building of long non-landlocked dam-like structures, e.g. with length of 30-50 km, in oceans or seas. These dams would create significant differences in water level in shallow coastal waters, such as those found in China, the United Kingdom and Korea. DTP systems usually consist of two- or three-bladed turbines. Several types of turbines are currently available, as discussed briefly in section 1.5.

The principle behind power generation from water flow is similar to that on which wind power technologies are based, i.e. the energy of a fluid flow is converted into electricity through the rotor. A rotor is a device that converts the kinetic energy of the flow, in this case water, into kinetic energy on a rotating shaft. The amount of power available by a given water flow is (Bahaj, 2011):

$$P_0 = \frac{1}{2} \rho A v_0^3 \quad (1)$$

In the equation that establishes the relationship between total flow power and flow speed, ρ is the density of water, in kg/m^3 ; A is the rotor cross-sectional area; and v_0 is the undisturbed flow speed, considered constant across the rotor cross section (Bahaj, 2011).

As seawater density is 800 to 1,000 times higher than air density, total power given by equation 1 will be considerably greater in water. Therefore, smaller tidal blades can be used to generate an equivalent amount of power compared to large-diameter wind turbines.

3.2 Tidal Turbines and design performance

A typical tidal stream turbine is shown in figure 6, which is an example of a horizontal axis tidal turbine (HATT). Although vertical axis tidal turbines and other concepts (such as oscillating hydrofoil, enclosed tip turbine and tidal kites) are also designed to harness tidal energy, most of the research and development efforts are focused on HATTs. This is primarily because of their higher technology readiness level (TRL), and similarity to commercial wind turbines.

Different authors have investigated the best parameters for drag-based hydrokinetic turbines to discover maximum efficiency and torque in different conditions. The performance of these turbines can be expressed in the form of a power coefficient C_p (equation 2) and torque coefficient C_m (equation 3) as a function of the tip speed ratio (TSR) (equation 4). TSR can be

expressed by the equation 4 (Altan et al., 2016):

$$C_p = \frac{\text{Actual Electrical Power Produced}}{\text{Power into turbine}} = \frac{P_{out}}{P_{in}} \quad (2)$$

$$C_m = \frac{T}{\frac{1}{2}\rho A v_0^2 R} \quad (3)$$

$$TSR = \omega D / v_0 \quad (4)$$

where ω is the angular velocity of the rotor (rad/s), v_0 is the flow's speed and D is the diameter of the rotor, which can be pictured in figure 6.

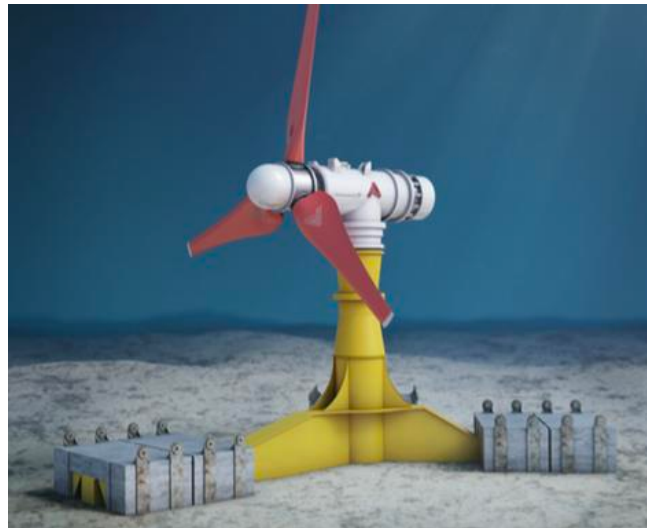


Figure 6 – Illustration of a 3-bladed rotor. Reproduced from Furtmayer (2016)

Figure 6 illustrates a typical 3-bladed rotor and its main parts, as well as the different constructive parameters. It has been defined in the literature that C_p characterizes the ratio between maximum power obtained from fluid-turbine interaction (P_{out}) and the maximum power available in the stream (P_{in}), being both expressed in Watts. C_m characterizes the ratio between the maximum torque obtained by the turbine and the available torque from the fluid. (Talukdar, 2012).

The values of C_p , C_m and TSR are highly influenced by two main geometric parameters

of a turbine, i.e. blade profile, number of blades. However, no consensus regarding the optimal values of these specifications is presented in the literature.

A typical C_p curve of tidal 3-bladed rotor can be seen in Figure 7:

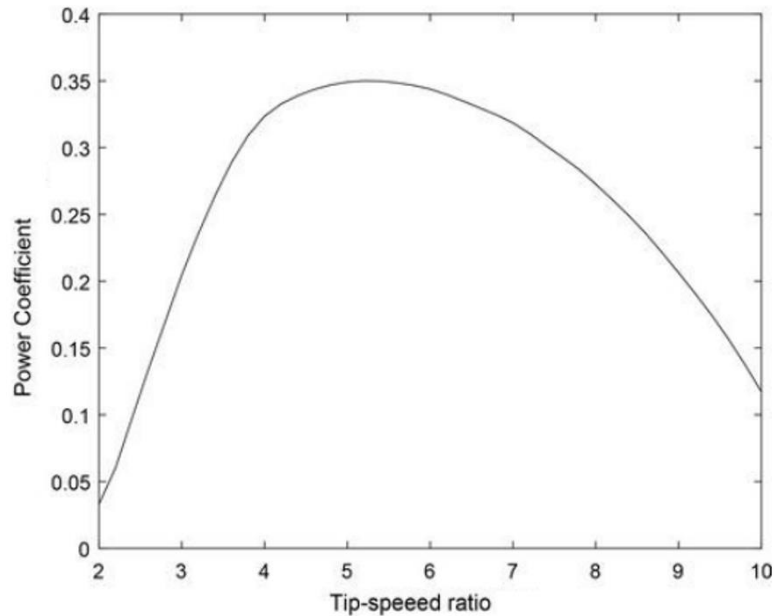


Figure 7 - A typical C_p for a tidal turbine with indicative values; these values do not reflect the maximum C_p in a tidal turbine. Reproduced from Faisal (2020)

3.3 Existing commercial turbines

Different companies are planning to put in the market 3-bladed turbines with diverse parameters to fit different applications, as seen in Table 1 representing relevant types of HATT turbines and manufacturers. It is important to mention that the turbines listed are still prototypes and produced in reduced scale. Bulk production is currently not available for the listed manufacturers. Table 2 summarizes turbines from different manufactures but focuses on a parameter level regarding power, nominal velocity, minimal velocity and number of blades.

Table 1 – Different manufacturers and their typical type of HATT. Adapted from Faisal (2020)

| Company name | Country base | Device type | Generator type _a | Device name _b |
|----------------------------|--------------|-------------|-----------------------------|--------------------------|
| Andritz Hydro Hammerfest | Norway | HATT | IG + GB | HS1000 |
| Atlantis Resources Limited | UK | HATT | PMSG + GB | AR1500 |
| Marine Current Turbines | UK | HATT | IG + GB | SeaGen S |
| Nautricity | UK | HATT | PMSG-DD | CoRMaT |
| Nova Innovation | UK | HATT | IG + GB | Nova M100 |
| Schottel Group | Germany | HATT | IG + GB | SIT |
| Scotrenewables | UK | HATT | IG + GB | SR2000 |
| Tocardo Tidal Turbines | Netherlands | HATT | PMSG-DD | T200 |

Table 2 – Different manufacturers and turbine parameters. Adapted from Carmo (2019).

| Type of the turbine | Dimensions (m) | Nominal Power (kW) | Nominal Velocity (m/s) | Minimal Velocity (m/s) | Number of blades |
|---|----------------|--------------------|------------------------|------------------------|------------------|
| Axial turbines with horizontal axis (HATTs) | | | | | |
| SeaGen | 18 | 1200 | 2,4 | 0,7 | 2 |
| Verdant Power | 5 | 35 | 2,2 | 0,7 | 3 |
| Tidal Stream | 20 | 1000-2000 | - | 1,0 | 2 |
| TidEl System | 18,5 | 2x500 | 2,3 | 0,7 | 2 |
| Hammerfest Strom | 20 | - | 2,5 | - | 3 |
| Tidal Stream Turbine | 18 | 1000 | 3,5 | 2,5 | 3 |
| Open Hudro | 15 | 1520 | 2,6 | 0,7 | multi |
| Amazon Aqua.Charger | 18 | 0,5 | 1,5 | 0,5 | 3 |
| Turbines with vertical axis | | | | | |
| EnCurrent Hydro Turbine | 1,6x0,8 | 12,5 | 4 | 2 | multi |
| Davis Hydro Turbine | 6,1 | 250 | 3 | 1,5 | 4 |
| Exim Tidal Turbine | 1x3 | 44 | 3 | 0,7 | 2 |
| Ponte di Archimede | 6x5 | 25 | 2 | - | 3 |
| Helicoidal turbines | | | | | |
| GCK Gorlov | 1x2,5 | 180 | 7,72 | 0,5 | multi |
| Lucid Energy Technologies | 1; 2; 3 | 40-150-360 | 4,5 | 0,5 | multi |
| Turbines built within pipes | | | | | |
| Underwater Electric Kite | 4 | 400 | 3 | 1,54 | multi |
| Rotech Tidal Turbine | 25 | 2000 | 3,1 | 1 | multi |
| Clean Current Turbine | 18 | 1700-5000 | 3,5 | 1 | multi |
| EnCurrent Hydro Turbine | 3x1 | 18 | 2,8 | 2 | multi |
| Clean Current Power System | 1,7; 2,9; 4 | 16;44;84 | 3 | 1,5 | 3 |

3.4 Calculation of turbine power through actuator disc models

In order to create a proper model to evaluate power output, it is necessary to predict and formulate how much energy each turbine can generate. Betz was one of the first authors to use analytical methods to determine limit values for energy extraction from a flow. The method developed by this author in the 1920s, known as one-dimensional linear momentum actuator disc theory (LMADT), is based on a model that assumes an infinite volume of air flowing around the rotor, which is often a suitable approximation to actual conditions in wind turbine applications (Burton et al., 2001). Although the mechanical behaviour of water is similar to that of air, airflow in the aforementioned applications is unrestricted, due to the low density of air, which circulates freely around the turbine (i.e. without restrictions or physical barriers). However, the behaviour of a tidal flow within a confined channel is necessarily different, not only due to the much greater density of water but also to the flow restrictions imposed by physical boundaries (Leclercq, 2011).

Therefore an improved theory that takes into account the channel restrictions is required to model the flow around an underwater stream turbine. In the next section we will present an improvement on the classical LMADT applicable to shallow channels.

3.4.1 Analytical modelling based on Betz's actuator disc model

Betz used basic assumptions to demonstrate that there is a maximum limit to energy extracted from the flow. Betz's model assumes that the fluid is homogenous, incompressible and in steady regime. Friction is not considered. Flow and forces under the rotor disc area are assumed to be uniform. Flow is supposedly unidimensional, which means that no trail behind the disc is considered. Moreover, calculations are based on an ideal actuator disc, i.e. the number of rotor blades is assumed as infinite meaning that the same homogeneous load is applied in the entire area of the rotor. Betz showed that if the rotor acts to extract more energy from flow available in the rotor area the bypass flow around the turbine will increase. Hence, there is a theoretical limit to the maximum energy a rotor can extract due to its effect on the incoming flow. In theory, a rotor can extract up to 59% of the available kinetic energy in the incoming flow, as will be demonstrated below. In practice the conversion rates of the most efficient turbines are around 40-50% (Bahaj, 2011).

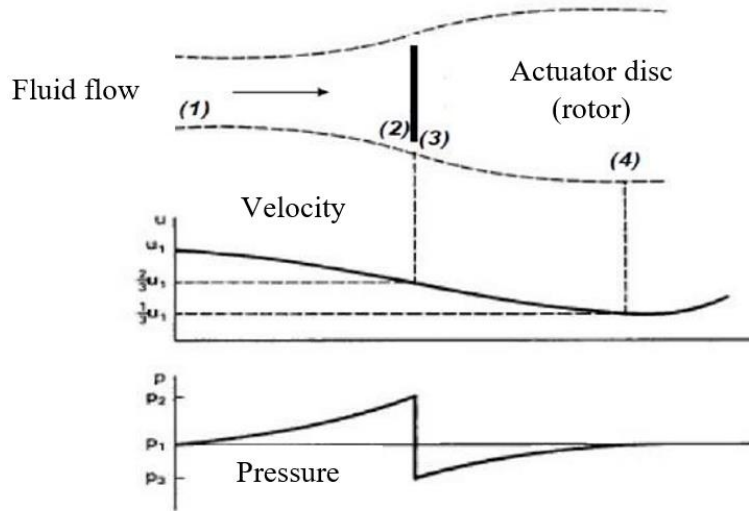


Figure 8 - Energy conversion device representation. Adapted from Leclercq (2012)

Different stations in the flow path through a rotor are shown in figure 8. The first point (1) is located upstream of the rotor, whereas the last point (4) is located far downstream. The remaining two points are located in the immediate vicinity of the rotor: point (2) is located right before and point (3) is located immediately after the rotor. It is assumed that the distance between points (2) and (3) is infinitesimal. Speed and pressure on the rotor are represented at the bottom. Flow speed gradually decreases in front of and behind the rotor, while a pressure difference exists across the rotor. As points (2) and (3) are very close, flow speed across the conversion device remains unchanged, i.e. $v_1 = v_2$. Since points (1) and (4) are located far from the rotor, pressure at these points is equal to the static pressure of the undisturbed fluid $p_1 = p_2 = p_{atmosphere}$ (Leclercq, 2011).

Considering the force applied by the fluid on the conversion device and conservation of linear momentum, thrust on the rotor (T) is given by:

$$T = A (p_2 - p_3) = \dot{m}(v_1 - v_4) \quad (5)$$

Since the mass flow is given by $\dot{m} = \rho A v_2$, equation 5 can be written as:

$$\rho v_2 (v_1 - v_4) = (p_2 - p_3) \quad (6)$$

Combining the equations above, the velocity through the rotor can be expressed as a function of the far flow speeds and the power P extracted by the turbine is given by:

$$P = T v_2 = \frac{1}{2} \rho A (v_1^2 - v_4^2) \frac{1}{2} (v_1 + v_4) \quad (7)$$

As $P_0 = \frac{1}{2} \rho A v_1^3$ is the total available power of the flow, we have that the maximum energy extracted from the device is the maximum point of this equation, yielding:

$$P = 16 / 27 P_0 \quad (8)$$

Where P is the power extracted by the turbine, which represents approximately 59% of total power. This is the maximum theoretical limit calculated by Betz for a horizontal-axis turbine. Details on this theory are widely found in the literature.

The model proposed by Betz is based on a few approximations, which may elicit criticism. As mentioned in the beginning of this section, only the axial component of velocity was considered, while the radial and tangential components were ignored. Moreover, the wake generated eventually disappears downstream of the turbine, as the turbulent flow mixes with the water that bypasses the device, after point 4. The infinite boundary condition means that pressure and speed are equal upstream and downstream of the turbine, which would mean that no energy is extracted. However, this assumption is incorrect, as the integral of an infinitesimal variation over an infinite area is a finite loss of energy. Moreover, the energy lost in restoring flow uniformity is also ignored.

Therefore, an improved theory that considers the restrictions of a confined flow in a blocked shallow channel is required to model the performance of underwater turbines in close proximity.

3.4.2 Actuator disc model based on a finite flow and constant pressure

Further details need to be inserted into Betz's model in order to increase similarity to real-world application. The energy lost as water that flows through the actuator disc can be calculated for a scenario where the equipment is exposed to a finite flow and pressure is restricted. In this scenario, it is assumed that the fluid flows within a confined area and that pressure is constant outside the dotted line (Figure 9), i.e. where the fluid bypasses the turbine. However, these conditions do not necessarily apply to practical applications.

The difference between this model and that described in section 3.4.1 is that point 5, which is sufficiently far downstream for flow to have become completely uniform and homogeneous, is now considered. The analysis is similar to that performed previously; the constant pressure condition entails that speed values at point 1 are equal in the turbine and bypass areas, i.e. Bernoulli's equations used for the areas between points 1 and 2, and 3 and 4, as well as the balance equation across the turbine, remain unchanged. This analysis has been performed by a research group and the results were presented in a University of Oxford internal report (Houlsby et al., 2008).

In the before-mentioned study, the author concluded that flow under these conditions is a function of a single parameter, α_4 , a dimensionless factor that relates inflow speed to outflow speed at point 4. The author also affirms that the trail transition area can be considered in the analysis conducted for a finite area. The value calculated using the momentum equation between points 4 and 5 (as no liquid force exists in this area) is:

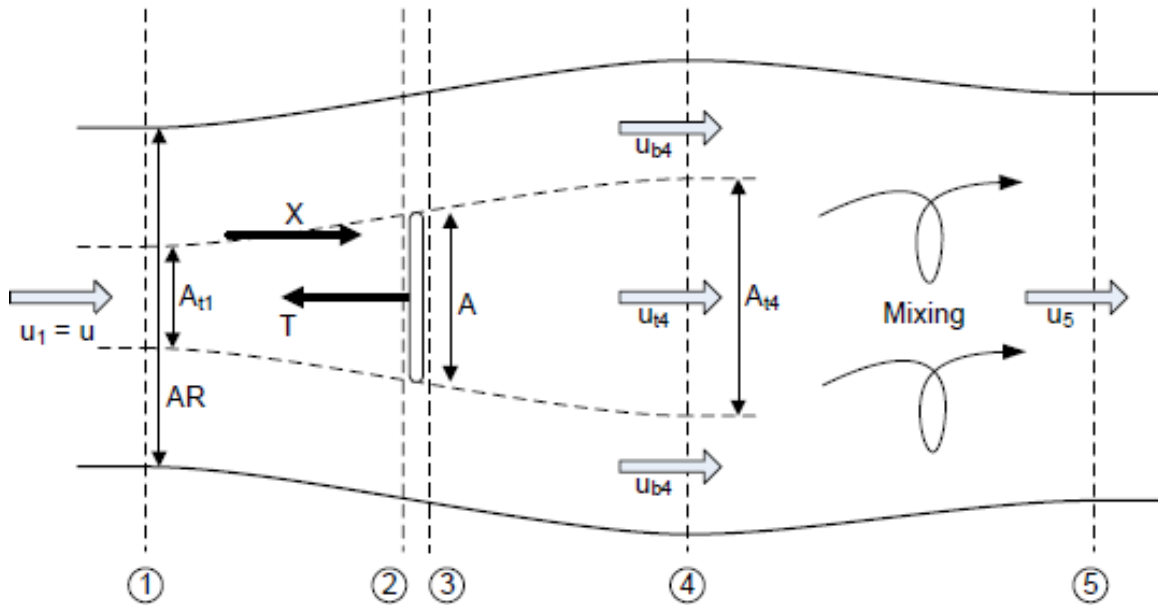


Figure 9 - Illustration of the analytical model of actuating discs in the channel, with constant pressure. Reproduced from Housby (2008)

Table 3 - Continuity relationships for flow shown in figure 9. Reproduced from Housby (2008)

| Region | | Station 1 | Station 2 | Station 3 | Station 4 | Station 5 |
|---------|-----------------|-----------------------------------|--------------------------------|-----------|---|-------------|
| Turbine | Area | $A_{1t} = A\alpha_2$ | $A_{2t} = A_{3t} = A$ | | $A_{4t} = A \frac{\alpha_2}{\alpha_4}$ | |
| | Velocity | $u_{1t} = u$ | $u_{2t} = u_{3t} = u\alpha_2$ | | $u_{4t} = u\alpha_4$ | |
| | Volumetric Flow | $q_{1t} = q_t = uA\alpha_2$ | $q_{2t} = q_{3t} = uA\alpha_2$ | | $q_{4t} = uA\alpha_2$ | |
| | Pressure | $p_{1t} = p$ | p_{2t} | p_{3t} | $p_{4t} = p$ | |
| By-pass | Area | $A_{1b} = A(R - \alpha_2)$ | | | $A_{4b} = A(R - \alpha_2)$ | |
| | Velocity | $u_{1b} = u$ | | | $u_{4b} = u$ | |
| | Volumetric Flow | $q_{1b} = q_b = uA(R - \alpha_2)$ | | | $q_{4b} = uA(R - \alpha_2)$ | |
| | Pressure | $p_{1b} = p$ | | | $p_{4b} = p$ | |
| Total | Area | $A_1 = AR$ | | | $A_4 = A \left(R - \alpha_2 + \frac{\alpha_2}{\alpha_4} \right)$ | A_5 |
| | Velocity | $u_1 = u$ | Varies | | Varies | u_5 |
| | Volumetric Flow | $q_1 = q = uAR$ | | | $q_4 = uAR$ | $q_5 = uAR$ |
| | Pressure | $p_1 = p$ | Varies | Varies | $p_4 = p$ | $p_5 = p$ |

Equation 7 can be derived from the equation used to calculate the quantity of motion between points 4 and 5, since no acting forces exist in this area:

$$uARu_5 = u^2 A \alpha_2 \alpha_4 + u^2 A (R - \alpha_2) \quad (9)$$

Power lost in restoring flow uniformity in the trail transition area, P_m , is given by:

$$P_m = P \frac{1-\alpha}{1+\alpha} \left(1 - \frac{\alpha_2}{R}\right) \quad (10)$$

Considering that P_m will not be converted into effective turbine work, the efficiency factor, i.e. the percentage of flow energy converted into work, can be calculated as $\eta = P/(P + P_m)$. The remaining energy is lost in restoring flow uniformity and fluid homogeneity at point 5. This second type of model will be utilized for the evaluation of power of the energy farm in the Business Case section.

However, for the development of practical tidal power generation systems making a meaningful contribution to the future energy supply, it is necessary to consider the efficiency of a number of turbines installed in a large tidal channel.

3.5 Physical modelling of turbines in a blocked channel

In order to further improve the physical model, it is necessary to consider the global effect of an array of turbines in a confined channel. The quasi-inviscid model of Garrett & Cummins (2007) suggests that the efficiency (limit of power extraction) increases as the channel blockage is increased by installing more and more turbines across the channel cross section. However, the efficiency is expected to decrease if too many turbines are installed as their hydrodynamic drag becomes significant compared to the drag along the (undisturbed) channel itself and hence the energy flux through the channel is reduced (Garrett & Cummins 2005).

Vennell (2010) combined the effects of the cross-sectional blockage and the channel choking effect in his tidal farm model, which explored the efficiency of a number of turbines homogeneously arrayed across the channel cross section and at several streamwise locations of

the channel. He assumed that the mass flux through the channel is constant in order to simplify the problem and thus focused on the combined effects of local and global blockages in an ideal tidal channel situation. It is noteworthy that, in a practical tidal channel situation, the above assumption may not fully hold as the hydrodynamic drag induced by the installation of the turbine array may become significant compared to the drag along the entire channel (Willden, 2014).

For such a case, a further extension of the model would be required to take into account the channel choking effect, perhaps in a similar way to the model of Vennell (2010) for homogeneously distributed turbines. It should also be noted that the model proposed in his work does not account for the effect of changes in water depth, which has been previously discussed, by Houlby et al. (2008); Whelan et al. (2009) and Draper et al. (2010).

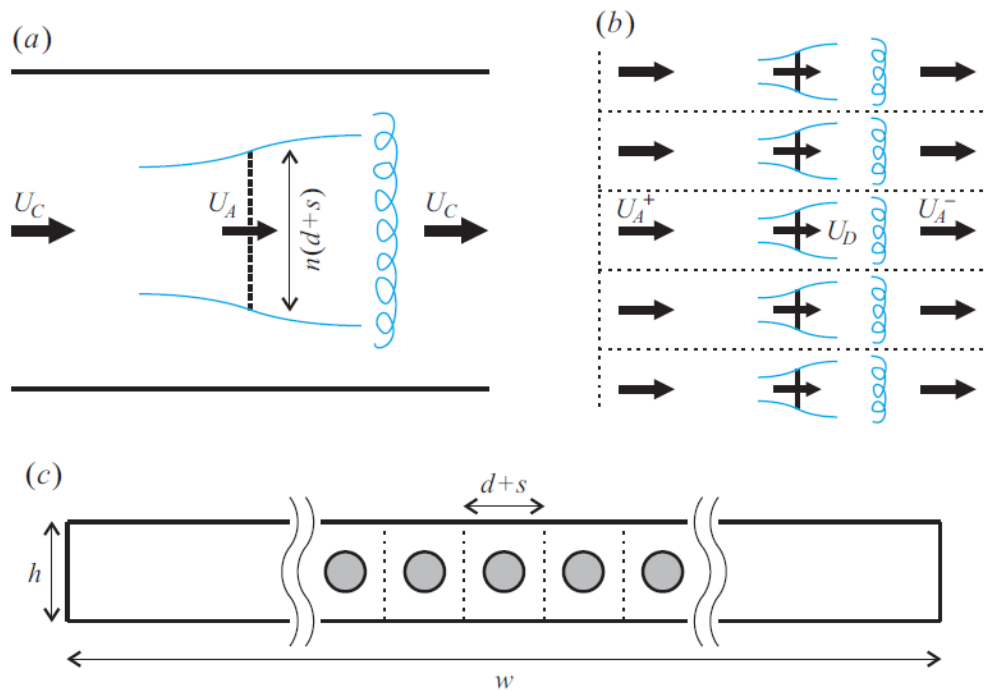


Figure 10. Schematic of the turbine array model: (a) array-scale - expansion and mixing, (b) device-scale flow expansion and mixing, and (c) cross-sectional view of the channel. Reproduced from Willden (2014)

Considering a large number N of turbine rotors of diameter d arrayed in a rectangular channel of uniform height h and width w (Figure 10). The intra-turbine spacing, s , is constant along the array; hence the spanwise length or width of the array is $n(d+s)$. As with the model of Garrett & Cummins (2007), the flow through the channel is assumed to be incompressible

and inviscid except for the far-wake region where mixing is allowed. The flow speed far upstream of the array is uniform and identical to the channel cross-sectional average of the streamwise velocity, U_C , which is fixed in Willden's model.

For the array-scale problem, the flow through the channel is assumed to be two-dimensional (as the channel height h is significantly smaller than its width w) and the array is considered as a single power-extracting fence of height h and width $n(d+s)$, blocking the channel cross section entirely in the vertical direction but only partially in the spanwise direction. Here the array blockage, B_A , can be defined as:

$$B_A = \frac{\text{(representative) array area}}{\text{channel cross-sectional area}} = \frac{h n(d+s)}{h w} \quad (11)$$

The local blockage B_L can be defined as:

$$B_L = \frac{\text{(single device area)}}{\text{local passage cross-sectional area}} = \frac{h n(d+s)}{h w} \quad (12)$$

The global blockage B_G can be defined as:

$$B_G = \frac{\text{(total device area)}}{\text{local passage cross-sectional area}} = \frac{h \frac{\pi d^2}{4}}{h w} \quad (13)$$

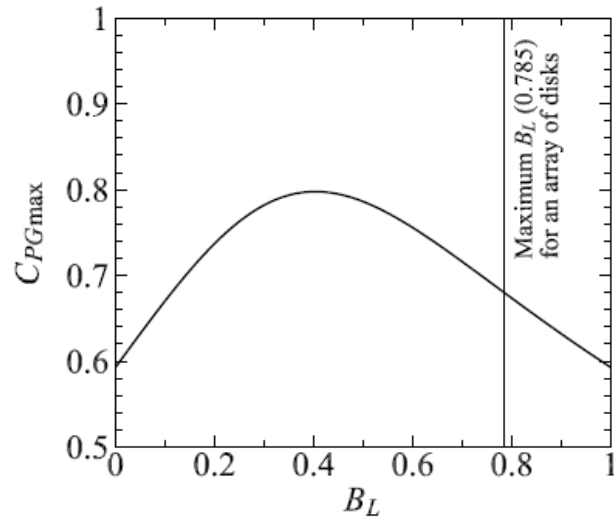


Figure 11: Effects of B_L on C_{PGmax} for given $w/nd \rightarrow \infty$. Reproduced from Willden (2012)

Willden (2012) showed that as the local blockage B_L is increased, the basin efficiency (to achieve C_{PGmax} for a given B_L) slightly decreases from $2/3$ for the *Lanchester-Betz* case (at $B_L = 0$) to 0.55 (at $B_L \cong 0,33$) and then it recovers as B_L is further increased. It should be noted, however, that this decrease in basin efficiency is the outcome of maximizing C_{PG} .

Therefore, it is possible to operate tidal turbines at a more sensible condition such that C_{PG} is slightly lower than C_{PGmax} so as to maintain a higher basin efficiency.

In the economic section that will follow a variable C_P depending on the blockage effect for an unique fence will employ Willden's approach. The greater the number of turbines, the greater will be the C_P until a certain point, upon which placing a greater number of turbines will decrease C_P accordingly.

4 REVIEW OF ECONOMIC METRICS FOR EVALUATING ARRAY DESIGNS

In the following section a review for the different economic metrics will be presented in order to evaluate the physical outputs of the turbines from a finance perspective. There is a great number of metrics that can be used to evaluate the performance of tidal energy arrays, presenting an analysis that does not take only into consideration array designs with too many turbines, but also the financial aspect of the venture. These metrics are a very important proxy as a decision-making tool for financial institutions and energy companies that decide to invest in specific energy ventures.

Financial institutions can provide capital at a lower cost for energy companies, and they find the returns from energy projects more attractive than those from traditional alternatives, such as government bonds. Building capabilities, infrastructure, and governance to support their activities in the energy industry, as well as developing the analytic skills and insight to identify opportunities as they emerge is very important, therefore a more detailed analysis into the decision-making metrics for evaluation a project in a finance perspective will be presented in this section.

4.1 Power

Many authors (Funke, 2014; Feu, 2017; Divett, 2013) proposed methods to optimise array design for power alone, such that the profit is a direct function of average power of the turbine. This can be an effective method of determining a suitable layout, especially if the size of the array is already specified, such as in Funke (2014) and Divett (2013).

In such cases the costs of implementation are relatively fixed, except for the costs that depend on the individual turbine locations, such as the cabling or distance and depth related installation costs (to be discussed in greater detail in the Methodology section). However, in general, maximization of average power of the turbine is a reasonable proxy for increasing the economic performance (Culley, 2016).

Problems in using the power alone as a functional arise when the number of turbines is also allowed to vary and becomes a free parameter within the array design optimization. Culley (2016) has shown that, when optimising power alone, the optimal design will feature an

impractically high number of turbines, where the overall power generation is at its maximum, but the capacity factor of the array, and therefore its profitability, is relatively low, also in accordance with Willden (2012).

The optimisation algorithms will keep adding turbines, which slow the flow velocity through the site, until a point is reached where the blockage is so high that adding any more turbines will decrease the overall power generation (Culley, 2016). However, the extracted power per additional turbine will diminish long before the threshold where the overall power decreases. Given the high cost of installing devices the optimal economic performance will be achieved at a far lower number of turbines than the optimal power.

Another problem of this approach regards the total cost of implementation. Private equity funds will prefer to acquire ventures for which the initial investment is reduced, if compared to a higher internal interest rate (IRR) project, which has a greater initial cash flow investment. Therefore, considering a reduced number of turbines instead of simply increasing the number of purchased turbines is also very important.

4.2 Break-even calculations

As already mentioned, adding additional turbines to an array may increase the overall power, but there comes a point where there are diminishing returns for each extra turbine installed, for example due to global blockage effects as well as the array being forced to expand into lower flow speed areas (Culley, 2016).

From a financial perspective it may be more advantageous to have a smaller array in which the average power per device is higher, because underwater turbines are relatively costly to manufacture and install. Goss (2018) showed that a break even power, P_{BE} , is included in the optimization functional to account for this problem and ensure that turbines are only added if they can generate enough power to cover their installation costs. Varying this parameter changes the trade-off priorities between the objectives of maximizing power generation and minimizing costs.

The break-even power is the average power over all turbines that needs to be generated so that the array can break even over its lifetime. A method for choosing a suitable break even power can be found by first using a simplified model for the expected cash flow J , such that:

$$J = Revenue - Cost = \sum_{i=0}^L (P_{avg} \times t_i \times T_E) - \sum_{i=0}^L (E_{Xi}) \quad (17)$$

where i is the year the costs are being evaluated, L is the lifetime of the array in years, P_{avg} is the average power generated by the whole array in MW, t_i is the number of hours of generation in year i , T_E is the electricity tariff, i.e. the price per MWh the electricity generated is sold at, and E_{Xi} is the sum of all array expenditure incurred in year i . If P_{avg} is assumed to be independent of the year it is possible to use this to find a critical average power per device that must be generated by the whole array to break even (Goss, 2012).

Therefore, for the array to generate a profit the average total power generated by the array must be more than the break-even power times the total number of devices. If an appropriate break-even power is chosen to reflect all of the costs, this choice of metric can effectively maximize the profit. It penalizes the addition of turbines which do not generate sufficient power to offset their costs, or which, due to hydrodynamic interactions, lead to reductions in the yield of other turbines.

When the costs are assumed to increase linearly with the number of turbines, the break even power is independent of the number of turbines and therefore can be used as a constant value (Goss, 2019). In practice that relationship will not reflect the true expenditure and the break even power will likely decrease as the number of turbines increases due to savings of volume. There are various ways this impact can be modelled, the simplest of which is to linearly decrease the break even power with the number of turbines.

Figure 12 shows that if the annual expenditure increases linearly with the number of turbines the break even power is fixed, however, if the expenditure declines quadratically with the number of turbines the break even power declines linearly with the number of turbines. Both rely on assumed relationships between the costs and number of turbines but are useful for initial investigations into how bringing costs and economies of volume into the functional affect the optimal array design (Goss, 2019).

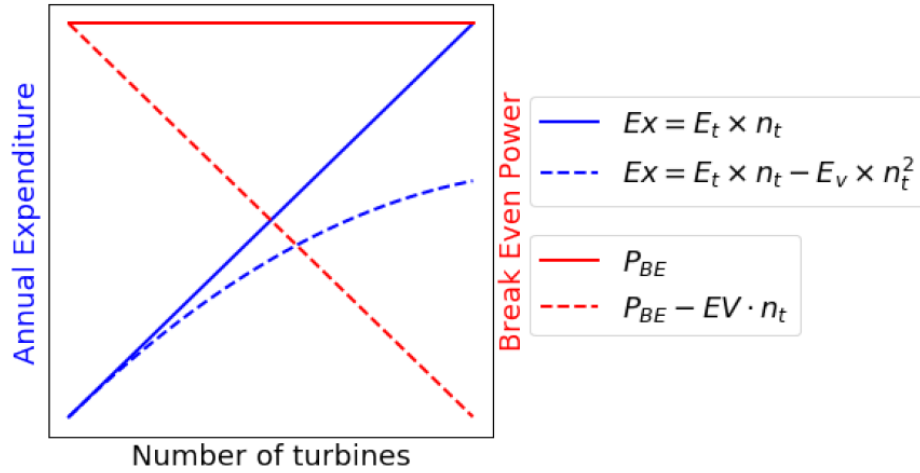


Figure 12: A demonstration of how the relationship between expenditure per year and number of turbines in an array corresponds to a fixed or linearly decreasing break even power. Reproduced from Goss (2019)

4.2 Net Present Value

The break-even equation describes the sum of all cash flow across an array lifetime, however in practice this value is rarely used by investors. Long term investments, such as tidal arrays, rely on discounted cash flow (DCF) analysis to quantify the idea that money today is worth more than money tomorrow to investors. Current funds have the ability to earn interest and increase in value in the future, so investors need to find a way to adjust future cash flow to enable the comparison between costs and revenue in different periods of time, in terms of their present day value. The Net Present Value (NPV) is a measure used to evaluate the profit of a project by summing all incoming and outgoing cash flows per year, i.e. the revenues minus the costs from each year, adjusted according to the time value of money by a discount rate, r , such that (Goss, 2019):

$$NPV = \sum_{i=0}^L (Revenue_i - Cost_i) / (1 + r)^i = \sum_{i=0}^L (P_{avg} x t_i x T_e - Ex_i) / (1 + r)^i \quad (18)$$

Using the NPV as the economic metric for tidal array optimization has many advantages. Unlike the previous metrics it takes into account the depreciating time value of money, which is important to investors. It allows for far greater flexibility in the financial modelling than the previous metrics (Goss, 2017). For example, instead of basing the analysis on a time-averaged power generation (P_{avg}) it can be replaced by a time-varying metric. This can be used to model

the impact that the power variation due to the cycles has on the economic performance of the array. It could also be used to include the effects of the anticipated degradation of the turbine performance, for example due to biofouling and algae build up and increase in required downtime due to a higher occurrence of faults with age, as commonly observed in the wind industry. However, using an average power generation is very useful while there is still a lot of uncertainty about the planned installation year and fault rates decades into the future.

A disadvantage of using NPV is that it is hard to compare between projects of different sizes. A smaller tidal array may have a far higher profit margin but a much lower NPV than a large tidal array. It is hard to interpret directly from the NPV how successful a project is, however investors use frequently NPV to decide in which project they will invest.

4.3 Net Present Value and Internal Interest Rate

There are several different economic metrics which can be derived when applying break even analysis to the Net Present Value method. Eq. 10 can be set to zero in order to obtain a value for the so-called break even point of an energy project. Then the resulting equation can be solved for each of the input variables, to determine the parameter value that would need to be achieved for the project to break exactly even over its lifetime. Each of these parameters at break even can be seen as the minimum requirement, and any improvement on these will result in a positive NPV and the project will generate a profit.

The most common metrics are derived by solving for the strike price, to obtain the levelized cost of energy (LCOE), solving for the lifetime, to obtain the payback period (PP), and solving for the discount rate, to obtain the internal rate of return (IRR).

All present value based calculations require summing all the cash flow over a lifetime and discounting them according to the time at which they occurred. The net present value calculation given in Eq. 10 is set so that the discount rate is applied on a yearly basis. Instead, it is possible to apply the discounting on different time intervals, e.g. semiannually, quarterly or monthly, or to use a natural log based formula to apply discounted cash flow analysis continuously.

Using the discrete compounding method, the present value (*PV*) of a future cash flow (*FV*):

$$PV = \frac{FV}{\left(1 + \frac{r}{p}\right)^{pi}} \quad (19)$$

where p is the number of compounding period per year (for example, $p=1$ for annual compounding, or $p=4$ for quarterly compounding), i is the number of periods into the future that the future cash flow occurs, and r is the annual discount rate.

By comparison, the continuous compounding method has no period over which the compounding is applied and can instead be found from where in this case i is a continuous value for the number of years into the future that the cash flow occurs.

A review into the use of discrete and continuous discount rates by Lewis et al. (2014) base on finance and engineering economics journals, found that the split between discrete and continuous discounting of future cash flows was fairly even. More mathematical papers tended to use continuous discounting, whereas more applied papers used discrete discounting (Goss, 2017).

In practice many tidal array developers are not likely to have precise knowledge of exactly when costs will be incurred, especially not at the stage of designing an array. Therefore discrete modelling on an annual, or quarterly, basis is sufficient for this application. In addition, analysis will be conducted for 10-year period as well as 20-year period, even though most hedge funds would not accept a longer period than 6-7 years to start divesting.

4.4 Levelized cost of energy

The levelized cost of energy (LCOE) is a proxy for the average price of energy, Te (\$/MWh), that an array must receive to break even over its lifetime. It takes into account discounting and is calculated by finding the Net Present Value of the unit-cost of electricity over the lifetime of the array, by setting NPV expression to zero and rearranging to find:

$$LCOE = \frac{\text{discounted cost}}{\text{discounted energy}} = \frac{\sum_{i=0}^L \frac{Ex_i}{(1+r)^i}}{\sum_{i=0}^L \frac{Avg^x t_i}{(1+r)^i}} \quad (20)$$

LCOE is usually focused as the main metric for economic comparison between different energy sources, such as wind and solar. It is an effective benchmarking technique for the

comparison of multiple technologies and multiple array designs. LCOE and IRR are effectively simplifications of NPV, where an input variable can be removed by investigating the parameters required to break even. (Goss, 2019)

The price of energy Te can vary greatly depending on subsidies available to early stage renewable energies, so LCOE predictions often encapsulate less uncertainty than IRR, because an assumption of Te is not required (Goss, 2019).

The LCOE is the most commonly used approach for estimating the cost of energy over the lifetime of a project, for both tidal energy and other renewables. Since it is not as sensitive to array size as NPV or other metrics, it enables a simple comparison across a range of different projects.

4.5 Pay-back period

Another metric that can be derived from break even analysis of the Net Present Value formula is the Payback Period (PP), which is the lifetime array must operate for in order to break even. If the planned lifetime of the array is longer than the PP the array can be considered to be generating profit, if the lifetime of the array is shorted than the PP it will be making a loss.

The Payback Period can be found by calculating the NPV of every year from 0, until the NPV becomes positive. The critical year is the last year before the NPV becomes positive, i.e. the year before the project breaks even. A payback period can be calculated by estimating how far through the year the project breaks even.

Hedge-funds and assets tend to choose projects which have a shorter pay-back periods. For energy generation endeavors, PP is usually around 6 to 7 years.

4.6 CAPEX, OPEX and DECEX

The expenditures in each year, $E X_i$, can be split up according to whether they occur before or after the array goes into production. In the cash flow model described above, the CAPEX would typically be the sum of all expenditures over the life-cycle period of the array:

$$CAPEX = \sum_{i=0}^L E X_i \quad (21)$$

Businesses typically describe all costs involved acquiring assets and setting up the business as Capital Expenditure (or CAPEX). An estimate break-down has been presented by Vasquez et al. (2013) and, in their work, it was estimated that the capital costs for a tidal stream array as 41% device costs, 26% foundations costs, 15% installation costs, 13% cable costs and 5% grid connection costs. By comparison, the MeyGen1A project found that the main contributors to the CAPEX were turbines (39%), onshore balance of plant (19%), offshore works (13%) and substructures (11%).

In more complicated arrays the CAPEX may include the expenses associated with upgrading physical assets. For example in arrays which expand from small demonstrator arrays to larger scale farms, the installation costs are still considered to be CAPEX even if they are incurred after the first turbines start generating. Within the business case section it will be assumed that all the capital expenditures occur in year $i=0$ and that the array will start production in year $i=1$. This is an easy assumption to be removed when applied to real tidal arrays, by developers who have full cash flow models of their anticipated costs (Goss, 2019).

The expenses of normal business operations are called the operational expenditure (or OPEX). OPEX is measured on an annual basis, here starting from year $i=1$ up to $i = L$, the operational lifetime of the array. Figure 13 illustrates the complexity of the required operations.

Typically OPEX includes costs such as rent, payroll, insurance and maintenance. For a tidal farm this may include standard inspections, maintenance, repairs and costs of vessels and staff to perform these tasks. Goss, 2019 presented in his work a cost break-down for the implementation of the MeyGen 1A which reported a £1.4m OPEX per year in its four turbine array, with its main components being lease and insurance (32%), unplanned maintenance (21%), planned maintenance (15%) and spare parts (14%).

The final costs to be considered in a tidal energy deployment are the decommissioning costs (DECEX). These are the costs of removing the turbines, anchoring and cabling from the water and safely ending the operation. There are a number of different ways in which these costs may be covered, from upfront cash security to accrual or insurance (Goss, 2019).

DECEX could either be incurred through an agreement as part of the CAPEX, or will be delayed to after the final year of operation (Goss, 2019). After speaking with diverse companies that implement energy farms in Brazil they reported that they usually disregard the decommissioning costs, also due to a non-existent after-market for the deployed materials (turbines, ballasts, etc.). Since it is not clear how to include these costs in an academic model

at this time, they will be simply disregarded during the business case section. This is a senior line of research that must develop quickly for the deployment of real tidal farms in the country.

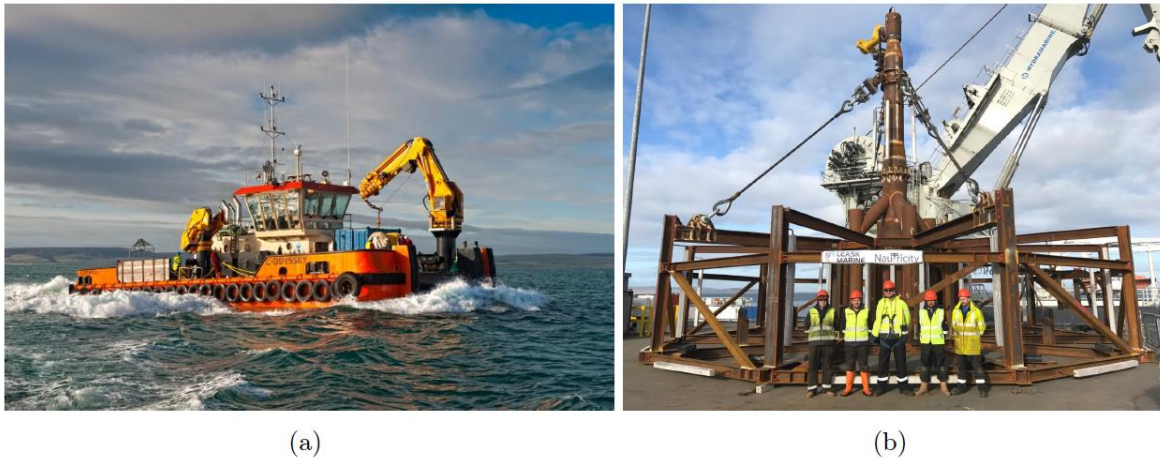


Figure 13: (a) The Leask Marine Ltd. MV C-Odyssey, an example of a multi-cat vessel used for installation and removal of turbines. (b) The Leask Marine Ltd. team after the successful removal of a Nautricity turbine’s base with a multi-cat vessel. Reproduced from Goss (2019)

An investigation into decommissioning costs by Marine Scotland (2018) found that many developers acknowledged that decommissioning had not been an explicit consideration on the design of devices, however a focus on reducing the cost of installation lead to designs which were inherently easier to remove. Technological advances which reduced the decommissioning cost included devices designed to be towed to (or from) location and devices that could be removed in modules for maintenance. Full decommissioning plans are not enforced by regulators at the marine licensing stage because the design may not be fixed. (Marine Scotland, 2018). Besides, the main cost driver is the cost of the vessels required to remove the infrastructure. Many tidal developers have designed devices to allow installation and removal with low cost multi-cat vessels (figure 13). In demonstration arrays material costs are low as many parts can be repurposed or stored. As arrays become larger the cost of dismantling and recycling the devices and foundations is likely to increase.

Marine Scotland (2018) estimated that floating tidal has a decommissioning cost of approximately USD 100,000 per device, with gravity-base foundations costing USD 200,000 per device and monopile foundations costing USD 500,000 per device. However, it is noted that these estimated could change substantially as design concepts and vessel rates change. Predicting these costs a couple of decades into the future leaves a lot of uncertainty for developers.

4.7 Alternative metrics to be considered

4.7.1 Environmental Costs

The metrics described before focus on the financial performance of a tidal array, however there are many other factors to be considered which the present work will not consider, only mention.

One of the most important, also related to the public perception, is minimizing the negative environmental and ecological impact of the arrays. There have been numerous studies on environmental impact assessment in tidal and other ocean energies (Falconer, 2012; Feu, 2019; Wilkinson, 2019). The most significant effects to account for are damage to habitat and health of marine species, and sediment transport. While the problem of assessing the environmental impact of a tidal stream array is well researched, there are limited studies on how to optimize array design whilst accounting for both the economics and the environmental impacts.

Feu (2017) uses the extent to which an array alters the flow in the region as a proxy for the environmental concerns and demonstrates a method of finding a Pareto front where there is a trade-off between the conflicting objectives of maximizing array yield while minimizing the change in the channel hydrodynamics.

This approach is useful for minimizing the negative impacts on marine ecosystems because alteration of the tidal flow can affect the dispersion of propagules (material used by marine organisms to propagate between areas, a key part of many marine life cycles), and there are habitats which are sensitive to flow speed, direction and level of turbidity, for example scallop nurseries (Eckman, 1989).

Eckman (1989) investigated the impact of different tidal arrays on two species, the acorn barnacle (*Balanus crenatus*) and the brown crab (*Cancer pagurus*), because the former prefers higher flows speeds and tends to react negatively to reductions in bed shear stress and the latter prefers lower flow speeds and reacts positively to reductions in bed shear stress. The relative importance of habitat suitability compared to profit is modelled by the choice of weights of each corresponding term in the function. While his paper demonstrated a useful method for incorporating the concerns of habitat suitability, each example site was only demonstrated for one species at a time, either the corn barnacle or the brown crab, and more work needs to be carried out to automate the combination of economics and environmental impact.

Nelson (2017) compared the energy extraction of small-scale array designs that considered

environmental constraints compared to those that do not. It was found that taking into account environmental constraints slightly decreased the overall power generation of the optimized array design slightly.

The present work does not include environmental impact in the economic analysis. As demonstrated by the studies discussed above, minimizing the environmental impact often leads to a trade-off where the array yield, and therefore profitability, are reduced. Nevertheless, environmental impact is an important aspect that cannot be neglected.

4.7.2 Location Based Costs

As already mentioned, expenditure is assumed to be a function of the number of turbines, but in practice it also depends on the turbine location. Depth and distance to shore are two topology factors that are most significant to tidal energy cost-breakdown that vary with location (Vasquez, 2016) and both have been demonstrated to be main cost drivers in offshore wind (Ederer, 2015). As depth and distance increase the installation and maintenance of the turbines become harder to carry out, and the costs increase proportionally. They also affect the environmental loads to which the turbines are exposed, the cable costs and electricity losses.

There have been some studies which optimize the design of tidal arrays based on the location dependent costs. On a macro-level Vazquez et al. (2016) assessed the spatial distribution of capital costs, coupled with a Navier-Stokes flow solver, to balance the capital investment against the energy productions and found a map of the levelized capital cost of energy. This is used as a decision parameter to identify the best sites to install tidal stream arrays. This can be done as a precursor to the array optimization methods where the number of turbines and their individual locations are optimized.

Studies in which the micro siting of tidal stream arrays is optimized with respect to location-based costs include Sullivan (2013) and Culley (2016). Both authors focused on optimization of a given number of turbines and their studies include a model for cable costs per meter and support structure costs that depend on the nature of the seabed, the depth and the peak moment resistance required. Both used genetic algorithms to minimize the cable length.

Optimization accounting for location-based costs can be computationally expensive, and usually comes at the sacrifice of other modelling capabilities (Goss, 2019). Sullivan (2013) used a genetic algorithm to optimize turbine location while taking into account variations in cable

and support structure costs, but only within the framework of a relatively simple 2D wake deficit based model, and only for uniform flow in one direction. Optimization of the cable routes can produce savings that are significant, but are a lower priority compared to optimizing the balance between power and number of turbines. As already mentioned, the turbine costs represent the most significant share of the CAPEX break down. For this reason, location varying costs will also not be included in this work.

Currently there is few publicly available information to build a model that can predict the costs as a function of different distances to shore, depths and number of turbines. Furthermore the sites selected for first-generation tidal turbine arrays are usually at a relatively short distance to shore and require depths of 25–50 m (Iyer, 2013). It is anticipated that later generations of tidal stream will be designed for operation in deeper water, where modelling of location-varying costs will become more crucial (Iyer, 2013).

4.7.3 Volume Savings

Costs can be reduced if they are spread across more turbines in an array – if the installed capacity in MW for a potential tidal site is increased, the effective cost per MW decreases – basically it is necessary to predict and plan for an optimal usage of resources. For example, the cost of mobilizing (preparing the vessel) and demobilizing (unloading and returning of the vessel) for offshore operations, installations, and maintenance falls per turbine as the number of turbines increases. For small arrays these activities take up a significant proportion of the total vessel time. (Coles, 2019). Coles also demonstrated that in MeyGen 1C the anticipated number of mobilization and demobilization days per turbine falls from 1.13 to 0.83 if the number of turbines increases from the current 4 to a planned 36, representing a significant cost reduction.

For the above-mentioned reason, the volume savings are very important for tidal endeavors. There are fixed costs in tidal array development, such as the site evaluation and substation costs, which lead to a reduced cost per MW when they are split across a greater number of turbines.

Potential cost reductions due to volume savings can also include bulk order discounts, reduced production costs per unit and savings due to serial production and standardization of common components. For example, dedicated manufacturing facilities for large-scale turbine

orders will be more cost-effective, but this is not possible for smaller arrays. Also, inter-array cable costs may increase approximately linearly with the number of turbines but the costs of a substation and the much more expensive export cables to shore will be roughly fixed, so the more turbines generating power, the lower the total cable cost per MW. (Goss, 2019)

Current tidal stream endeavors in the UK have only been implemented in arrays with small numbers of turbines; for example, the world's first arrays had three turbines (Nova Innovation) off the coast of the Shetland Islands and four turbines installed by MeyGen in the Inner Sound of the Pentland Firth. Even without cost reductions due to experience or improved technology, substantial cost reductions could be seen in the immediate term, just by moving from these demonstrator sized arrays to commercially sized ones. (Goss, 2019).

It is worth noting that while costs are expected to fall with time and volume, there are more significant cost reductions to be made while tidal energy is a relatively new industry. The cost reductions as the tidal industry advances from small demonstrator arrays to the first large-scale commercial arrays will be significant, but as the industry develops the potential to reduce costs will diminish (Goss, 2019). Some aspects of tidal arrays are already well-established, building on what can be learnt from other offshore energies. For example, electrical connection to the grid (which makes up around 5% of the lifetime costs of tidal arrays) has less potential for dramatic cost reduction due to developments already being carried out by the offshore wind industry, so the learning reductions have to some extent plateaued.

However, there is still potential for significant volume savings to be achieved on these costs through subsea hubs which will allow the electrical connection of multiple devices resulting in cheaper configurations.

4.7.4 Scale Savings

Scale savings refer to the cost reductions gained from moving to larger rotor, higher power turbines (i.e. increased scale of the turbines themselves) and not to the effects of increasing the number of turbines).

Coles et al. (2016) demonstrated the significant impact that turbine scale could have regarding the overall budget of the project, by investigating the predicted yield of the 1.5MW rated AR1500 device compared to the 2MW rated AR2000. The AR1500 is currently operational as part of the MeyGen Phase 1A, the AR2000 is the next generation device by

SIMEC Atlantis Energy, which is expected to be deployed in future phases of the MeyGen project. Both devices are capable of accommodating a range of physical options, but Coles et al. (2016) assessed an 18 m diameter AR1500 with a hub height of 14 m to a 20 m diameter AR2000 with a hub height of 15m. Coles estimated that properly scaling turbine could lead to a reduction in LCOE of 17%, 20% or 23% due to the 29% uplift in anticipated yield when progressing from the AR1500 to the AR2000, depending on whether the CAPEX increases by 10%, 5% or 0% between the two devices. It is difficult to predict how much CAPEX will increase between the turbine designs, because the costs are commercially sensitive and not much information is present on the literature.

Turbine cost is likely to increase due to higher loading from larger blades, increased generator size and hub height, but the AR1500 for instance was designed to meet conservatively high loads, and through the proof of concept in MeyGen 1A, the AR2000 may not require as conservative a design. Therefore, for different CAPEX scenarios simulation, small achievable changes to the turbine specification can result in significant near-term reductions to the LCOE of tidal energy (Goss, 2019).

Foundation costs also make up a significant proportion of the lifetime costs of an array, so some developers plan to use several rotors on the same supports to spread the foundation costs over a higher rated power, and achieve scale savings.

4.7.5 Energy generation

In order to build a complete financial model, income must be accurately predicted, as well as expenditure. For a tidal farm, income depends primarily on two factors: the net energy output and the tariff at which this energy is sold to the grid (which may well be higher than the market price due to subsidies and other government schemes or vary greatly throughout year seasons).

Since early-stage tidal energy deployments often receive a fixed price per MWh, through subsidy, most hydrodynamic models used for optimization of tidal array design produce an average power estimate for the array, P_{avg} , rather than a time varying prediction of the instantaneous power over the whole lifetime. Therefore, the energy generated in each year E_i is assumed to be constant, such that:

$$E_i = t_i \cdot P_{avg} \quad (22)$$

where t_i can be approximated as the number of hours in a year minus the anticipated number of hours of downtime for maintenance.

For instance, the MeyGen Phase 1A reported an average availability of 95% in 2020 (having entered its operational phase in 2018), with a higher availability of 98% in the summer compared to 90% in the winter. Increased experience in planning and predicting operations and maintenance could see these downtime windows decrease and availability increase in future tidal projects. When used in industry the availability could be modelled to depreciate throughout an array's lifetime, to account for decreases in efficiency as devices age, e.g. due to component wear or bio-fouling. This effect has been well documented in the wind industry. However, for simplicity it can be kept constant for initial investigations (Goss, 2019). This is a reasonable assumption because there is limited information on the rate of degradation of tidal stream arrays, with few years of operational experience to date. Also, due to the high discount rate currently used in tidal the latter years of the array's generation (where degradation would be highest) contribute significantly less to the NPV and LCOE. Finally, the net energy output can be found from the gross energy output by a factor to account for electrical efficiency losses.

In practice, even when evaluating metrics such as NPV and LCOE on an annual level, lunar nodal cycles cause variations in the yearly average yield. Since the earlier years of generation count more towards these metrics, due to discounted cash flow, this could lead to an effective difference in the performance of the array depending on which stage of the tidal cycle it begins generating in.

In preliminary economic models it can be assumed that arrays receive a constant price per unit energy, however more accurate models could estimate P_{avg} over smaller time scales and use this in conjunction with a fluctuating energy price to determine the impact on revenue. More information regarding this topic will be presented below.

4.7.6 Revenue inputs

In financial models the income must be estimated to properly analyse the cost/benefit balance of different array designs. Assuming that the main source of income for an array operator is from selling the energy generated, then the revenue, in year i , can be approximated by:

$$Revenue = P_{avg} \cdot t_i \cdot T_e \quad (23)$$

where P_{avg} is the average power generated, predicted using a hydrodynamic model of the array, and either used as an average over the whole lifetime of the array, or calculated over smaller time scales, for example to take into account variation due to the lunar cycle. t_i is the number of hours of generation each year, which can be multiplied by the average power, to find the gross energy output in MWh. Below, in the end of this chapter, we present an explanation on factors that affect the ratio of operational hours to hours downtime. T_e is the electricity tariff, i.e. the price per MWh the electricity generated is sold at. This price is greatly dependent on the subsidies and other schemes available to developers, and the schemes available worldwide are briefly discussed later in this work. Besides, the market price may fluctuate over days and years, however government schemes can often make this value more predictable and stable.

4.7.7 Relationship between cost and size of array

Firstly, information on how CAPEX and OPEX in the wind industry varies in relation to the number of turbines is used to justify the relationship assumed in equations of CAPEX and OPEX having a fixed cost and variable cost depending on the number of turbines.

Wind energy is a more established industry and can therefore be used to help predict the cost reductions that can be achieved through volume savings for tidal energy. CAPEX and OPEX values are commercially sensitive and hard to establish, and while there have been several studies which have communicated with many different developers of varying sizes (Smart, 2018), they often anonymize this data by converting to a metric that is independent of array size, such as cost per MW installed capacity.

Much of the available information found in this literature review on the costs of tidal turbine arrays is given as a CAPEX/MW for an array of a certain rated capacity. Figure 14 extracted from Goss (2019) showed how the total CAPEX increases with the number of turbines if a linear relationship between them is assumed.

This can be used to show the relationship between CAPEX/MW and number of turbines, by dividing the total capacity of the array (n_t turbines, each with a rated capacity of MW_t) to get:

$$CAPEX/MW = \frac{CA_f + CA_t \cdot n_t}{n_t \cdot MW_t} \quad (24)$$

where CA_f represents the fixed costs for CAPEX, CA_t represents the costs that are turbine dependent. Figure 14 illustrates the behavior of variation taking into consideration different number of turbines.

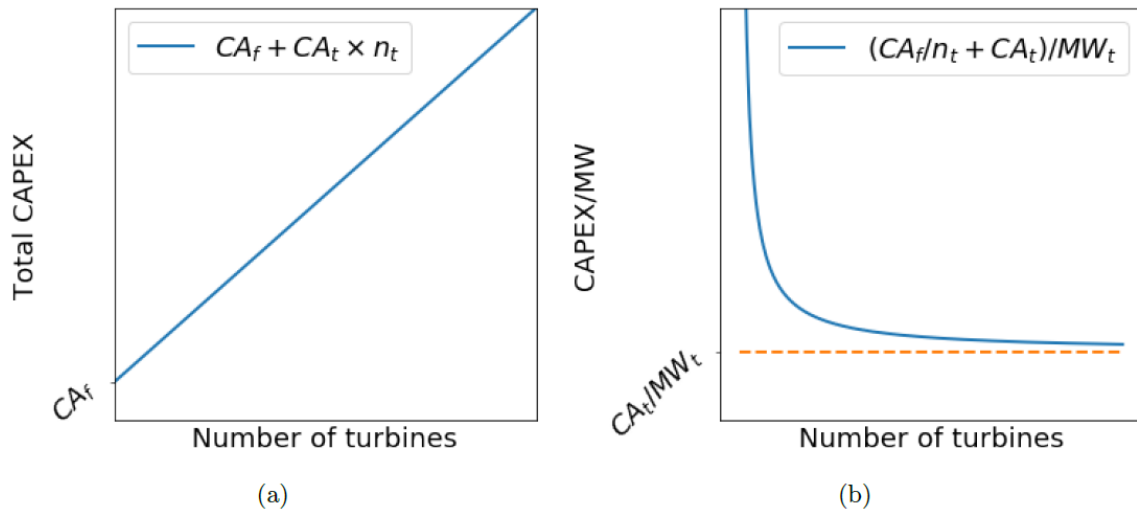


Figure 14: Variation in the total CAPEX of an array and the CAPEX per MW installed capacity as functions of the number of turbines. Reproduced from Goss (2019)

4.7.8 Discount rate

The discount rate, r , is a key parameter when evaluating the economic success of a project over its lifetime as it determines the present value of future cash flows. It is the interest rate used in discounted cash flow analysis. It reflects that future cash flow has less value than current cash flow to investors due to opportunity costs and risks. In general, higher rates are applied to less developed technologies, to account for the greater risks and uncertainty associated with the novel design and speculative cost estimation. Determining an appropriate discount rate is important for any economic metrics, such as net present value (NPV), LCOE and payback periods (PP).

Ouyang and Lin (2016) investigated the LCOE of different renewable energy technologies in China and the appropriate subsidies and policies to support them. They found the discount rates required for different forms of renewables varied through 5, 8 and 10%, with the higher rates being needed for novel renewable energy sources, such as tidal, which are seen as more risky compared to more established forms of renewables, such as onshore wind or solar PV. In general it can be shown that a transition to lower discount rates will help renewable energy

become more cost competitive against fossil fuels. Khatib (2016) performed a review of generation costs in OECD countries and found that as the discount rates fall from 10% to 5% more capital intensive forms of energy, such as nuclear, wind and tidal, become more cost competitive compared to coal and gas. Both papers used a common discount rate across the whole energy market due to limited data to distinguish the relative risks for different technologies. Common discount rates have been criticized for not reflecting these risks appropriately, and more recent studies have suggested specific values for the tidal compared to other ocean energy industries, which are on the higher end of the spectrum due to their novelty and perceived risk. (Goss, 2019)

A report on the cost of ocean energy, by SI Ocean for the European Commission used a discount rate of 12% for both wave and tidal, but also investigated how changes in the rate chosen could have a significant impact on the LCOE. Reducing r from 12% to 6% results in a decrease in their predicted LCOE of demonstrator arrays, from 0,32 USD/kWh (\$300/MWh) to 0,23 USD/kWh (\$220/MWh).

The OREC 2018 report estimated a discount rate at 10MW cumulative tidal capacity of 10%, but their models predicted this would fall to 8,4% by 100MW, 8,0% by 200MW and 7,1% by 1GW global installed capacity, reflecting the potential that scalability has to reduce the cost of capital. It was also demonstrated that each percentage point reduction in discount rate leads to a significant LCOE reduction (of approximately 6%), for example the discount rate changing from 7,1% to 6,1% would reduce their 1GW cumulative capacity LCOE estimate from USD 94 per MWh to USD 85 per MWh (2012). This is consistent with SI Oceans' results, which fell by 6,4% on average per percentage point reduction in discount rate. Falls in r could be achieved as the industry matures and investment in tidal energy is seen as less of a risk.

The Carbon Trust predicted that the first commercial marine energy schemes would have a discount rate of around 15%, which could fall to 8% as the technology matures (Goss, 2019). Vazquez and Iglesias (2014) used a discount rate of 10% in their Levelized CAPEX of Energy tool. In another paper these authors argued that tidal stream energy projects have greater technological risks, compared to conventional types of energy generation, and high capital costs which results in a conservative discount rate being needed of between 10% and 12% (Goss, 2019)

Allan et al. (2012) used a high and low discount rate of 15% and 6% respectively, with 10% used as the central value when finding the LCOE of wave and tidal, which is often used

as a common rate across multiple different technologies (Goss, 2019). Allan et al. (2014) noted that higher discount rates adversely affect technologies with longer lifetimes and high CAPEX as a proportion of the LCOE. Both factors apply to tidal, so it is anticipated to be highly sensitive to variation in the discount rate. Culley et al. (2014) also used a 10% discount rate for their study into cost modelling and micro-siting of tidal stream and found that this amounted to a 35% reduction in income when compounded over an assumed 20-year array lifetime. Coles et al. (2014) used a discount rate of 12% when investigating mechanisms for reducing the LCOE of tidal energy. Dalton et al. (2015) suggested a discount rate of 8% to 15% is typical in UK ocean energy, however they noted that more in-depth economic studies could use multiple rates within one project to reflect the different risks of individual cash flows. Klaus et al. (2005) assumed a financial discount rate of 10% but also tested the impact of varying it over the range 5–15%. They emphasized the importance of a thorough investigation into the choice of the discount rate, by demonstrating the results of LCOE comparisons between technologies can be inverted as the discount rate is varied through its conventional range.

This present study therefore will consider a discount rate of 3 to 15% with a typical value of 10%. However, due to the high sensitivity of LCOE to the discount rate, sensitivity analysis of the final LCOE prediction should be performed.

4.7.9 Lifetime of array

The lifetime of the array is the number of years that the tidal project is planned to operate. It is normally determined by contracts and insurance based on the assumed time an array can perform well before there is too much degradation due to environmental conditions. Vazquez and Iglesias (2010) used an expected lifetime of installation of 20 years in their Levelized CAPEX of Energy tool. Likewise, Dalton et al. (2015) and the report by SI Ocean (2018) assumed a lifetime of 20 years. The Department of Business, Energy and Industry Strategy (BEIS) of Spain assumed an operating period of 22 years for tidal streams in their 2016 generation costs report.

The world's largest and currently operating project, the MeyGen 6MW array in the Pentland Firth, announced in 2018 that it had entered into its 25th year operations phase. Similarly, Johnstone et al. assumed a lifetime of 25 years in their techno-economic analysis of tidal energy, and as did Coles et al, 2012. As the technology becomes more tested and proven

lifetimes are likely to increase even further. Therefore, a typical value of 25 years with an upper and lower bound of 30 and 20 years respectively was used in this study. From an investment perspective, 10 years was also considered for the IRR calculation.

Tidal energy is currently perceived as a relatively risky investment, and therefore has a high discount rate, this makes the NPV and LCOE less sensitive to the choice of array lifetime because both revenue and costs many years into the future are heavily discounted (Goss,2019).

At a discount rate of 10% cash flows 20, 25 and 30 years into the future have a present value reduced by 85%, 91% and 94% respectively, so adding additional years to the project lifetime does not contribute much to the overall LCOE. If the discount rate falls to 5% then the present value reductions fall to 62% 70% and 77% respectively. (Goss,2019)

4.7.10 Cost model inputs

Goss (2019) proposed adopting a maximum, minimum and mean values of the cost parameters and other economic inputs (discount rate and lifetime of an array) across all the sources discussed should be taken at different levels such as the Pessimistic, Optimistic and Typical. It should be noted that the cost information summarized in this review is based on the limited publicly available information at the time of writing and that there is a significant difference between the optimistic and pessimistic values due to the high degree of uncertainty in this relatively new industry. These estimates are suitable for academic modelling and optimization of tidal stream arrays, but in practice tidal developers should use their internal cost information for more accurate economic array design. (Goss, 2019)

Table 4: Summary of parameters.

| Symbol | Description | Optimistic | Typical | Pessimist | Units |
|--------|-----------------------|------------|---------|-----------|-------|
| r | Discount rate | 0,05 | 0,1 | 0,15 | n.a. |
| L | Lifetime of the array | 30 | 25 | 20 | years |

4.7.11 Downtime and degradation

Availability is a measure of the time that an array is available for operation. Availability can be calculated from the number of downtime hours over a given period, such that:

$$Availability = 1 - \frac{downtime\ hours}{total\ hours} \quad (25)$$

Therefore, the number of hours of generation in year i , as used in the LCOE expressions, can be predicted as t_i by multiplying 365 days by 24 hours minus the anticipated availability in year i . In the wind industry it has been found that turbines often have lower availabilities during high-wind periods, where the production and loads are higher so faults are more likely to occur. To account for this effect, availability is sometimes calculated in two ways: as a time-based availability or as a production-based availability, found as the percentage of the actual energy produced over energy expected. The former is easier to calculate but the latter is a better representation of the energy lost. (Goss, 2019). Downtime in high winds often results in the percentage of energy lost is higher than the percentage of hours lost, with one study finding that a 3% non-availability in time resulted in an 11% reduction in energy generated in the Irish wind farm investigated by Coles et. al. (2016). The production-based availability can be improved by scheduling maintenance, where possible, during periods of low resources. A similar study for tidal energy was not found, so this study will consider a 3% non-availability value.

Hours of downtime, or non-availability, can have several causes; turbine availability can include scheduled or unscheduled maintenance or faults in the turbines causing periods of non-operation, grid availability can include periods of time where the grid is unable to accept electricity due to lack of capacity or grid failure, or balance of plant availability, where electricity generated at the turbines is lost due to failure of supporting components and auxiliary systems. (DNV-GL White Paper, 2017)

Turbine suppliers will often guarantee a minimum turbine availability rate when they sell their turbines to operators and if turbine failures cause the availability to drop below that value the suppliers will pay compensation to the operators. This contractual availability is negotiated during the turbine supply agreement. In wind energy a typical value of 97% is used as the

industry standard (Conroy, 2011). There is limited operational data to form conclusions about the typical time-based versus production-based availability in tidal, but the MeyGen Phase 1A guaranteed a contractual availability of 95%, and anticipated that the turbines would exceed their target performance in practice. (DNV-GL White Paper, 2017)

When more data becomes available from operational tidal stream arrays, it may become possible to model the downtime as a function of time (Goss, 2019). There are likely to be cyclic patterns in the number of downtime hours needed in a year for scheduled maintenance, as some operations may need to occur on a five-year cycle, for example. There is also evidence from the wind industry that failure rates vary greatly depending on the year in the operating lifetime (Gonzales, 2018). Faulstich et al. (2017) demonstrated that wind farms often follow a “bathtub curve” where there is a high failure rate in the early life due to teething problems or ‘infant mortality’, followed by a period where the failure rate is approximately constant and low, with just intrinsic random failures occurring and a wear-out period near the end of an array’s lifetime, where damage accumulates and the failure rate increases. This degradation could be due to increased component wear or bio-fouling impacts. (Goss, 2019)

4.7.12 Final considerations regarding the economic metrics

As discussed above, there are a great number of metrics that can be used to evaluate the performance of tidal energy arrays. These include power alone (which results with array designs with too many turbines if the number is not pre-specified) and purely economic metrics such as break-even power analysis, NPV, LCOE, IRR and PP. Some studies have expanded upon performance metrics further to include the trade-off between economic performance and environmental impacts of the arrays, however this requires decisions on the relative weightings of each criteria. Many of these economic metrics can be estimated for large-scale arrays by assuming a linear relationship between CAPEX and OPEX (perhaps DECEX) and the number of turbines, and therefore, splits each of these expenditures into their fixed and turbine-dependent components is an interesting strategy to evaluate an array optimization.

With the collected information, the present work will employ an IRR model to evaluate the feasibility of a renewable energy farm in the section “Business Case” section. Since the range of subsidy schemes are not the same worldwide, it is important to identify possible upper and lower bounds on strike prices, however it is noted that the actual value will be highly

dependent on the state of the industry and levels of government support at the time. It should be noted that there is a great deal of uncertainty in each of the economic input estimates and they should be used for the purpose of providing a reasonable range for academic studies and may not reflect the real economic performance of a potential tidal site. These estimates are useful in the absence of real financial data from developers, which is often highly commercially sensitive, and can be used for proof of concept when demonstrating new techniques for optimizing tidal array designs. In practice, array design studies should be repeated with internally-validated financial models from developers and manufacturers.

5 METHODOLOGY

This chapter presents a methodology to assess and evaluate the economic and financial characteristics of a tidal farm project. Based on previous studies discussed in the past chapters, we hope to present a tangible method to critically analyze the feasibility of such an enterprise. The method employed in this work is developed in two stages:

1. Construction of a cost assessment model
2. Conduction of a business case calculation in order to evaluate the proposed model in a specific geographic region

For the current implementation, four different cost pillars have been studied representing the total costs of a tidal farm deployment in its entire life cycle. The evaluation method proposed for the economic feasibility of these energy projects is based on the LCC (life-cycle costs) of the project and the determination of the annual energy produced (AEP). The LCC represents a pulverized breakdown to account for the different project stages of a tidal farm. Here, the goal is to estimate the associated costs of a project during its implementation and service life.

It is important to emphasize that the development of a methodology for the economic assessment of projects based on LCC is a simplified representation of the real world based on the main characteristics and relations of the project and their corresponding cost estimations. In order to carry out an adequate LCC for tidal energy projects from the perspective of environmentally sustainable economic efficiency, it is fundamental to understand the life cycle of this sort of project and the activities to be performed at all the stages. (Segura, 2017). Hence, as shown in figure 15, the stages of which the proposed methodology is composed are:

- Concept and definition costs: C_1 ;
- Purchase costs: C_2 ;
- Installation costs: C_3 ;
- Operation costs: C_4 .

So that the total LLC is:

$$LCC = C_1 + C_2 + C_3 + C_4 \quad (26)$$

| Life-cycle costs for tidal energy projects | | | |
|---|---------------------------------|---------------------------------|------------------------------------|
| Concept Costs (C1) | Purchase Costs (C2) | Installation Costs (C3) | Operation Costs (C4) |
| Market research costs (C11) | Turbine Costs (C21) | Transportation Vessels (C31) | Insurance Costs (C41) |
| Environmental studies costs (C12) | Exportation Power Systems (C22) | Submarine Cables (C32) | Blade Cleaning (C42) |
| Engineering Design (C13) | TEC Structure (C23) | Ground Exportation Cables (C33) | Light Preventive Maintenance (C43) |
| | | TEC Installation (C34) | High Preventive Maintenance (C44) |
| | | | Corrective Maintenance (C45) |

Figure 15 – Break-down of costs in this study.

In the following sections of this work, further information will be provided concerning site parameters (channel depth, tidal energy statistics, weather windows, distance from shore, etc.) and turbine characteristics (geometry, configuration, power curve, etc.) to estimate the total energy produced and, consequently, the revenue generated from a possible commercial exploitation of the tidal energy project.

Cost and energy generation will be combined and analyzed by means of several indicators (NPV, IRR and LCOE) that will influence the decision to invest in the tidal energy project and will allow comparative studies with other renewable energy sources. It is important to note that the estimated costs and the estimation of the total energy included in the methodology for the economic feasibility of tidal energy projects have been obtained by studying the current scientific literature, internal information at the University of São Paulo and Segura (2017) containing internal technical reports generated at the University of Madrid (UPM – Universidad Politécnica de Madrid), as well as information provided by companies that specialize in tidal energy projects.

The following subsections will present the details required to describe the proposed methodology.

5.1 Concept and market research costs

The concept and market research costs (C_1) are attributed to various activities whose objective is to guarantee the project's viability. Focusing on tidal energy projects, the following costs are typically included:

Market research costs (C_{11}): It is necessary to determine the current state of the market as regarding tidal energy generation and to analyze the economic viability of the tidal energy project on the basis of environmental information, site information (water depth, tidal energy resource, weather windows, distance from shore, etc.), device information (geometry, configuration, power, materials, etc.), export power system information (farm topology, connectors, cables, transformation platform, converters, etc.), and so on.

Therefore, this subtopic includes the hiring of engineers and companies to proceed with the aforementioned research and will be considered as a constant value.

Environmental studies costs (C_{12}): These include costs with certification and regulation, such as environmental studies (seabed surveys, local species and ecosystem surveys, coastal process surveys, etc.), social impact surveys and the authorization of the installation. These costs are usually constant, with the exception of the authorization of the installation of the tidal farm, which depends on the surface required to install the tidal energy project, therefore it has a considerable variation depending on the project's location.

Engineering design costs (C_{13}): costs related to fulfilling the specification of the project requirements and providing proofs of its compliance. They typically include costs regarding: project management, the inclusion of reliability, maintainability and activities for environmental protection; detailed documentation for the design, determining the installation/maintenance steps required for the park, the selection of the suppliers and quality management.

All these costs can be modeled as a constant value. Once these costs have been attained, the concept and definition costs C_1 is obtained by the sum:

$$C_1 = C_{11} + C_{12} + C_{13} \quad (27)$$

5.2 Purchase Costs

The purchase costs (C_2) represent the sum of the turbine costs, export power system and turbine structure, meaning, the material and infrastructure that will be purchased for the construction of the tidal farm:

Turbine costs (C_{21}): This represents the cost for the purchase of the turbines, which will depend on the design of the turbine, the manufacturer and discount rate provided, depending on the number of the machines and discount eligibility provided by the manufacturer.

Export power system costs (C_{22}): This represents the cost to acquire and build the power exportation system, to integrate the energy into the electricity grid and can be calculated by summing the price of umbilical cables (estimated by considering the length of the umbilical cables and the price per meter), summed with transformation platform and converters (estimated by considering the number of turbines installed, the power of each and the cost per MW of the rectifiers and inverters).

Turbine structure costs (C_{23}): This represents the costs to build the structure to support the turbines, consisting of base support, transition structure, vertical column, concrete ballasts, special concrete bags and other infrastructure costs related to the installation.

Once these costs have been attained, the purchase costs, (C_2) is simply:

$$C_2 = C_{21} + C_{22} + C_{23} \quad (28)$$

5.3 Installation Costs

Installation Costs (C_3) for tidal farms is difficult to determine because of the uncertainties of the offshore operations and the volatility costs of vessels used in these operations. Several concepts need to be considered if these costs are to be estimated in an appropriate manner (Segura, 2017), as summarized below.

Specialized vessels: The evolution of offshore wind farms and the development of advanced offshore technologies result in the advancement of infrastructure and specific solutions for these particular sectors. When designing the installation and O&M (operation and maintenance) procedures, it is essential to search for specialized vessels and crew with which to perform these activities. Without such specialized vessels, the costs of these operations would

be so high that the economic viability of these offshore systems might be seriously compromised (Segura, 2017).

Base port: When studying the implementation of a tidal farm, it is important to determine the location of nearby industrial base ports. These ports need to be equipped with sufficient means for the reception of materials and components and have the capabilities to load and upload these materials and components, along with the means to perform turbine maintenance tasks. The location of the port base has a great influence as regards ensuring a reduction in the installation and O&M costs (Segura, 2017).

Weather windows: Weather phenomena, such as wind velocity, wave height and tidal current velocity, need to be studied in order to perform the installation and the O&M procedures in safe conditions. The definition of favorable weather windows throughout the different seasons of the year is fundamental for the safe planning of the installation and the O&M tasks are to take place (Segura, 2017).

Hence, the installation costs (C_3) represent the sum of the transportation vessels, submarine cables and ground exportation cables to install the turbines, as follows:

Transportation vessels costs (C_{31}): This represents the cost to lease the transportation vessels and crew that will carry the turbines and the necessary equipment for the installation.

Submarine cables costs (C_{32}): This represents the cost to install the submarine cables (which depends on the cost of technical labor), the cost of operations in the port and the specialized vessels to install the cables.

Ground exportation cable costs (C_{33}): This cost is estimated by considering the number and length of submarine exportation cables, the length of the submarine exportation cable, the cost per m of this element, the cost of technical labor, and the distance from the tidal farm to the base port, and costs related by the weather windows.

Installation of the turbines (C_{34}): This cost is estimated by summing the cost of leasing the vessels, the cost of technical labor, cost of operations in the port, which depend on the distance from the tidal farm to the base port, and weather windows.

Once these costs have been attained, the operation and maintenance costs C_3 is obtained:

$$C_3 = C_{31} + C_{32} + C_{33} + C_{34} \quad (29)$$

5.4 Operation and Maintenance Costs

In the case of tidal energy projects, manufacturer procedures to operate and maintain turbines make up an important part of the design of the turbines and will have a direct and important repercussion regarding the time it takes to get the turbines working properly and, consequently, the energy generation capacity of the tidal farm. A reduction in time spent on these tasks substantially influences the reduction in the cost of energy (Astariz, 2015).

Additionally, the execution of the maintenance tasks should be carried out in periods of small tidal currents in order to ensure safe conditions when raising the nacelle and carrying out insertion operations to minimize energy losses during the time spent on these operations (Lyding, 2019).

During the development of an effective maintenance plan for the tidal farm (and the cost structure), it is necessary to estimate the downtimes that each component requires, the failure probability of each component, the specialized vessels used in these tasks and the weather windows in which these tasks can be performed. Furthermore, it is very important to include the insurance costs and fixed expenses in the operation and maintenance cost structure, because they are some of the most expensive factors in the offshore renewable energy sector (Connor, 2013).

Bearing the previous considerations regarding the cost structure in mind, the following costs are considered at this stage:

Insurance costs and fixed expenses (C_{41}): The estimation of this cost is an area that needs to be studied in depth within the offshore renewable energy sector. According to the scientific literature, two possible metrics can be used to estimate these costs (Conor, 2013): a percentage of the total capital expenditure (CAPEX); or cost per MW generated. For example, the Irish Wind Energy Association (2017) includes an estimation of the insurance cost of 15,000 USD per MW. In this work, the insurance costs and fixed expenses will be estimated as a percentage of the total CAPEX.

Blade cleaning (C_{42}): This cost takes into consideration the removal of algae, microorganisms and fouling from the blades of the rotor. This cost depends on the number of rotors installed on the farm, the downtimes spent on this process, the weather windows, the transport costs, the labor costs, and the costs incurred as the result of production losses.

Light preventive maintenance (C_{43}): This involves light general maintenance (grease changes, review of painting defects, etc.) in the turbines (nacelle and supporting structure).

High preventive maintenance (C_{44}): This implies more in-depth maintenance (bearing replacements, inspection of the nacelle and the structure components, etc.) in the turbines (nacelle and supporting structure) and the export energy system. The estimation of this cost category will be carried out by considering the number of turbines purchased, the downtimes spent on this process, the weather windows, the transport costs, the labor costs, the material costs, and the costs incurred as the result of production losses.

Corrective maintenance (C_{45}): This cost involves repairing the turbines (nacelle and supporting structure) and the export energy system. The computation of this cost category is developed by including the number of turbines purchased, the failure probability of the components of the tidal farm, the downtimes spent on this process, the weather windows, the transport costs, the labor costs, the material costs and the costs incurred as the result of production losses.

Once these costs have been attained, the operation and maintenance costs, C_4 are:

$$C_4 = C_{41} + C_{42} + C_{43} + C_{44} + C_{45} \quad (30)$$

5.5 Costs not considered in this methodology

As mentioned before, decommissioning costs are not considered in this stage. These costs are presented as C_5 in Figure 16, but will not be implemented. After speaking with several companies and investment stakeholders, a feasible solution for decommissioning is still not present and not considered during design and implementation phase of the energy farms.

It is also important to mention that decommissioning costs (DECEX) will not be considered at this stage, although these are very important costs for future models. These costs are not currently taken into consideration because current data and experience to subsidize analysis in this regard are lacking. Hence, implementation of renewable projects in Brazil do not typically consider this cost in the business case. In spite of this, DECEX is already a very established cost metric in other countries.

5.6 Proposed methodology

This section will integrate cost methodology with the economic and financial model, utilizing the metrics described in the literature review. After computing the LCC as seen in section 4.1, it is necessary to compute the annual energy produced (AEP) of the project before performing a feasibility analysis (economic and financial model).

Annual Energy Produced (AEP): one of the most important proxies to indicate the decision regarding the installation of a tidal farm, is the calculation of total energy produced per year. In order to estimate AEP and the income generated if the electric tariff is known, it is necessary to determine a model that considers the characteristics of the flow (speed, direction, distribution, etc.), the ability of the device to capture energy and its performance in converting and exporting energy. The following items are required to estimate AEP:

- Availability factor
- Tidal farm topology
- Physical model

For the *availability factor*, the turbine does not always work properly owing to device breakdowns and maintenance periods as previously discussed. This availability factor needs to be estimated on the basis of the information obtained from the maintenance procedures used, weather windows, and so on, therefore a statistic value will be used taking into consideration Segura (2017).

Tidal farm topology influences the final value of AEP, and it is necessary to evaluate the performance of each turbine installed on the basis of the position (row, column) that it occupies within the tidal farm. For this part, the farm blockage (B_G), as well as local blockage (B_L) need to be computed depending on L (width of the channel) and chosen turbine geometric characteristics.

The physical model presented in previous chapters is employed to calculate AEP. Different physical models that consider other aspects of the farm can also be employed. During the literature review, two models have been presented (Betz's classic theory and an improved model considering channel blockage) each producing a maximum C_p depending on farm arrangement. For the models to be implemented, it is important to select the most appropriate turbine and define the diameter D of the rotor. To estimate channel flow speed, statistical data from an annual dataset will be analyzed for a specific site, which, in the present study, will be

based on the work of Fortes (2016).

The physical model of the tidal farm will be combined with the economic model in an algorithm to produce data for the financial study. The effect of key variables over the cash flow will be investigated for specific farm arrangements. Cost parameters will be estimated employing in the theory discussed before, as well as estimates of revenue. Figure 16 represents the structure of the algorithm combining the physical and financial models. The arrows represent the flow of deformations through the various calculations with input and output parameters. More details on the calculations will be given in the next chapter.

As far as the financial study is concerned, the present work will consider the revenue cashflow and the IRR analysis. After interviewing private equity funds and other companies that currently invest in ventures in Brazil, a typical investment return rate (IRR) of 25% can be considered as a proxy for decision-making.

Regarding the economic analysis, the algorithm will consider the value of strike energy calculated as an average of Enel's tariff throughout 2019 and 2020 (in BRL/kWh). It is important to mention that prices for the electricity energy in Brazil will depend on auctions and market-related specificities, therefore a simplification of the pricing model was used (Enel's tariff average).

Estimation of the channel flow speed at the depth of the rotor will be supplied by the histograms of the current velocity presented by Fortes (2016) for a site located in São Sebastião Channel of the coast of São Paulo state. These histograms provide information about the occurrence (number of hours) of a given current velocity in a year. This will make the business case studied in the next chapter.

5.6.1 Physical limits of the proposed model

It is also important to mention that the gradient pressure effect due to obstruction of the channel is not considered. After installing the stream turbines the blockage effect over the island would increase and therefore water flux would be increased outside the channel. Hence, more water would pass throughout the edge of the continent, and this effect is not considered in this model. The hydrodynamic load of the downstream turbines is also not considered. A sensitivity scenario with stochastic modelling was also not constructed, as the idea of the work is to present a tool to evaluate economic feasibility by inserting physical parameters of the channel.

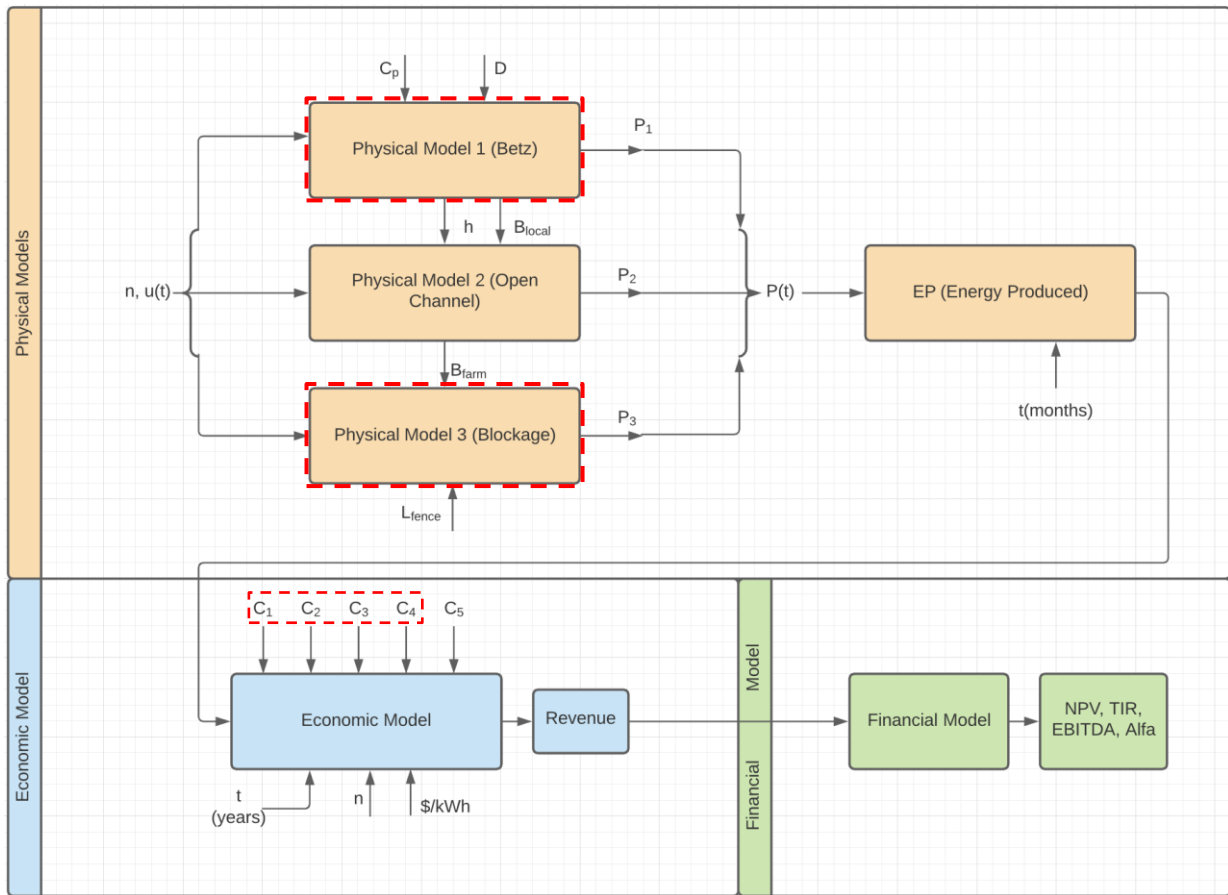


Figure 16: Summary of the computation of the physical, economic and financial models. The red-dashed lines represented the inputted data and that the open channel physical model was not used, as well as decommission costs C_5

6 BUSINESS CASE DEFINITION

The algorithm proposed in the previous chapter will be employed in a business case to verify the proposed methodology and the financial output of a potential energy farm to be installed in a real location in Brazil.

6.1 Characterization of the São Sebastião Channel

The channel of São Sebastião in the State of São Paulo, Southeastern region of Brazil, has been chosen because of the available information present in the literature and for being known to have strong currents, possibly representing a suitable place for a tidal farm installation. These characteristics will be explained along this section, clarifying the reason for choosing this location.

The channel between São Sebastião Bay and the São Sebastião Island (marked by a red dot in figure 17) is used for various economic activities (for example tourism, oil and gas offloading), however it is not explored by the renewable energy industry. Therefore, the study of the spatial distribution of a turbine farm located in this region becomes interesting, both from an environmental and socioeconomic point of view. (Fortes, 2018)

This location has one of the greatest potential for extraction of electricity from the ocean in the State of São Paulo. Thus, it is necessary to explain the main characteristics of the region in order to correctly model the studied scenario. According to the nautical charts provided by the Brazilian Navy, a maximum depth in the channel is around 40 meters, but vessel traffic in such regions implies restrictions on anchoring and the impossibility of implementing a farm of tidal turbines over the full width or length of the channel.

Thus, due to the physical restrictions imposed by the continent and the island on the channel flow, the local current has its magnitude amplified, reaching average velocity values close to 0,3-0,6 m/s, according to studies performed by Kirinus and Marques (2015). From the study, we know the flow speeds in the channel are much lower than the typical sites for tidal farms in the North Sea, which may reach velocities of about 2 m/s.

In his work, Fortes (2018) employed sECOM (Stevens Estuarine and Coastal Model), a three-dimensional, hydrostatic, coastal and estuarine circulation model to estimate flow speeds in the channel. The code is based on primitive equations that provide the prediction of sea level,

period and significant height of waves and three-dimensional fields of currents, temperature, salinity, density, viscosity and diffusivity. The results of his work are presented in table 5, compared with field data of average and maximum values for currents and power densities for the red dot in the São Sebastião Channel (figure 17) for currents at 5m and 15m below the free surface.

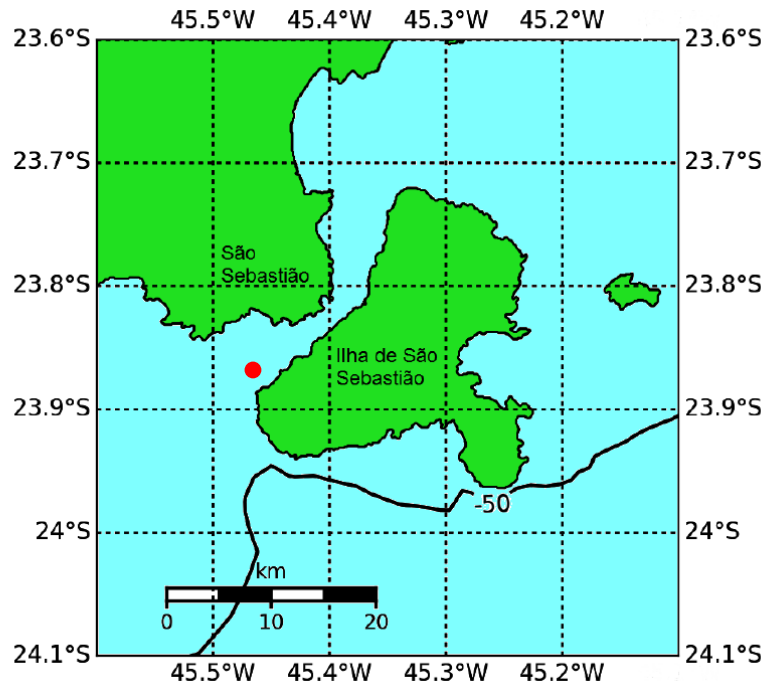


Figure 17: Region of São Sebastião chosen as area of study. Reproduced from Fortes (2018)

Table 5 - Maximum and average values (with their standard deviations) for the flow speeds and power densities for the analyzed time series. Adapted from Fortes (2018)

| | Current (m/s) | | | Power density (W/m ²) | | |
|-------------------------|---------------|--------------------|---------|-----------------------------------|--------------------|---------|
| | Average | Standard deviation | Maximum | Average | Standard deviation | Maximum |
| sECOM – average column | 0,2 | 0,21 | 1,53 | 26,3 | 108,6 | 1853,3 |
| sECOM – average surface | 0,32 | 0,31 | 2,23 | 93,8 | 344,8 | 5693,0 |
| Currentographer average | 0,32 | 0,18 | 1,25 | 36,2 | 63,0 | 994,7 |
| Currentographer bottom | 0,23 | 0,17 | 1,11 | 19,4 | 46,3 | 700,2 |

It is noteworthy, however, that Fortes (2018) states that oceanographic research in São Sebastião shows that the dominant of the current in the channel comes from wind energy, with the tidal component being comparatively insignificant. As such, currents tend to be highly seasonal, but with two directions (Fortes, 2018). The interval between July 1, 2016 and June 30, 2017, was chosen in order to contemplate periods in which there was data collected in the Fortes' work.

In order to assess the energy potential of currents in the region, average power density maps were modeled in the period for the study area. Since the power density (PD) is proportional to the cube of the current velocity ($PD = \rho v^3$), a small increase in the flow velocity may imply a significant growth in the PD. Furthermore, it is possible to see that the average velocity at the surface is around 50% greater than in the water column, making the energy density near the surface much higher, as seen in figure 18.

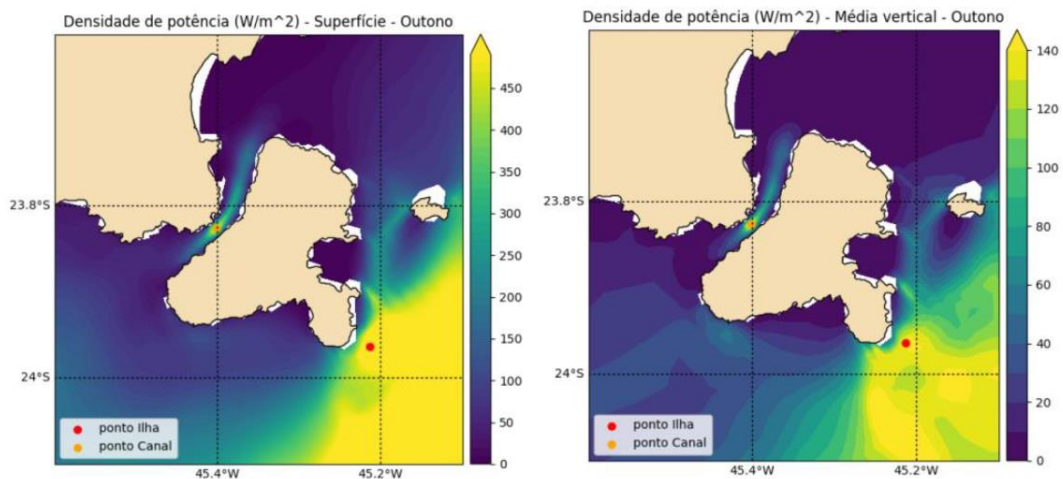


Figure 18 - Power Density of the currents in the São Sebastião Channel. Reproduced from Fortes (2018). The red dot marks the highest intensity.

Despite having a lower energy density when compared to the red-dotted point outside Ilha Bela Island in figure 18, the São Sebastião channel is attractive for such energy exploration due to natural constraints. In Fortes' work, the main characteristics were addressed in order to model this region regarding available energy resource. But within the scope of the present work, it was decided to adopt an initial velocity close to 0.5 m/s in the Southwest-Northeast direction, as will be detailed in the subsequent chapters, a condition that is similar to that observed in the central region of the channel.

Fortes (2018) also assessed the temporal variation of the current, which is reproduced in

figures 19 and 20. Figure 19 presents the evolution of average power density in the water column for the two most intense points of study: one in the channel and the other off the island.

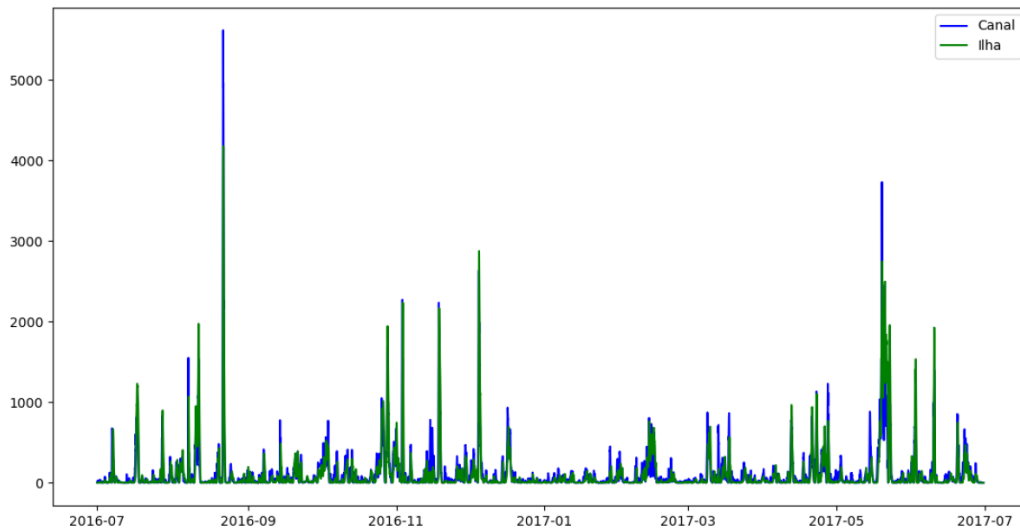


Figure 19: Time series of the vertical mean of the power density in the water column over 12 months in W/m², for the channel (blue) and the island (green) stations. Reproduced from Fortes (2018)

When the data is averaged for one month, a clearer idea of the potential power density along the year is obtained, as seen in figure 20. The annual mean power density for the channel flow was estimated by Fortes (2018) in 119,3 W/m². The power density varied greatly throughout the annual period studied and, in all the time series, it falls below 100 W/m² most of the time. However, in several moments it has peaks that are one order of magnitude greater than the average.

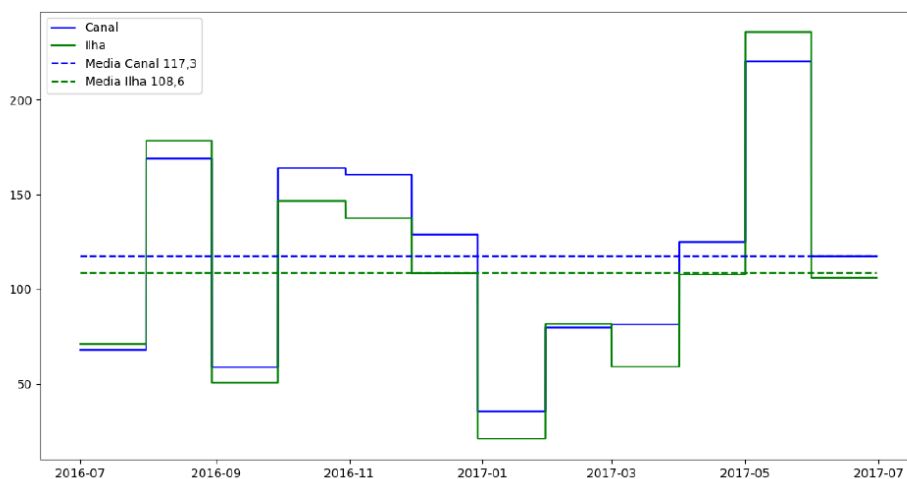


Figure 20: Monthly and annual averages of the average vertical power density across the entire water column in W/m² for the island (green) and channel (blue) stations. Reproduced from Fortes (2018).

Annual averages, ranging between extremes of 108,6 W/m² to 473,2 W/m² are considered low when compared to other very energetic places, especially with strong sea currents, which may present values in the order of 1 kW/m² (Cornett, 2006; Ferreira, 2011; Borthwick et al., 2013; Vanzwieten et al., 2014). In some places it can exceed 10 kW/m², as in in China (Liu et al., 2011). However, these values are higher than others found in research focused on the southern region of Brazil, such as in Fischer et al. (2015), who found a maximum of 9 W/m² of PD in current data for the region of Rio Grande, RS and Kirinus and Marques (2015) who found about 35 W/m² in the region of Lagoa dos Patos, RS. Therefore, the São Sebastião channel is not immediately discarded as a potential site for energy generation. Figure 21 offers an estimate of velocity distribution along the year in the channel, highlighting that a dominant flow speed around 0.5 m/s is a conservative choice.

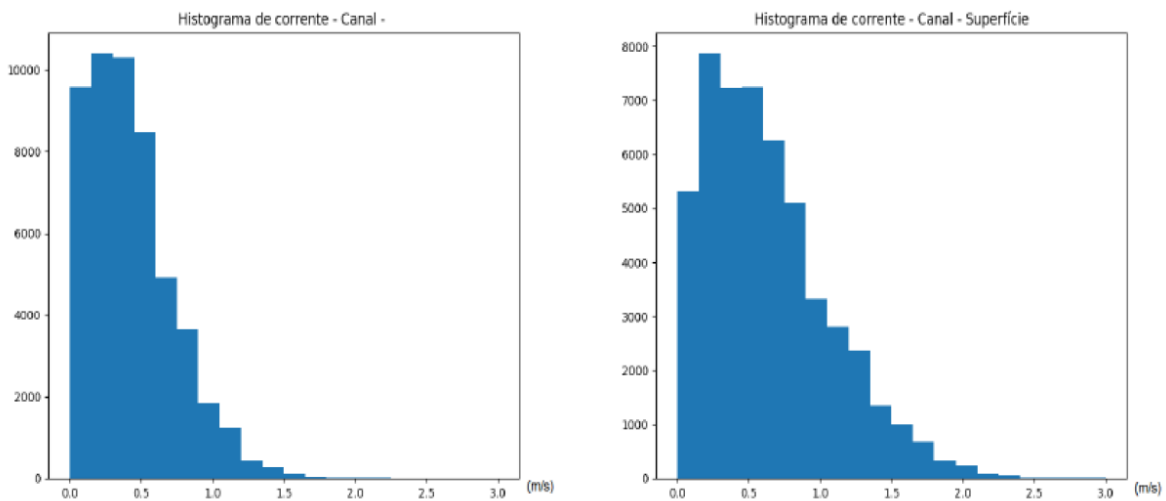


Figure 21 - Histogram of annual current velocity measurements for the São Sebastião channel. Left: vertical mean in the water column. Right: vertical mean on the surface. Reproduced from Fortes (2018)

The predominant direction for the current in the São Sebastião channel is the Northeast-Southwest direction (dominated by geographical constraints) and the average velocity at the surface is around 50% greater than that in the water column, making the energy density near the surface much higher. For this reason, we will keep the rotor near the free surface setting the height of the turbine structure in the next section.

Fortes (2018) also quantified the energy potential of the oceans in the São Sebastião region estimating averages of 22,3 kW/m of wave energy and power density of currents of 473,2 W/m². This may suggest that in both wave and current energy exploration could be viable, especially

taking into account the fact that the region has a well established naval technology, which can reduce the costs of installation, operation and maintenance. To these advantages, there is also the proximity of the coast and energy consuming centers, which reduces the possible losses in the transport of electricity.

One limitation in Fortes’ data was the fact of analyzing a given period of one year, what makes the means for each station, for example, not representative of seasonal climatology. For this, a longer-lasting study would be necessary preferably with greater range of collected data.

Finally, as far as the present study is concerned, the key parameters of the current in the channel employed in our analysis are summarized in table 6. Please note that the ballast height (h_l) is the parameter adjusted to keep the rotors near the free surface where flow speed is maximum.

Table 6: Summary of parameters considered for the topology of the channel and tidal farm construction. Source: Author

| Parameter | Value |
|---|--------------|
| Height of the channel (h) | 40 m |
| Height of the turbine ballast (h_l) | 30 m |
| Channel width (w) | 1000 m |
| Flow velocity (u) | 0.5 m/s |

6.2 Characterization of the renewable energy farm

The proposed current farm is composed of a range to be studied between 10 to 1000 turbines of Verdant’s Gen5Rotor of 45 kW. The TECs selected have an open rotor configuration whose axis is parallel to the flow (see Figure 22). The nacelle of the turbine can be separated from the structure in order to facilitate the maintenance tasks, but when the nacelle is mounted on the structure, its orientation is fixed, thus making it mandatory for it to have a pitch controllable blade system so as to maximize the energy captured in both current directions. The

diameter of the blades is 5 m, and the TEC is fixed to the seabed by gravity, i.e., the structure that supports the turbine is supported on the seabed by means of a substantial mass. Finally, the tidal farm will be composed of a small number of rows, with variable number of turbines per row, in order to minimize the shadow effect in the last rows and maximize the total energy captured by the tidal farm.



Figure 22: Illustration of 3-bladed rotor and nacelle by Verdant Rotor. Reproduced from Verdant (2014).

Table 7: Summary of the turbine parameters considered for the business case analysis.

| Parameter | Value |
|---|--------------|
| Turbine Diameter (D) | 5 m |
| Nominal Power of the individual turbine (P) | 45 kW |

6.3 Characterization of costs for São Sebastião channel

This section will be present the computation method of the costs for the farm installation to properly mensurate the budget involved in the complete project and will be divided into two parts: installation procedures and maintenance procedures.

6.3.1 Installation Procedures

For the case study developed, the following considerations and installation procedures have been kept in mind for the tidal farm during its expected service life of 20 years.

The prices considered in this section will take Segura's work as a reference and replicate the installation procedure. It considers the installation price of HF4 Vessels selected designed by MojoMaritim. This vessel is characterized by its dynamic positioning and the fact that it can work under extreme conditions. The use of this vessel makes it possible to obtain larger weather windows for the development of the installation and O&M procedures and, consequently, helps substantially reduce the total life-cycle costs. An additional advantage of the vessel selected is that it allows the transportation of all the equipment required to install one TEC or the transportation of three nacelles at the same time, which helps reduce the maintenance tasks.

Base port: the port selected for its operative qualities is the Port of São Sebastião. The distance from the base port to the location of the tidal farm is approximately 9 km. This distance, although small, cannot be ignored since, owing to the nominal velocity of the vessel selected (14 knots), it would spend 30 min on the displacements. Weather windows: Bearing the vessel characteristics and the climatological considerations in mind, the percentages of time during which operations can be performed in each season will be considered similar to Segura's work. These are the following: (a) spring: 75% (68 days); (b) summer: 95% (87 days); (c) autumn: 50% (46 days); and (d) winter: 15% (14 days). These percentages show that it is possible to operate around 215 days a year, which is sufficient time to satisfy the installation and maintenance procedures of the tidal farm. The price considered these time windows for the installation of up to 20 turbines, so the figures presented in Segura's work will consider the complete installation project and a breakdown showed in the sections below will compute an individual price for each turbine. Using equations (18) and (19) a CAPEX projection for a higher number of turbines will be calculated and this estimation will be used for the business case results.

Installation Sequence: after studying the seabed on which the tidal farm will be located, it is necessary to study the zones in which the turbines will be situated in order to find the optimal route for the cables that belong to the turbines and the umbilical cables that join the turbines to the transformation platform, as well as to define the optimal route for the exportation cable

(Segura, 2017). Similar approach has been conducted regarding the base port for the cost calculation.

Figure 23 illustrates an example of the installation procedure of the turbines.

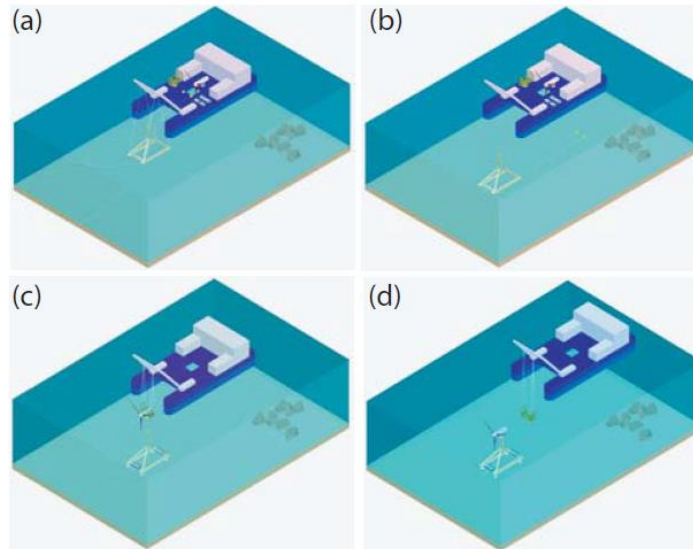


Figure 23: Installation procedure: (a) controlled descent of the base structure; (b) support structure on the seabed and deposited guide wires; (c) controlled descent of the nacelle; (d) removing the tool for nacelle installation and unstressing the guide wires. Reproduced from Segura (2017)

6.3.2 Maintenance procedures

For the case study the following maintenance plan is considered for the São Sebastião tidal farm during its expected service life:

Blade Cleaning

Although the blades should be protected with copper paint, which acts as a biocide, one of the essential tasks is that of cleaning the blades to guarantee the performance of the system. The task of removing the algae, microorganisms, etc., is performed once a year through the use of pressurized water in the installation vessel. It is also necessary to consider the processes of recovering and lowering the nacelle during this procedure.

Light Preventive Maintenance

All the components of the turbines need a general maintenance and periodical inspection about every two years. This includes the following operations: changing the grease in the thrust

bearing and the gearbox, filling the bottles of compressed air, inspecting all of the components, blade cleaning or checking the paint for defects.

High Preventive Maintenance

This procedure is more complicated than those described above, and therefore more complex operations on the nacelle need to be computed. This procedure is carried out every four years. In this case, the nacelle is moved from the tidal farm to the base port and is then completely disassembled. The following operations are carried out: bearing replacement of the thrust bearing and the gearbox, the replacement of grease in the seal ring, a detailed inspection of all the nacelle components, painting the entire nacelle.

Corrective Maintenance

On a medium size tidal farm, it is supposed that faults may occur in a TEC that were not foreseen in the maintenance plans. The greater or lesser speed of action needed to solve the problem depends on factors such as the availability of the vessel, the particular weather window at that time, the current climate conditions and even the availability of an additional nacelle.

6.4 Cost overview

A cost-break down will be presented considering the data from Segura (2017) and Frangoul (2020). An explanation of each item will be presented subsequently:

C_{11} : Market Research Costs (fixed cost). This cost will consider the site information survey (water depth, tidal energy resource, weather windows, distance from shore, etc.), as well as the device information study (geometry, configuration, power, materials, etc.) and the export power system information (farm topology, connectors, cables, transformation platform, converters, etc.)

C_{12} : Enviromental Studies (fixed cost). This cost will consider all relevant project management costs: obtaining certificates and regulations, such as environmental studies (seabed surveys, local species and ecosystem surveys, coastal process surveys, etc.), social impact surveys and the authorization for the installation of the current farm. The complete cost

presented in Segura (2017) has similar topology conditions to this business case therefore the value will be applied to the farm area in the São Sebastião channel.

C_{13} : Engineering Design (fixed cost). This cost will consider all engineering costs for headcount and engineers necessary to calculate and manage the project. Given the similarity of this business case with that of Segura (2017) this study will reproduce the value found in that work (table 8).

C_{21} : Turbine Cost (fixed cost per turbine, but variable depending on the number of turbines of the farm) – direct costs of commercial turbine are a very difficult information to gather for research in an early-development topic. Hence, the cost of acquisition of turbine will be inferred from approximation, as seen below:

- i. Since the chosen turbine must fit the physical location parameters, a 45 kW turbine by Verdant Power will be employed. A tidal power project in New York in 2020 employed the same turbines (Frangoul, 2020).
- ii. 30 Turbines that generate approximately 1MW should cost about 2,2 MiO USD. This information has been extracted from the turbine datasheet provided by Verdant Power
- iii. Hence, the cost of a single turbine can be approximated by $2,2 \text{ MiO USD} / 30 = 73\text{k USD}$ (Frangoul, 2020). This will be the individual base cost per turbine employed in our study.

C_{22} : Exportation Power System (variable cost). This is the cost related to extracting energy from the farm. It will consider:

- i. Equipment Nacelle and Base: considering number of turbines, power of each turbine (15kW), cost per MW protection switch, mass of submarine connector, cost per kilo of connector.
- ii. Umbilical Cables and Exportation Cables: cost given per meter of cable.
- iii. Transformation platform and converters: This cost is estimated by considering the number of turbines installed.

C_{23} : Turbine Structure (variable cost). This is the infrastructure cost to hold the turbines in position, which will consider:

- i. Cost per farm considering the number of turbines installed.
- ii. Base Support: this cost will be calculated by the number of turbines multiplied by the mass of the base (in kg) and the cost per kg.
- iii. Transition Structure: this cost is estimated by considering the number of turbines installed.

The fixed costs C_{11} , C_{12} and C_{13} for this business case will reproduce the costs presented by Segura (2017), since a great increase in the number of turbines would not necessarily alter these costs. In addition to that, after speaking with stakeholders (assets and private equities) it has been confirmed that environmental studies do not alter greatly depending on the number of turbines. On the other hand, all values taken as variable i.e C_{12} , C_{22} , C_{23} , combined with the installation costs C_{31} , C_{32} , C_{33} and C_{34} , as well as operations costs C_{41} , C_{42} , C_{43} , C_{44} and C_{45} will be calculated. To compute the individual cost per turbine, our study will parametrize data from Segura (2017) in which 40 turbines were installed and divide the total value per 40 turbines to find an individual cost per turbine. The variable costs will increase proportionately to the number of turbines that will vary in our study (section 6.5).

The LCC obtained for the case study from Segura (40 turbines) is summarized in table 8. Upon analyzing the results obtained for the tidal energy farm, it can be observed that the highest costs correspond to the most important components in the energy conversion system. Furthermore, the purchase costs of the turbines make a significant contribution to the total costs:

Table 8: Cost break down per topic.

| Fixed Costs | Price considering 40 turbines | Source |
|---|-------------------------------|---------------|
| C1 - Concept and Definition Costs | | |
| Market Research Costs | \$ 302.500,00 | Segura (2017) |
| Environmental Studies Costs | \$ 4.934.400,00 | Segura (2017) |
| Engineering Design Costs | \$ 240.000,00 | Segura (2017) |
| Selection of the Service Providers | | |
| Quality Management | | |
| Total fixed cost for farm implementation | \$ 5.476.900,00 | |

| Variable Costs | Price considering 40 turbines | Source |
|---|--|-----------------|
| C2 - Purchase Costs | | |
| Turbine Costs | Variable (individual turbine costs \$ 73k) | Frangoul (2020) |
| Exportation Power System | \$ 1.500.000,00 | Segura (2017) |
| Equipments Nacelle and Base | \$ 300.000,00 | |
| Umbilical Cables and exportation cables | \$ 1.200.000,00 | |
| Submarine cables and ground cables | \$ 1.300.000,00 | |
| Base Support | \$ 800.000,00 | |
| Transition Structure | \$ 1.155.600,00 | |
| Columns & Ballasts | \$ 1.382.400,00 | |

| C₃ - Installation Costs | | | |
|---|-----------|-------------------|------------------|
| Transportation vessels | \$ | 1.440.000,00 | Segura (2017) |
| Submarine Cables | \$ | 1.600.000,00 | |
| Ground Exportation Cables | \$ | 706.096,00 | |
| Turbine Installation | \$ | 914.400,00 | |
| C₄ - Operation and Maintenance Costs | | | |
| Insurance Costs | \$ | 628.000,00 | Segura (2017) |
| Blade Cleaning | \$ | 422.268,00 | |
| Light Preventive Maint. | \$ | 1.018.656,00 | |
| High Preventive Maint. | \$ | 1.396.800,00 | |
| Corrective Maintenance | \$ | 258.000,00 | |
| Total variable cost per turbine (sum of the variable costs divided per 40) | \$ | 418.734,57 | |

Segura's work presents a very complete model for the evaluation of costs, which has been extensively used in this work. It does not present, however, a market study of the current stream turbine manufacturers. Besides, the results of business case in her work lacks the physical modelling of the blockage effect and the variation of the stream velocity. These two physical parameters are extremely important as they sharply vary the production of energy. This work will characterize the turbine farm problem considering existing turbine (real acquisition values) and will present a more extensive physical modelling of the hydrodynamic problem.

6.5 Characterization of the turbine farm problem

The objective of any optimized farm arrangement is to produce the greatest amount of energy given the available physical space and other restrictions. Therefore, the turbine described by Verdant Power was selected (main dimensions in table 9) and will serve as input data for the physical model. Such a turbine is just a real example that could be used for the

conditions of the studied channel, but other turbines could easily be included in the model.

Table 9 - Characteristics of the selected turbine (Source: Verdant)

| Parameters | | Value |
|-------------------|--------------------------------------|---------------------|
| 1 | Turbine diameter | 5 m |
| 2 | Area of the rotor | 78,5 m ² |
| 3 | Turbine height (center of the rotor) | 25 m |
| 4 | Nominal flow speed | 1,5 m/s |
| 5 | Nominal power of the turbine | 45 kW |
| 6 | Nominal C_p of the turbine | 0,35 |

Given that the scope of the work involves the ideal turbine model, it was decided to use the main geometric parameters, such as the diameter and height of the turbine.

According to the “Energy Yearbook of the State of São Paulo”, the municipality of Ilha Bela consumed approximately 80 GWh in 2018 in this city. In these values, the main consumers are homes and commercial properties, which represent, respectively, a consumption of 46 GWh and 24 GWh.

As a target, this study will consider a scenario in which the regional energy demand will be met, making a technically viable farm whose number of required turbines will be analyzed through the energy potential of a turbine disposed separately in this channel.

6.5.1 Definition of premises

The region of choice along the coast of Ilha Bela has been the region with maximum flow speed, closer to the terminal. In a first simplified study, navigation restrictions are not taken into account. No residual value after life cycle of machineries will be considered and the inflation of the period analyzed will be 4% per year, as already pronounced by Brazilian Central Bank as a target for the next 20 years (BACEN, 2020).

It has also been considered that the linear scaling factor for turbine costs, which represent

the curve in that several machines purchased at the same time would have greater a discount, will not vary greatly. Companies, during business case calculation, vary the scaling factor from 0,8 (maximum discount) to 1,0 (no discount at all) for their calculations, taking into consideration that the individual price of a turbine does not change considerably, therefore a maximum factor of 0,8 will be utilized during modelling. A linear variation in assembly costs was considered, following Goss (2019), hence CAPEX and OPEX will vary linearly.

This model does not take into account the loss of efficiency over the life of the system. It also does not take into account the likely increase in the operating cost due to the increase in the system's useful life. Further research is required for these features to be implemented.

Farm configuration will always be considered as centered in the channel width. The layout of the installation considers that all turbines within the same row are aligned with each other and no other variations with hydrodynamic interference were calculated, such as a staggered configuration.

The first analysis presented will compare the first physical model (Betz) with the second physical model (blockage) in order to represent the difference in power generated by choosing more turbines and comparing the difference considering blockage – this is important to evaluate the topology of the array.

In order to calculate the cash-flows and later on, the AEP (total energy produced in one year), the electric tariff considered is 0,10 \$/kWh, calculated as an average of the tariff charged by Enel (Brazilian Regulation - SP) converted to USA dollars using a 1 USD = 5 BRL exchange rate. This value will increase by 4% every year (according to projected inflation).

Several scenarios will be analyzed because the model will plot different power outputs depending on the number of turbines in the topology analyzed. For the tidal farm topology, the number of rows and columns will be varied and an availability factor of 0,9 will be considered. (Segura, 2017)

It is important to mention that this example merely illustrate the methodology and the number of turbines, hence all values except the fixed ones, will vary in the calculation presented in the next section. Below the table of physical variables and their respective values:

Table 10: Physical variables and values considered for the computation of model.

| Variables | Value | Comments |
|-----------|---------|-----------------------|
| v | 0,5 m/s | Flow speed |
| L | 1092 m | Width of the channel |
| H | 40 m | Height of the channel |

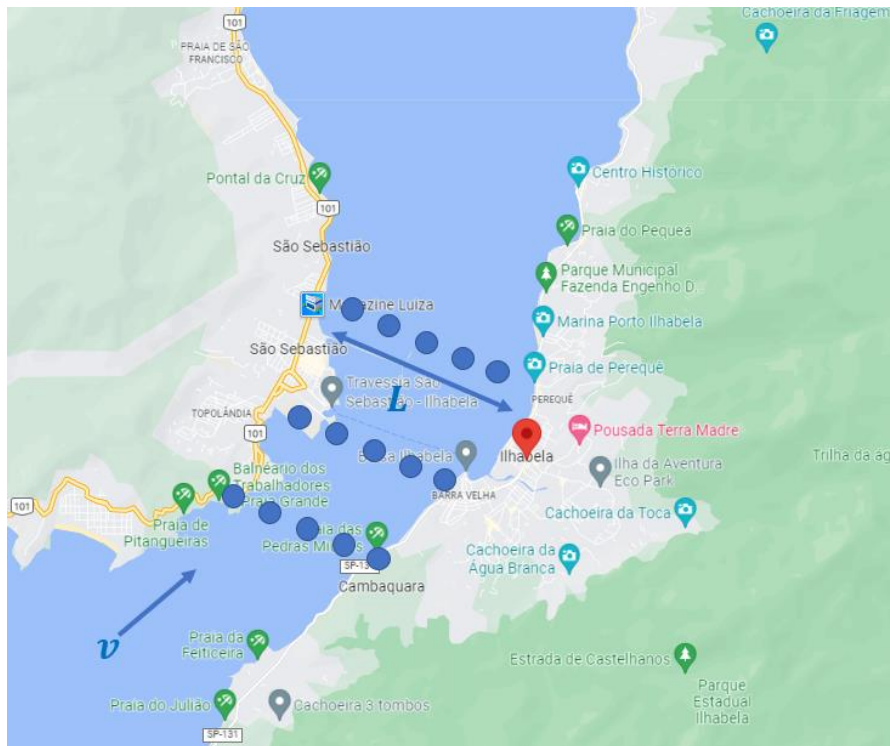


Figure 24: Illustration of the physical variables and values of the island and the continent where the tidal farm would be placed.

Navigation of commercial vessels in this part of the island will not be considered after the placement of the turbines. The choice of this region is justified by the amount of available information in the literature.

7 BUSINESS CASE RESULTS

In this section, the result of the proposed methodology using specific data from São Sebastião will be presented. This section will compare the output using two different physical models, a thorough analysis of the variation of C_p depending on the array topology and finally, a calculation of the economic metrics varying physical parameters such as flow velocity and number of turbines.

7.1 Results of C_p by altering the arrangement of the turbine array

The present section focuses on varying the number of turbines until a great number of turbines (N) is achieved, taking into consideration the comparison of the results of the two physical models: Betz model and blockage model. As seen before, hydrodynamic interference can increase turbine C_p due to channel blockage, an effect that makes a considerable difference in the power output for larger highly blocked farms. (Willden, 2012) The total number of turbines ($N = n.m$) will depend on the number of n turbines equally distributed in m rows.

The variation of local and global blockages and C_p (as a function of blockage) can be evaluated for a single fence, as shown in table 12 and figure 25.

Table 11: Variation of B_L , B_G and $C_p(B)$ by altering the number of turbines (n) within a single row ($m=1$)

| m | n | N | B_L | B_G | $C_p(B)$ |
|-----|-----|-----|-------|--------|----------|
| 1 | 1 | 1 | 0,785 | 0,0118 | 0,61 |
| 1 | 5 | 5 | 0,785 | 0,0589 | 0,64 |
| 1 | 10 | 10 | 0,785 | 0,1178 | 0,69 |
| 1 | 15 | 15 | 0,785 | 0,1767 | 0,72 |
| 1 | 20 | 20 | 0,785 | 0,2356 | 0,75 |
| 1 | 25 | 25 | 0,785 | 0,2945 | 0,77 |
| 1 | 30 | 30 | 0,785 | 0,3534 | 0,79 |
| 1 | 35 | 35 | 0,785 | 0,4123 | 0,79 |
| 1 | 40 | 40 | 0,785 | 0,4712 | 0,79 |
| 1 | 45 | 45 | 0,785 | 0,5301 | 0,77 |
| 1 | 50 | 50 | 0,785 | 0,5890 | 0,75 |
| 1 | 55 | 55 | 0,785 | 0,6479 | 0,73 |
| 1 | 60 | 60 | 0,785 | 0,7068 | 0,70 |
| 1 | 65 | 65 | 0,785 | 0,7657 | 0,68 |

The behavior of C_p has been plotted considering the number of turbines, so the model correctly implements equation (7) according to Nishino (2012).

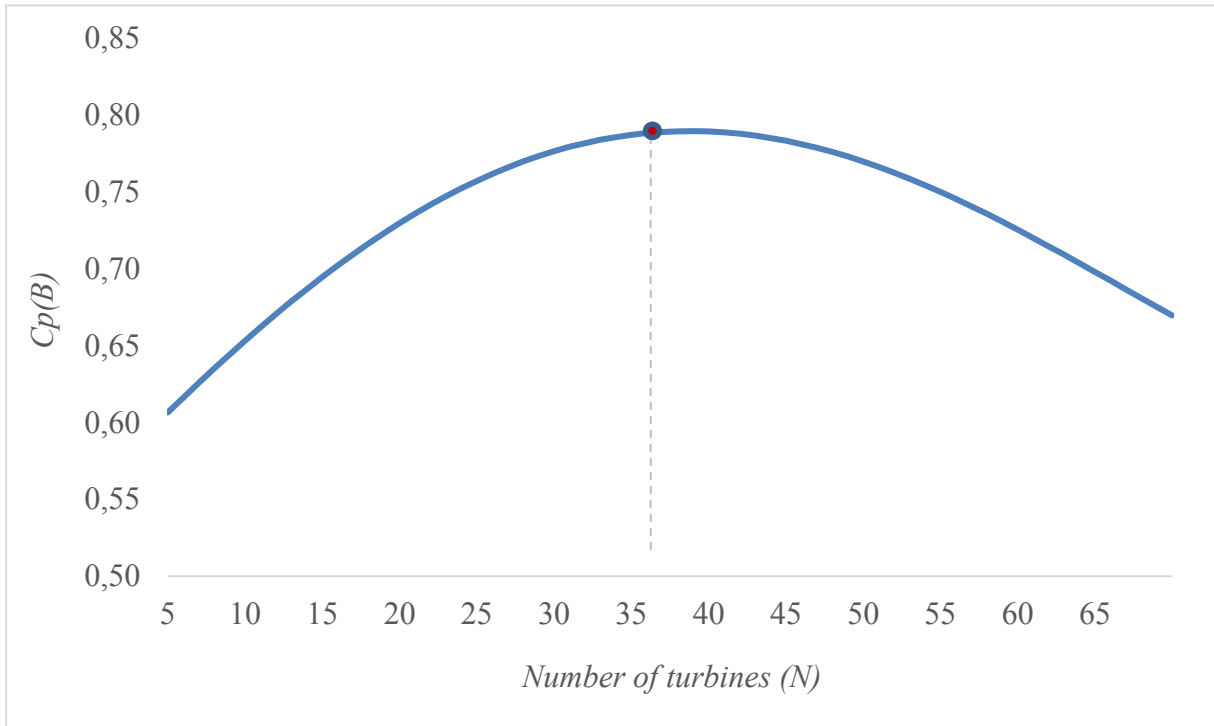


Figure 25: Behavior of C_p depending on the blockage effect varying as a result of the increasing number of turbines within a single fence.

Now that we have implemented a model to calculate the variation of C_p due to blockage, we are able to estimate the power output of the farm by varying the total number of turbines (N). It is also possible to visualize that the optimal blockage point happens approximately when $N = 35$ turbines. From this point onwards, we will start constructing an m by n array of turbines considering this fact. Bear in mind that hydrodynamic interference between row is not considered in this model.

7.2 Comparison of generated power employing two physical models

Several simulations have been conducted to evaluate the difference in power extraction given certain conditions. The first scenario predicts the power generated by the whole energy farm considering the first physical model (PM1), which considers the idealized C_p from the Betz theory for each turbine. The first model will be illustrated by the red curve in figure 26. The second physical model (PM2) implements the blockage effect of a LMADT in a finite flow

with constrained pressure, allowing for an enhancement of C_p due to channel blockage; the second model will be visualized by the blue curve in figure 26.

The second turbine array (blue curve) is constructed by placing turbines side by side until they physically complete the whole width of the channel (considering the minimum gap between them). When there is no place left, the next row starts to be filled with new turbines. Considering that $N = 35$ turbines per row produces the optimal C_p due to blockage effects, the following rows will add 35 turbines to the farm. For example, a farm with $m = 4$ rows of turbines will have $N = 140$ turbines with optimum C_p .

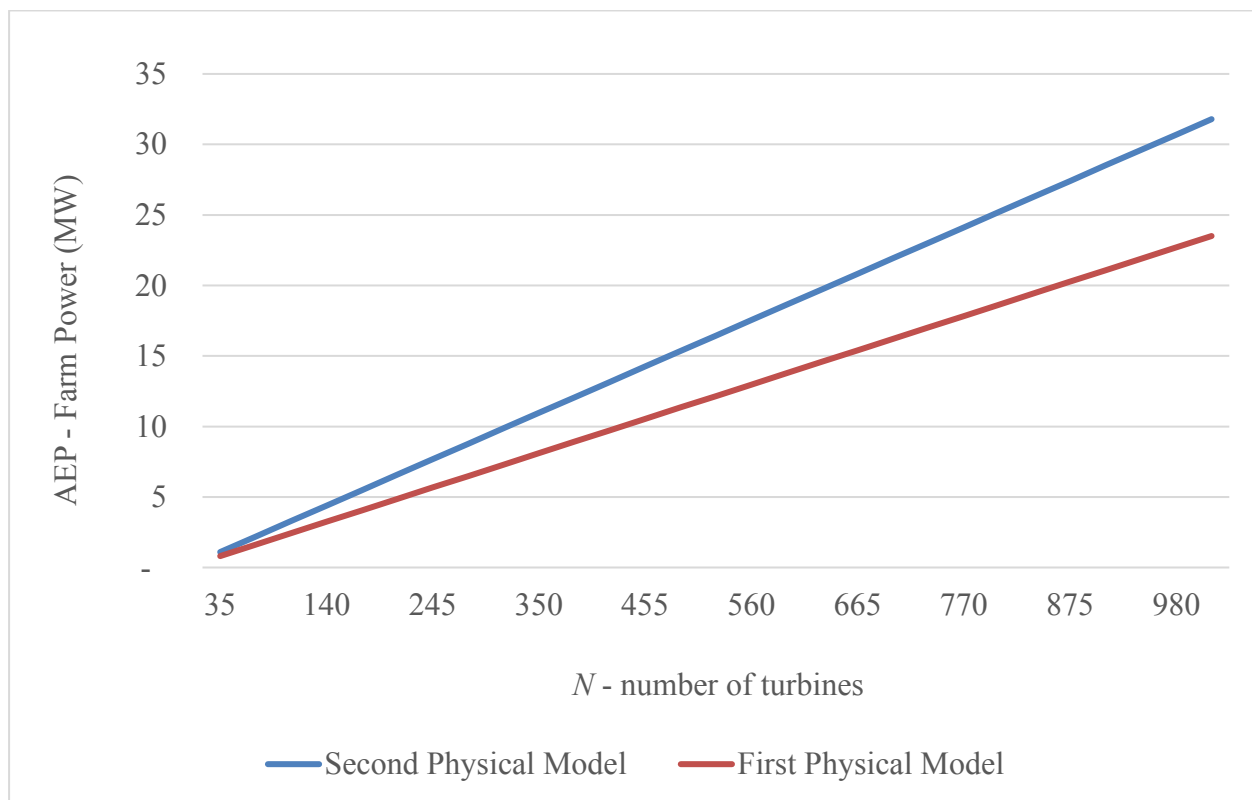


Figure 26: Comparison of the different physical models to evaluate farm output. The first physical model represents simple Betz implementation, and the second physical model has an optimized farm scaling and placement.

Figure 26 represents the difference of power generated by the same number of turbines given the physical variations of the two models. The first physical model (PM1) considers a linear approach (section 3.3.1) and the second (PM2) considers a creation of farm arrays where the C_{p_g} tends to be maximum, following an array set-up of variable numbers of turbines per

array.

The blockage effect contributes to a greater power generation. Having more turbines, naturally increases the difference between the power output of the models. For instance, when $N = 1000$ the result of PM2 can be computed as 20% greater than that of PM1, highly impacting large ventures and decision-making of investors. Therefore, for smaller ventures, a good approximation can be estimated using the idealized Betz model.

It is important to mention that such a great number of turbines (of the order of a thousand) is never expected in real applications. However, since the goal of this report is to present a tool to evaluate the IRR of the endeavor it is interesting to understand how the increasing number of turbines would impact the power output, as well as to compare the output of the two physical models.

And now that we have calculated the output power as a function of N we are able to evaluate the IRR of the business endeavor.

7.3 Power, IRR, and cashflow for $N=105$

In this subsection the calculation of the IRR will be presented using $v = 0,5$ m/s for the channel flow velocity. The first step is to calculate energy extraction, convert to power and use the electricity tariff to convert these values into revenue. As an example, table 13 presents the revenue for a farm with $N = 105$ turbines, while table 14 shows the associated costs (initial investments) and cashflow for the following years.

Table 12: Example of revenue for $N = 105$

| | |
|---|--------------|
| Power generated by each turbine individually (kW) | 31 |
| Power generated by the whole farm (kW) | 3.115 |
| Energy produced in a month (kWh) | 692.826 |
| Electricity tariff (\$/kWh) | \$ 0,10 |
| Revenue per year | \$ 695.639 |
| C_1 - Concept and Definition Costs | \$ 5.476.900 |
| C_2 - Machine Costs (Purchase) | \$ 7.775.148 |
| C_3 - Installation Costs | \$ 7.186.266 |
| C_4 - Operation and Maintenance Costs | \$ 338.682 |

Hence, the cashflow for a farm with $N = 105$ turbines is presented in the figure 27. The whole investment is computed in year 0 and subsequently reinvested with the revenue each year to compute the IRR:

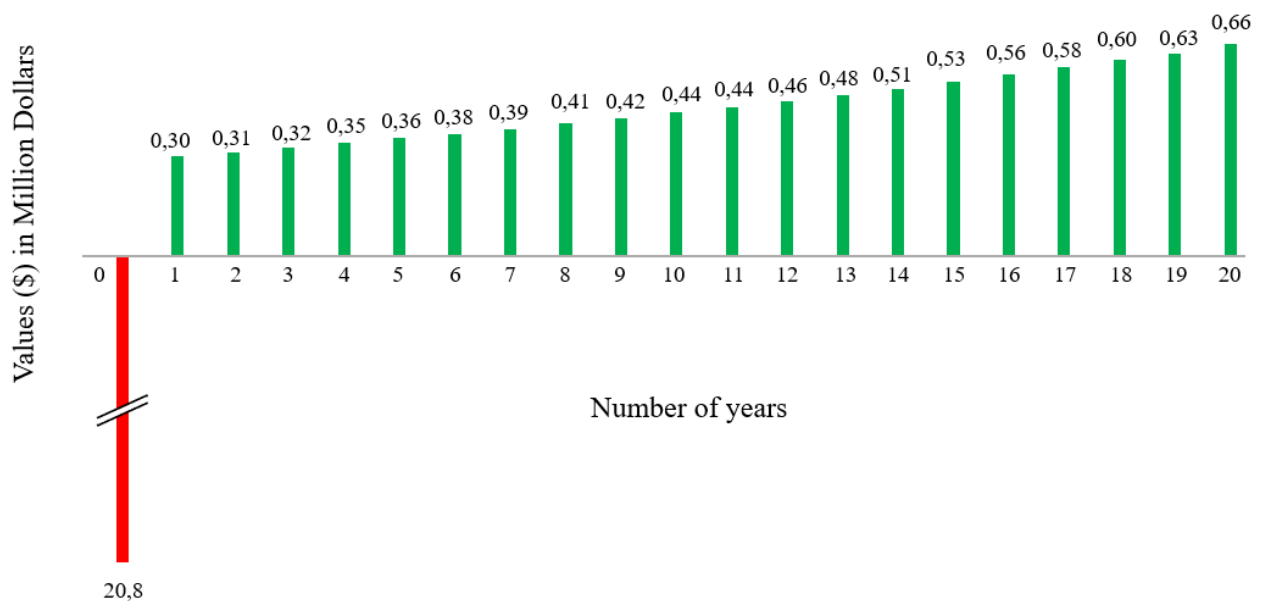


Figure 27: Representation of cashflow generated for the number of 105 turbines.

As a result, a positive return on investment could not be reached over the 20-year lifetime of the array. This means that the sum of cashflow generated by a farm containing 105 turbines and average flow speed of 0,5 m/s would not overcome the initial investment during the analyzed period. From a finance perspective (and to facilitate comparison) this cashflow can be translated into a curve (Figure 27) in which it is possible to visualize the NPV. In this type of representation, when the curve crosses the X-axis would represent the PP in years (section 3.2.5) According to Segura (2016), a typical value of PP would be around 7-9 years.

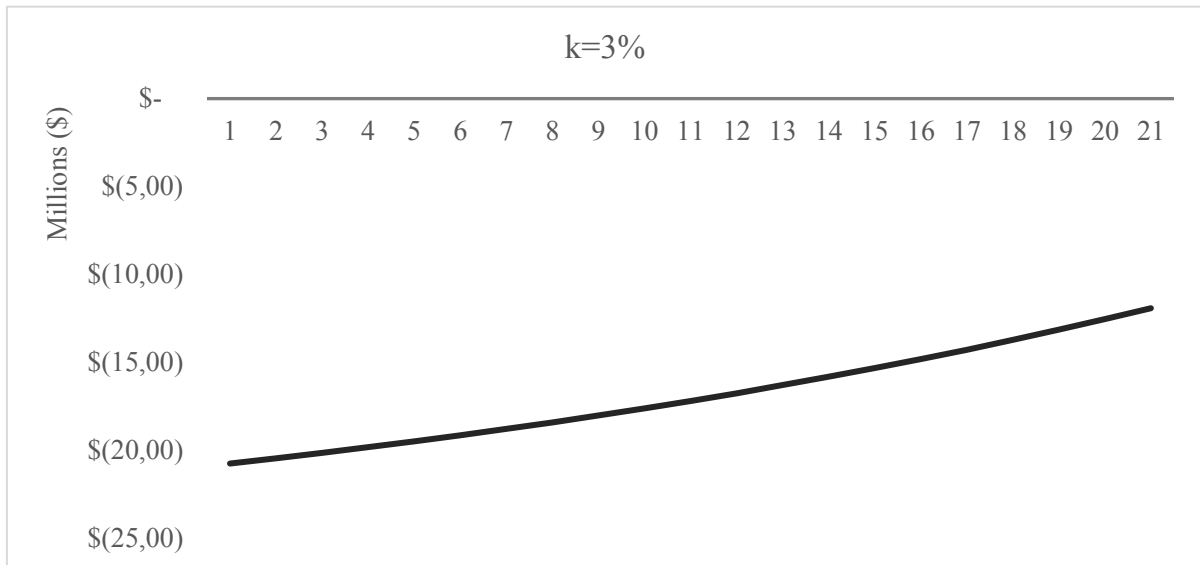


Figure 28: Graph of cashflow to visualize PP and NPV considering $N = 105$.

Taking those parameters into consideration and lowering interest rate ($k=3\%$) there is no economic feasibility because the project would take more than 20 years to pay off.

The table below represent the results of 10 years and 20 years: naturally the IRR increases by having a longer lifetime array:

Table 13 – Calculation of the IRR of the example of 100 turbines for 10 and 20 years.

| IRR | Period |
|------|----------|
| -26% | 10 years |
| -6% | 20 years |

Therefore, we can calculate that $NPV = \$ -11.934.183,95$ and $EBITDA = \$ -9.547.347,16$. This mathematically implies that $NPV < 0$ meaning that project is not viable.

The question that remains is whether by increasing the number of turbines it would be possible to find an $NPV > 0$, representing a viable project. This will be covered within the next section.

7.4 Power, IRR, and cashflow varying the number of turbines

The figure 29 shows different results of cashflows after changing the number of turbines, to visualize weather the said endeavor would return positive values inside the lifecycle of 20 years. The figure shows different cashflows when $N=250$ and $N=1690$ following the calculations of power coefficient from section 7.2.

Such number of turbines are chosen strategically. It is possible to see that the difference of cashflows from the Figure 28 and Figure 29 (a) varies greatly. However, Figure 29 (a) and Figure 29 (b) do not vary with same intensity. In this case, (a) and (b) are rather similar. The number $N=1690$ is chosen to physically fulfil the whole channel with turbines. The results presented in Figure 29 make sense from a finance perspective, because from a certain point (more specifically around 200-300 turbines and therefore we chose $N=250$ to visually express this result) simply increasing the number of turbines alters the purchase costs directly, which represent a large part of the investments and therefore NPV and IRR do not vary greatly from $N=250$ to $N=1690$.

It is also important to mention that altering interest rate k is not as impactful as altering the flow speed of the channel (see section 7.5 as the power output sharply increases when flow velocity increases proportionately). Also, no great differences can be seen by altering $k=3\%$ to $k=5\%$ for example, therefore it is important to study flow velocity in depth.

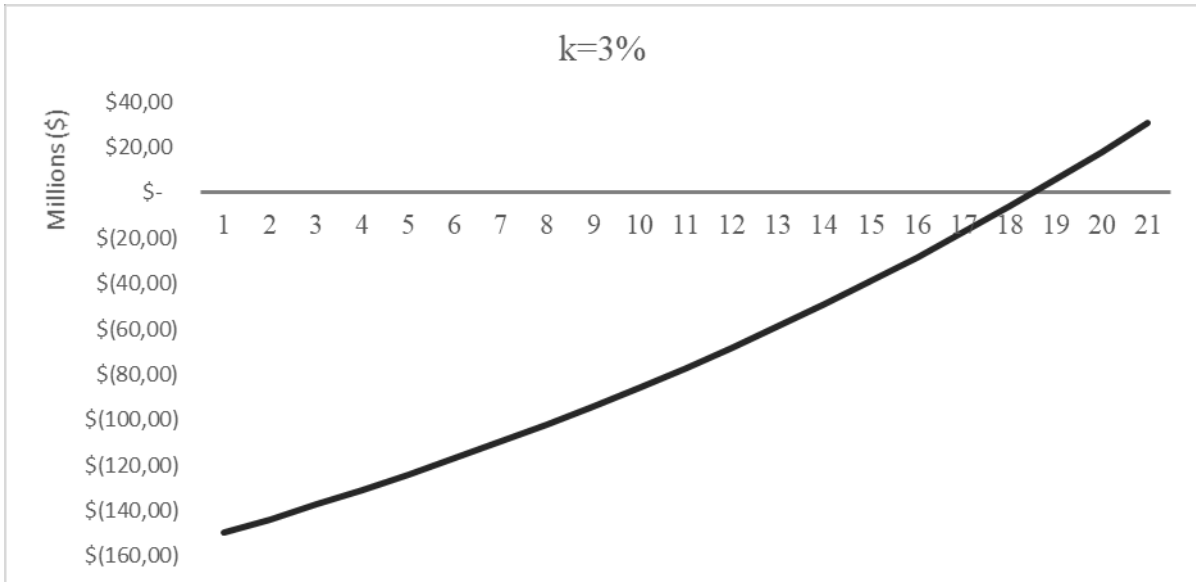
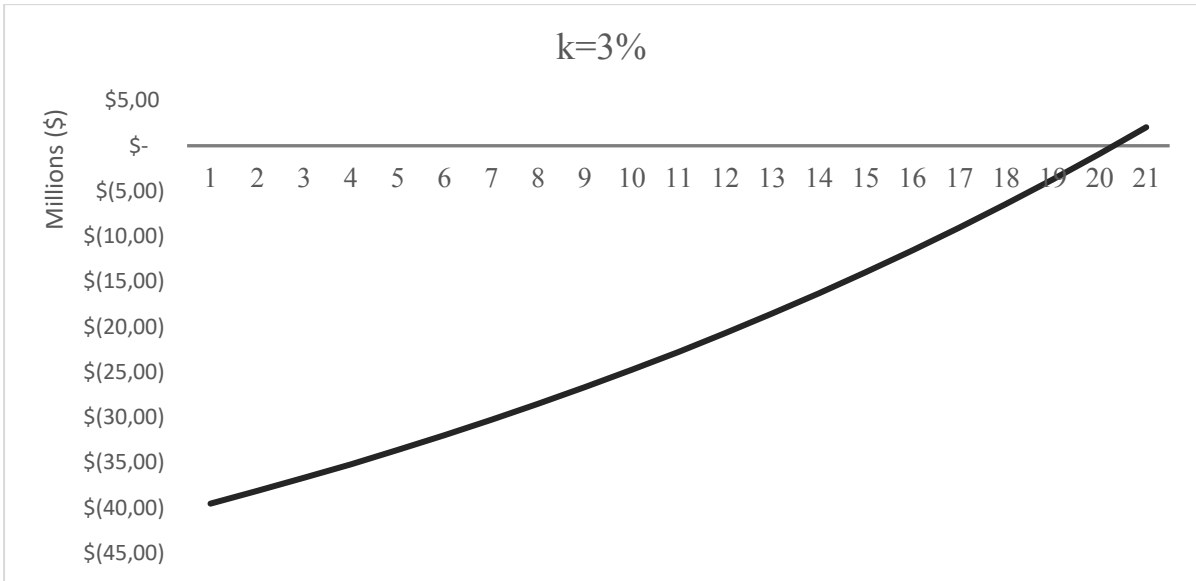


Figure 29: Illustration of the different cashflows taking into consideration different number of turbines. (a) Top: $N = 250$; (b) Bottom: $N = 1690$.

As mentioned in earlier sections, simply increasing the numbers of turbines will present a more interesting scenario, however investors will not support the project because of the high costs of implementation. They will prefer smaller initial investments and higher IRR.

Considering all other real parameters (and mainly $v = 0,5$ m/s), the Ilha Bela case would be positive only for a number of turbines = 331 and greater, for the 20-year lifecycle. In this case we would have the following outputs:

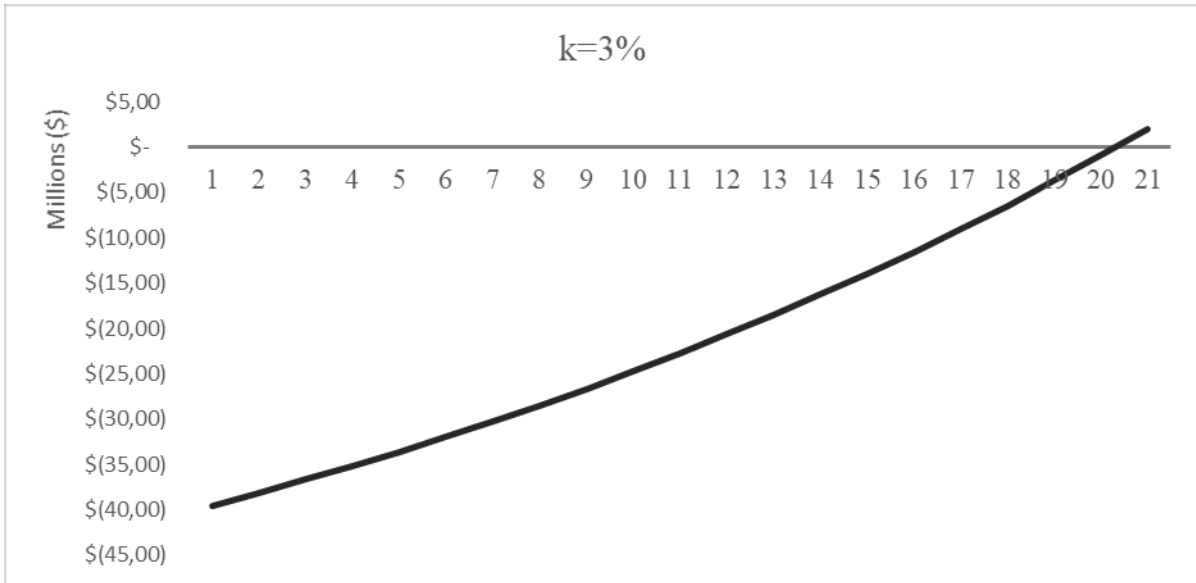


Figure 30: Illustration of the cashflows of 331 turbines that cross exactly in the 20-year mark for the selected channel.

Table 14: Summary of the different values computed for $N = 331$

| | |
|---|---------------|
| Power generated by each turbine individually (kW) | 33,6 |
| Power generated by the whole farm (kW) | 12.137 |
| Energy Produced in a month (kWh) | 2.621.623 |
| \$/kWh | \$ 0,10 |
| Revenue per year | \$ 2.516.758 |
| C_1 - Concept and Definition Costs | \$ 5.476.900 |
| C_2 - Machine Costs (Purchase) | \$ 25.735.740 |
| C_3 - Installation Costs | \$ 7.186.266 |
| C_4 - Operation and Maintenance Costs | \$ 1.121.037 |

In conclusion, taking those parameters into consideration and lowering interest rate ($k=3\%$) the project would be economically feasible only after 20 years, which is the PP (time for the investment to pay off). The initial investments, however, are not extraordinarily high ($PV = 157$ Million Dollars) which is in the range of a middle market M&A boutique. Again, however, we would like to emphasize that no private equity firm would wait this long to invest in such an endeavor.

7.5 Results by increasing flow speed

As seen above, the major parameter to decide the location of the implementation is not the number of turbines. As seen in the literature review, flow velocities in excess of $v=2,0$ m/s are necessary to make this type of endeavor economically feasible. The model correctly predicts this value, as in $v=2,0$ m/s it is possible to reach an IRR of 40% with 160 turbines, what would make an endeavor feasible from a finance perspective.

In the previous analysis we focused on the break-even period. If we now alter flow speed, what value of flow speed and number of turbines would be needed to arrive at break-even values? In this section this calculation is presented considering a life cycle of 20 years. Therefore, the study in this section has been conducted utilizing the proposed tool and the figure 31 represents different velocities for the considered topology. After increasing flow speed to 1,5 m/s it is possible to increase the IRR to 20% when $N=320$ turbines is implemented. This represents an interesting investment scenario from a finance perspective.

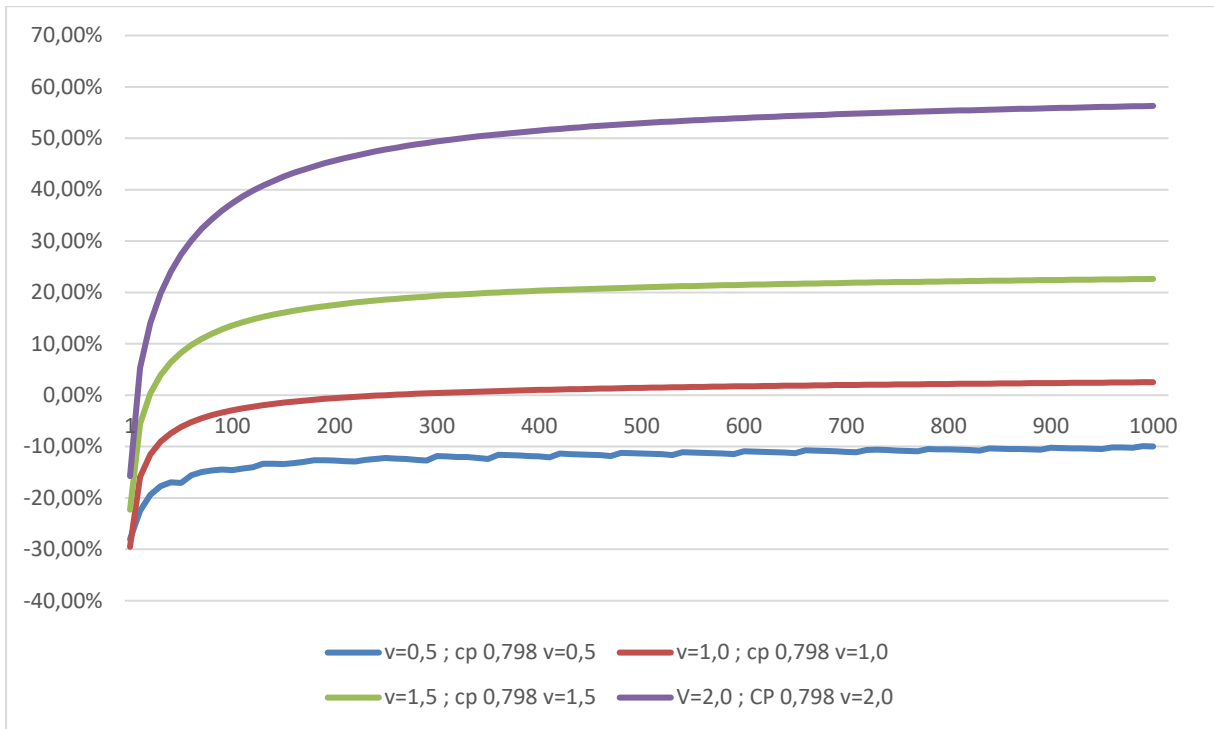


Figure 31: Different IRRs by altering flow speed, from 0,5 m/s to 2,0 m/s.

This analysis was carried out until $N = 1000$ turbines because after this point, no considerable change can be seen in the graphs. Besides, no real endeavor would contain more than 1000 turbines because of the necessary implementation costs would be too high.

7.6 Calculation of IRR depending on the number of turbines, using $v=2,0\text{m/s}$

This subsection will present economic metrics for a fictional endeavor taking into consideration the topology of Ilha Bela, however increasing the velocity to $v = 2,0$ m/s.

First off, analyzing one single fence, the IRR “deaccelerates” as the number of turbines increases. This is consistent with the previous analysis, presenting that a greater number of turbines increases the IRR, as well as the blockage effect that increases C_p proportionally with the number of turbines. (Figure 32).

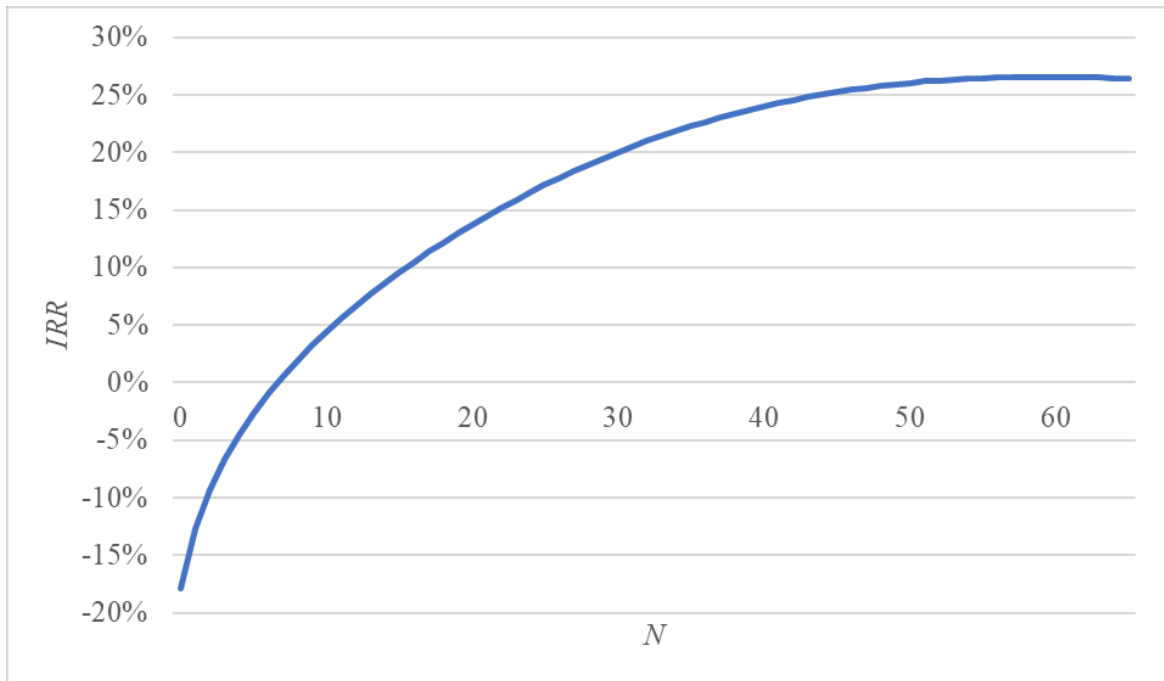


Figure 32: Alteration of IRR by increasing the number of turbines for a single fence

7.7 General result varying speed and suggestion of location

An analysis of the IRR will be presented considering both first and second scenario. The only difference is that a fictional flow velocity of 2,0 m/s is considered, showing that the main parameter for the feasibility is the velocity. In the first scenario, the Betz model will provide a constant C_p of 0,59 which is the represented by the yellow curve (physical model 1). In the second scenario, a comparison of C_p and IIRs is presented depending on the blockage effect (physical model 2). The optimal condition of $C_p = 0,79$ (Nishino) is presented in the orange curve. However, this condition cannot be achieved, because of the necessary space between turbines and depth of the channel. A more realistic approach is presented considering a variable C_p , depending on the number of turbines per fence. The blue curves were constructed by altering the number of turbines per row and this variation is consistent with the fact that, by altering the number of turbines C_p also alters the farm output. For example, when $N=40$, the center topology considers two fences of 20 turbines, having a lower C_p than when $N=35$ therefore the sawed effect.

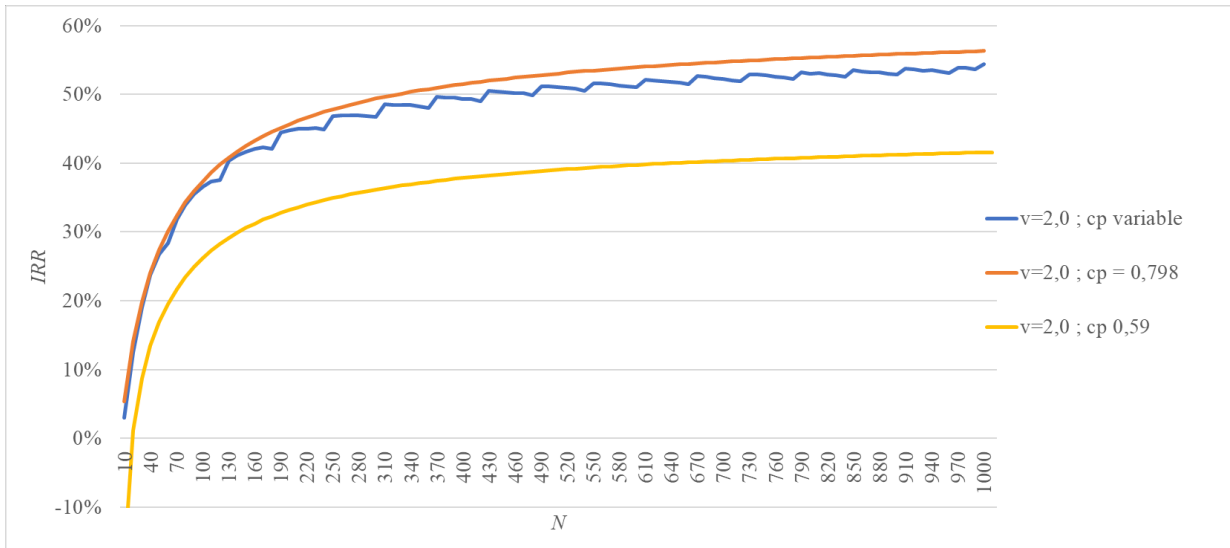


Figure 33: Comparison of the different physical models to evaluate output difference. PM1 represents simple Betz implementation and PM2 has an optimized farm scaling and placement, considering a variable C_p and therefore a variable power output.

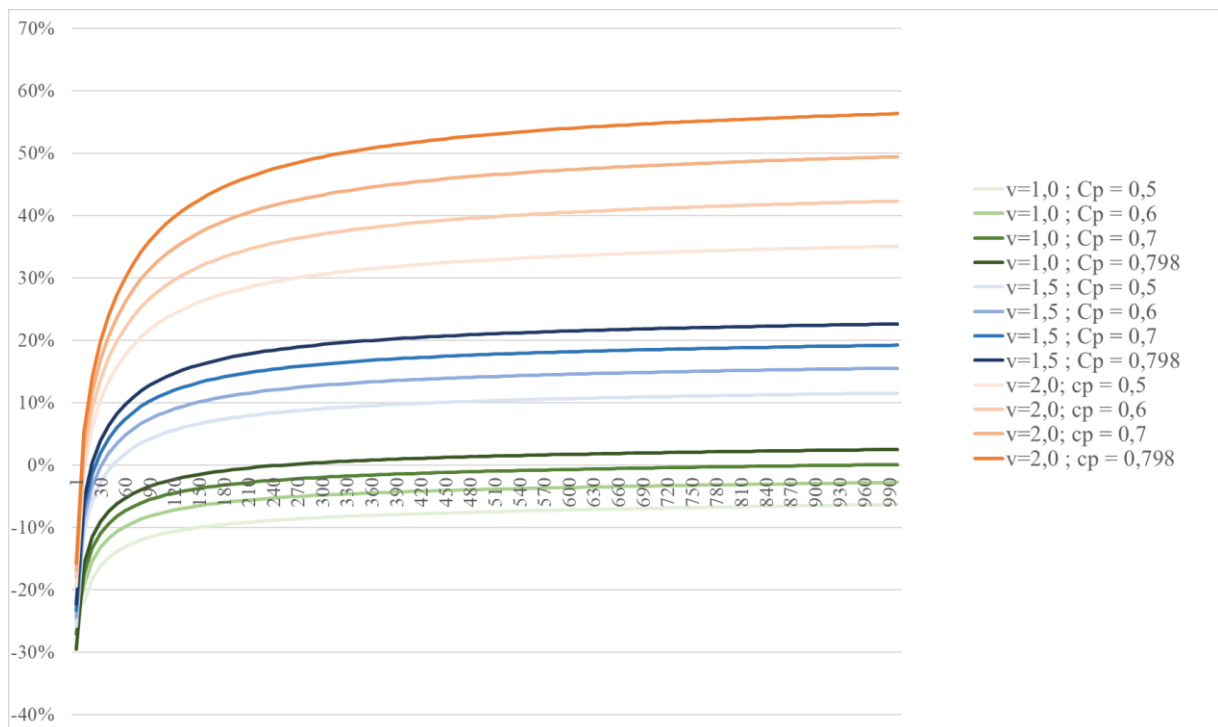


Figure 34: Comparison of the different physic models to evaluate output difference. MF1 represents simple Betz implementation and MF2 has an optimized farm scaling and placement, considering a variable C_p and therefore a variable power output.

In real applications, however, velocity plays a much more important role than C_p , therefore it is important also to visualize the behavior of IRR of different velocities. The figure 34 represents minimum and maximum values for each velocity analyzed starting off with $v=1,0$; $v=1,5$; $v=2,0$ but varying C_p in each one.

The following conclusion can be drawn from Figure 34: when $v=1,0$ m/s the NPV>0 is reached when $N = 260$ turbines approximately if $C_p = 0,798$; however, no feasibility can be reached when $C_p = 0,59$. When $v=1,5$ m/s the economic conditions become much more interesting and both C_p represent positive NPV i.e. $N = 400$ when $C_p = 0,59$ and $N = 30$ when $C_p = 0,798$. However, having this velocity independently of the C_p a condition of IRR greater than 25% is never reached.

On the other hand, when $v=2,0$ m/s reaching an IRR greater than 25% becomes possible when $C_p= 0,59$ for $N = 30$ and $C_p = 0,798$ for $N = 12$. This result is consistent with previous works, taking into consideration the reduced number of tidal turbines in most seen endeavours nowadays.

Previous works consider that tidal stream turbines require peak flow speeds in excess of 2 m/s for economically viable energy extraction, however, by increasing the number of turbines and consequently C_p , the IRR of the endeavor also changes considerably, as it can be seen by the results above.

8 CONCLUSIONS

This work presents a cost assessment methodology and economic model tool to evaluate the economic feasibility of marine stream energy farms. The methodology presented is based on the life-cycle costs of the complete project, which are concept, purchase, installation, and operation costs. The proposed model determines the total energy produced and consequently the total revenue generated by considering different aspects of the tidal farm, such as farm topology and different turbine characteristics.

Marine stream energy presents a significant and worthwhile opportunity as a predictable and renewable source of energy in different countries, especially with significant tidal resources. Different locations benefit from established offshore energy sectors and present considerable hydraulic potential, presenting an interesting scenario taking into consideration current climate challenges and the necessity to drive renewable energy exploration. In order to drive carbon reduction transition in current economies, not only costs must be reduced but also the economic aspect of the energy ventures must be taking into consideration.

It has been seen that in the channel of São Sebastião, located in the Southeast coast of Brazil, with $v = 0,5$ m/s there would not be a financially viable endeavor. However, by looking for a channel of similar dimensions with higher flow speeds then that would be possible to see IRRs as great as 40% and PP as low as 6-7 years, which would be of interest for most private equity and M&A companies.

The economic assessment of stream energy technologies is very important to coherently quantify the costs of these technologies, discovering their economic viability and simultaneously attracting investment in these technologies.

The compilation of data is analyzed to determine the feasibility analysis of the project using different economic and technical indicators. This allows the profitability of the project to be calculated and, as a result, proper comparison to peer investments can be conducted to guide decision-making stakeholders. If an investors want to conduct an initial assessment of a tidal farm, they can use this tool to generate the income statement, balance sheet and cash flow of the endeavor by imputing the required physical and economic parameters into the model. Obviously, the tool varies with different turbine powers.

It was also discussed that there are a great number of metrics that can be used to evaluate the performance of stream energy arrays, such as LCOE, PP, NPV and IRR, although this work

utilizes the NPV and IRR, presenting an analysis that takes into consideration array designs with several turbines and the financial aspect of each venture, ranging from $N=1$ until $N=1000$. The analysis showed that velocity is a main factor to be considered when studying the implementation of a tidal energy farm and the correlation between IRR and flow velocity has been analyzed. Tidal stream endeavors can reach economic viability by increasing the number of turbines and consequently C_P , as the IRR of the endeavor changes considerably.

Within the business case section, the proposed methodology was used to study the viability of a tidal farm in the region of Ilha Bela Island, a location that presents interesting tidal potential exploration. The results obtained after carrying out economic metric analysis (NPV, IRR) are the following: the project would not be economically feasible if the average flow velocity used were 0,5 m/s as presented in Fortes' work, even by increasing greatly the number of turbines. Moreover, different velocities were analyzed, into which different IRRs were calculated. When speed is in the range of $v=2,0$ m/s IRRs as high as 40-50% can be achieved, representing very interesting endeavors from an investment perspective.

Financial institutions can provide capital at a lower cost, and they find the returns from energy projects more attractive than those from traditional alternatives, such as government bonds. Building capabilities, infrastructure, and governance to support their activities in the energy industry, as well as developing the analytic skills and insight to identify opportunities as they emerge is of extreme importance in current scenario.

Renewables have developed from niche technology to global industry. With environmental concerns rising to the top of global and regional agendas, the debate has shifted from when renewables will take off, to how much faster will they grow, because the cost of renewables continues to fall sharply, and their growth rates soar. The need for clean power in emerging economies only adds to the momentum and drive this inevitable change.

A winning strategy for renewable energy exploration will focus on international expansion and scale, focusing on regions such as South America or Northern Europe which present considerable potential. As companies grow and expand across borders, their ability to reap benefits of scale will depend on establishing global operating models with clear responsibilities for effective working across continents, cultures, and time zones. Key capabilities, such as regulatory management and auctioning, will need to be deployed globally, which will require a deep understanding of the specifics of individual markets and regulations. As companies will need to develop sophisticated asset-allocation and pipeline-management capabilities to ensure

that they focus on the projects that create the most value, tools such as the one presented in this paper to evaluate the economic potential of energy endeavors will be extremely handy.

8.1 Suggestions for future work

The present work aimed to present the aspects of energy extraction using tidal energy. The main theories and mathematical models for energy extraction were reinforced and discussed in detail. A method of economic analysis and cost assessment for the installation marine stream turbines has been presented, however, further details can increase the accuracy of the model. For instance, a more realistic physical model could be implemented, taking into consideration topology, bathymetry, the height variation of the channel's surface due to the effect of the turbine constraint, turbulence intensity, restriction for navigation, etc. Also, a decommission cost estimation could be presented, if real values were provided after the life-cycle of the endeavour, for instance, if the turbines could be recycled in 30 years after deployment. Lastly, future work could consider cost assessment models that take into consideration the loss of efficiency over the lifetime of the system.

REFERENCES

- Ahmed, M., Ohamed, H. "Design Optimization of Savonius and Wells Turbines". Fakultät für Verfahrens- und Systemtechnik der Otto-von-Guericke-Universität Magdeburg. 2011.
- Altan, B. 2016. Investigation of 3D printed Savonius rotor performance. *Renewable Energy* 99, 584-591
- Aquaret, J. 2008. Aquatic renewable energy technologies.
- Arinaga, R., & Cheung, K. 2012. Atlas of global wave energy from 10 years of reanalysis and hindcast data. *Renewable energy* , 49-64.
- Bahaj, A. S., Molland, A. F., Chaplin, J. R. & Batten, W. M. J. 2007 Power and thrust measurements of marine current turbines under various hydrodynamic flow conditions in a cavitation tunnel and a towing tank. *Renewable Energy* 32, 407–426.
- Bryden, I. G., Couch, S.J., Owen, A. and Melville, G. 2007. Tidal current resource assessment. *Proc. IMechE, Part A: J. Power and Energy*, Vol. 221, 125-135.
- Burton, T., Sharpe. D., Jenkins, N., Bossanyi, E. 2001. *Wind Energy Handbook*. John Wiley & Sons, Ltd. West Sussex, England.
- Çengel, Y., & Cimbala, J. 2010. *Fluid Mechanics Fluid Mechanics*, 2, 853-920. Mc Graw Hill Professional.
- Draper, S. "Modelling tidal energy extraction in a depth-averaged coastal domain". Volume 4, Issue 6, November 2010, p. 545 – 554
- Denny, E. "The Economics of tidal energy". *Energy Policy* 2009; 37, 1914-1924.
- Elghali, S.E.; Benbouzid, M.E.H.; Charpentier, J.F. "Marine Tidal Current Electric Power Generation Technology: State of the Art and Current Status". *Electric Machines & Drives Conference*, 2007; 1407-1412.
- Fortes, J. F., "Avaliação do potencial de energias marinhas na região de São Sebastião". Instituto Oceanográfico da Universidade de São Paulo. MsC Programa de Oceanografia. 2018.
- Furtmayr, F. "Windkraftanlagen mit vertikaler Achse (VAWT): Der C-Rotor im Windkanalversuch und Strömungssimulation in Star-CCM+". Abschlussarbeit zur Erlangung des akademischen Grades. 2013.

- Garrett, C. and Cummins, P. 2004. Generating power from tidal currents. *J. Waterway, Port, Coastal, Ocean Engineering*, Vol. 130, 114-118.
- Garrett, C. and Cummins, P. 2007. The efficiency of a turbine in a tidal channel. *J. Fluid Mechanics*, Vol. 588, 243-251.
- GE Power Conversion (2017) -
- Gupta, R., Deb, B. "Performance Analysis of a Helical Savonius Rotor with Shaft at 45° Twist Angle Using CFD". Department of Mechanical Engineering, NIT Silchar Assam, India. 2013.
- Kirinus, E. P. 2018. Long-term simulations for ocean energy off the Brazilian coast
- Leclercq, M. Harvesting energy from the sea. Master of Science Thesis, KTH School of Industrial Engineering and Management. Energy Technology EGI-2012-001MSC, SE-100 44 STOCKHOLM
- McNaughton, J. 2016. Tidal-stream power and turbine produced electricity quality for the Energy Power variability of tidal-stream energy and implications for electricity supply
- Mechanics, Vol. 588, 243-251. Whelan, J., Thomson, J., Graham, J.M.R. and Peiro, J. 2007. Modelling of free surface proximity and wave induced velocities around a horizontal axis tidal stream turbine. Proc. 7th European wave and tidal energy conference, Porto, Portugal.
- Menet, J. L., Bouraba, N. "Increase in the savonius rotors efficiency via a parametric investigation". Ecole Nationale Supérieure d'Ingenieurs en Informatique Automatique Mecanique Énergetique Électronique de Valenciennes (ENSIAME). 2012
- Patel, V., 2006. Theoretical study on the prediction of the hydrodynamic performance of a Savonius turbine based on stagnation pressure and impulse momentum principle
- Prasad, D. 2018. Studies on the performance of Savonius rotors in a numerical wave tank
- RETEC, 2016. Revista de Tecnologias (Technology Magazine) - v. 9 n. 1
- Rouse et. al. 2008. Enhancing local distinctiveness fosters public acceptance of tidal energy: A UK case study
- Sargolzaei, J. "Prediction of the power ratio and torque in wind turbine Savonius rotors using". Department of chemical engineering, IRAN. 2007.

- Sarma, N. K. 2014. Experimental and computational evaluation of Savonius hydrokinetic turbine for low velocity condition with comparison to Savonius wind turbine at the same input power.
- Whelan, J., Thomson, J., Graham, J.M.R. and Peiro, J. 2007. Modelling of free surface proximity and wave induced velocities around a horizontal axis tidal stream turbine. Proc. 7th European wave and tidal energy conference, Porto, Portugal.
- DNV-GL White Paper, 2017 - Definitions of Availability Terms for the Wind Industry,” Tech. Rep., 2017.
- S. W. Funke, P. E. Farrell, and M. D. Piggott, “Tidal turbine array optimisation using the adjoint approach,” *Renewable Energy*, vol. 63, pp. 658–673, 3 2014. [Online].
- Vogel C., 2016. The power available to tidal turbines in an open channel flow. *Proceedings of the ICE - Energy* 170(1):1-10
- Z. L. Goss, M. D. Piggott, S. C. Kramer, A. Avdis, A. Angeloudis, and C. J. Cotter, “Competition effects between nearby tidal turbine arrays-optimal design for Alderney Race,” in 3rd International Conference on Renewable Energies Offshore, Lisbon, 2018, pp. 255–262.
- T. Divett, R. Vennell, and C. Stevens, “Optimization of multiple turbine arrays in a channel with tidally reversing flow by numerical modelling with adaptive mesh,” *Philosophical Transactions of the Royal Society A: Mathematical, Physical and Engineering Sciences*, vol. 371, no. 1985, p. 20120251, 2 2013.
- Z. L. Goss, S. C. Kramer, A. Avdis, C. J. Cotter, and M. D. Piggott, “Economic optimisation of large scale tidal stream turbine arrays,” in 13th European Wave and Tidal Energy Conference, Naples, 2019, pp. 1598–1598.
- Z. L. Goss, M. D. Piggott, and S. C. Kramer, “An English Channel Model for the Optimisation of Tidal Turbines in the Alderney Race,” in Oxford Tidal Energy Workshop, Oxford, 2018, pp. 10–11.
- Z. L. Goss, S. C. Kramer, A. Avdis, C. J. Cotter, and M. D. Piggott, “Variations in the optimal design of a tidal stream turbine array with costs,” in Oxford Tidal Energy Workshop, Oxford, 2019, pp. 33–34. [Online].
- D. M. Culley, S. Funke, M. Piggott, and A. Peter, “The modelling and design optimisation of

tidal stream turbine arrays,” Ph.D. dissertation, Imperial College London, 2016.

S. Song, W. Shi, Y. K. Demirel, and M. Atlar, “The effect of biofouling on the tidal turbine performance,” Tech. Rep.

Frangoul, Anmar. In New York’s East River, a tidal power project takes shape. CNBC, New York, 11 November 2020. s12. Available at <https://www.cnbc.com/2020/11/24/in-new-yorks-east-river-a-tidal-power-project-takes-shape.html>